Valorization of brines in the chlor-alkali industry. Integration of precipitation and membrane processes.

Doctoral Thesis presented to the
Chemical Engineering Dept.
Universitat Politècnica de Catalunya
by

Sandra Casas Garriga
sandra.casas@upc.edu

October 2011

Advisor: J.L.Cortina

Submitted to reviewers on October 2011.
Final deposit on November 2011.

Abstract

Reuse of brines in the chlor-alkali industry can be benefitial both in terms of new material source for the industry and environmental impact reduction of the brines disposal. In this thesis, reuse of Seawater Reverse Osmosis Desalination brine as well as potash mine brine is studied.

Seawater Reverse Osmosis from the El Prat Desalination Plant and potash mine brine from the Llobregat brine collector pipe were used for this study. These kinds of brines were chemically characterized using different analytical methods that had to be adapted to the high salinities of the samples. According to the composition results obtained and the literature reviewed, several treatments were evaluated to reach the membrane electrolysis process requirements of the chlor-alkali industry. Potash mine brine had high sodium chloride concentration and in consequence, only purification was studied.

Electrodialysis, nanofiltration and precipitation were studied for brines concentration and primary purification. Experiments in the laboratory and in pilot plants were carried out. Pilot plants were designed and operated to determine the optimal conditions to treat the brines and design a feasible system to valorize the brines in the chlor-alkali industry using membrane electrolysis cells.

Electrodialysis was demonstrated a feasible technology for SWD-RO brine concentration, as it concentrated the brine and at the same time produced some useful by-products that could be further valorized. Performance obtained was highly dependent on inlet temperature and current densities used. The optimal ED

operation point was determined when working in a continuous mode at $0.5kA/m^2$ were 18L/h of 244 g/L NaCl with 0.16 kWh/kg NaCl energy consumption were obtained. A first purification of polyvalent ions was reached using ED.

Nanofiltration efficiently removed polyvalent ions from both brines studied. The optimal operation point was around 20 bar in both cases. In the pilot plant, pressures higher than 20bar could not be evaluated due to fixed inlet flow. Removal of sulphates, calcium and magnesium was higher than 90%, 50% and 70% in both brines studied whereas NaCl was only removed by 12% maximum at 20bar, which was benefitial for its reuse. Removal of minor elements was also studied and depended on ionic radii as well as ionic charge.

Precipitation using NaOH and Na_2CO_3 reagents was evaluated to remove calcium and magnesium from the brines at different inlet temperatures. Temperatures over 65°C increased calcium purification performance, especially on SWD-RO brines which contained all the antiscalants of the RO process that avoided calcium carbonate and sulphate precipitation. In consequence, the amount of reactants needed to reach the optimal purification point was higher than the values reported in the literature. Nevertheless, purifications efficiencies higher than 95% could be obtained. Reactant order addition effect on the purification performance results obtained was not considered significant Precipitates obtained during the purification process could be further valorized.

Integration of membrane and precipitation process was needed in order to efficiently treat the brines studied. Finally, a mathematical model to predict the concentration performance and design future experiments was developed and validated with the results obtained in the pilot plant.

Acknowledgments

Glossary

General Terms

BAT   Best Available Technology

CIP   Cleaning in place

CF   Concentration Factor

CTM   Technological Center of Manresa

EC   Energy consumption (kWh/m^3 or kWh/kg NaCl)

ED   Electrodialysis

ED-SWD-RO   Concentrated SWD-RO brine by ED

EDR   Electrodialysis Reversal

I   Current intensity (A)

I_d Current density (kA/m^2)

IC   Ionic Chromatography

ICP	Inductively coupled plasma mass spectrometry
IEX	Ion Exchange
IT	Irreversible Thermodynamic approach
LCD	Limiting current density (kA/m^2)
MCr	Membrane Crystallization
MD	Membrane Distillation
MS	Maxwell-Stephan
MSF	Multidestilation Flash
MWCO	Molecular weight cut-off
NF	Nanofiltration
NP	Nerst-Planck
PFR	Permeate flow rate (L/m^2 bar)
PTFE	Polytetrafluoroethylene
PWP	Pure Water Permeability (L/m^2h bar)
R	Rejection of an ion (%)
RO	Reverse Osmosis
SEM	Scanning Electron Microscope
SWED	Sea Water Electrodialysis
SWD-RO	Sea Water Desalination Reverse Osmosis
TOC	Total Organic Carbon
UF	Ultrafiltration
XRD	X-ray Diffraction
ZDD	Zero Desalination Discharge
ZLD	Zero Liquid Discharge
α	Selectivity of the rejection of an ion in nanofiltration
η	Current efficiency in ED (%)
S^A_B	Membrane selectivity

ED modelling

C_{d_i}	Inlet NaCl concentration (mol/L) of the diluate stream
$C_{c\_i}(t=0)$	NaCl concentration in the tank at the beginning of the experiment (mol/L)
C_{d_o}	Outlet NaCl concentration (mol/L) of the diluate stream
C_{c_i}	Inlet NaCl concentration (mol/L) of the concentrate stream
C_{c_o}	Outlet NaCl concentration (mol/L) of the concentrate stream
C_{d_cm}	Concentration of NaCl (mol/L) on the cation membranes in the diluate compartment
C_{d_am}	Concentration of NaCl (mol/L) on the anion membranes in the diluate compartment
C_{c_cm}	Concentration of NaCl (mol/L) on the cation membranes in the concentrate compartment
C_{c_am}	Concentration of NaCl (mol/L) on the anion membranes in the concentrate compartment
$C_{NaCl}^{sat}(25ºC)$	NaCl saturation concentration (g/kg) at 25°C
D	Ion diffusion flux (mol NaCl/h)
$D_{Cl^-\_am}$	Coefficient of chloride ion diffusion in the anionic membranes (dm^2/h)

$D_{Na^+\_cm}$	Coefficient of sodium ion diffusion in the cationic membranes (dm^2/h)
D_w	Osmosis flux (mol H_2O/h)
D_{w_am}	Coefficient of water diffusion in the anionic membranes (dm^2/h)
D_{w_cm}	Coefficient of water diffusion in the anionic membranes (dm^2/h)
F	Faraday constant (C/mol e$^-$)
h_{Cl^-}	Hydration number of chloride ions (adim)
h_{Na^+}	Hydration number of sodium ions (adim)
k_m	Mass transfer coefficient (dm/s)
M	Ion migration flux (mol NaCl/h)
M_w	Electro-osmosis flux (mol H_2O/h)
Mw_{NaCl}	Molecular weight of NaCl (g/mol)
Mw_{H_2O}	Molecular weight of water (g/mol)
N	Number of cells
Q_{d_i}	Diluate stream inlet flow (L/h)
Q_{d_o}	Diluate stream outlet flow (L/h)
Q_{c_i}	Concentrate stream inlet flow (L/h)
Q_{c_o}	Concentrate stream outlet flow (L/h)

$Q_{tan\,k}$	Overflow of the concentrate tank (L/h)
Q_w	Water flow transported from diluate compartment to concentrate compartment (L/h)
S	Effective membrane area (dm^2)
t_{Cl^-}	Anionic transport number
t_{Na^+}	Cationic transport number
t_{Cl^-am}	Anionic transport number in the anionic membranes (adim)
t_{Na^+cm}	Cationic transport number in the anionic membranes (adim)
t_{SS}	Time to reach the maximum NaCl concentration in the tank (h)
t_f	Ending time for the model to run (h)
t_w	Water transport number (adim)
V_{cell}	Cell volume (L)
$V_{tan\,k}$	Volume of concentrate tank (L)
$\rho_{NaCl}^{sat}(25^oC)$	NaCl saturated solution density at 25°C (g/L)
ρ_w	Water density at room temperature (g/L)
σ_{cm}	Thickness of the cationic membrane (dm)
σ_{am}	Thickness of the anionic membrane (dm)

Table of contents

Chapter 1

Introduction and objectives

Water stress and water scarcity are critical issues in many regions all over the world. More than 1.100 million of people are currently living without access to potable water, whose availability has diminished by 37% in the last 30 years *(AGUA 2007)*. Still, water demand is expected to increase as a combined result of population rise and the uncontrolled expansion of industrial and agricultural activities *(Meneses et al. 2010)*. If no measures are taken, it is expected that two thirds of the world population will suffer from water stress by 2025 *(WWC 2000)*.

Obtaining new fresh water sources to supply the expected increasing demand has become a hot topic of study nowadays. The major water reservoirs in the earth are the oceans, which stand for the 97% earth's water; therefore, solving the problem of water scarcity by seawater desalination has become a general worldwide trend in the recent years.

Desalination in Spain started in the 60s to supply the water demanded in the Canary Islands. In the 80s, the number of plants grew in all the territory due to the increasing water demand from tourism and agriculture. Nowadays, there are more than 700 desalination plants installed in Spain with a production capacity of more 800 hm^3/day, where almost 47% of them come from seawater *(Meneses et al. 2010)*. Spain has become the European country with highest desalination capacity installed and it is also the fourth country in the world with the highest water production from desalination *(Fritzmann et al. 2007, Palomar et al. 2010)*. One of the European biggest

desalination plants was installed in Barcelona in 2009 within AGUA program. AGUA program was launched by the Spanish Government in order to promote desalination in the Mediterranean basin. Barcelona desalination plant uses reverse osmosis (RO) technology and is able to produce 240.000 m^3/day of fresh water to supply 20% of the city water demand (*Palomar et al. 2010*).

Reverse osmosis (RO) and multi-stage flash (MSF) are the most worldwide used desalination technologies. The decision for a certain technology is influenced by several factors such as feed water salinity, required product quality available area, energy cost, local demand for electricity, etc. *(Moch 2002)* Reverse osmosis (RO) is the currently most used membrane technology for seawater desalination in Europe due to its lower energy consumption compared to other desalting technologies *(Fritzmann et al. 2007).*

Up to 40-50% of the treated seawater in RO process is rejected as high salinity brine with all the chemicals used in the process. The main drawback of this desalting technology is then the disposal of the rejected brine, which is generally drained back into the sea due to economic reasons. Other methods such as dilution with seawater or with other streams have been studied (*Meneses et al. 2010, Mickley et al. 2006*) but are not commonly applied because of their extra cost.

The direct RO brine disposal into the sea generates environmental impacts in the reception point such as diminishing the amount of flora and creating salinity, temperature and alkalinity gradients (*Palomar et al. 2010, Latorre 2004, Gacia et al. 2007, Sanchez-Lizaso et al. 2010, Fernandez Torquemada et al. 2006*). General growth predictions expect an increase of 180% in the desalination capacity of the Mediterranean region *(Fritzmann et al. 2007)* and total capacity is expected to reach 94 million m^3/day in the world by 2015 (*WHO 2007*). Thus, the environmental impact generated by this technology will also increase and new reuses of this by-product will be needed in order not to damage the Mediterranean ecosystems and to assure seawater quality.

Taking this challenge into account, the research project SOSTAQUA was leaded by the water supply company of Barcelona (SGAB) in cooperation with 16 different other companies in order to develop a sustainable water cycle through the use of innovative technologies (*Sostaqua 2011*). The SOSTAQUA project was focused on different activities such as the reuse RO reject, diminish the water consumption, develop new water treatments, reuse other water cycle rejects and optimize the energy consumption in the water treatment processes.

This thesis was developed within the SOSTAQUA project and it is focused on reusing and valorization of the brine rejects produced in the urban water cycle in the chlor-alkali industry. Two different types of brines, both with a high salinity content, were studied: the RO brine of the desalination plant in Barcelona and the reject of the potash mining industry located in El Bages (Barcelona). Although the reject of

the mine brine is not coming from the urban water cycle, it was decided to include it in the project because of its disposal difficulties and the environmental impact that is creating in the Barcelona area.

Both studied brines have high salinity content and are currently discharged into the Mediterranean Sea, generating an environmental impact. Therefore, the reuse of these brines can be promising in terms of reducing the environmental impact generated, giving value to by-products and creating synergies between industries.

The potential reuse was considered to be in the chlor-alkali industry as a feed product because of the high salinity of the brines studied. Chlor-alkali industry uses nearly saturated NaCl brine as a raw material to produce chlorine gas, hydrogen gas and sodium hydroxide. Usually, this raw brine comes as a solid salt such as rock or solar salt, and the feed brine is prepared by dissolving it (*Elliot, 1999*). Nevertheless, other sources have been studied lately as alternative feed brine for the chlor-alkali industry in order to substitute the solid salt (*Turek et al. 1995, Blancke 2006, Blancke 2007*).

In order to reuse the brines studied in this thesis in the chlor-alkali industry, purification and concentration steps should be carried out to reach the composition requirements of the process, as represented in Figure 1.1. Membrane electrolysis is the BAT for the electrolysis process and it is expected that by 2020 it will be the predominant technology for chlorine production worldwide. Membrane electrolysis cell requirements are strict and huge purification steps must be carried out. In this thesis, different purification and concentration technologies are studied for both brines in order to reach the membrane electrolysis process requirements.
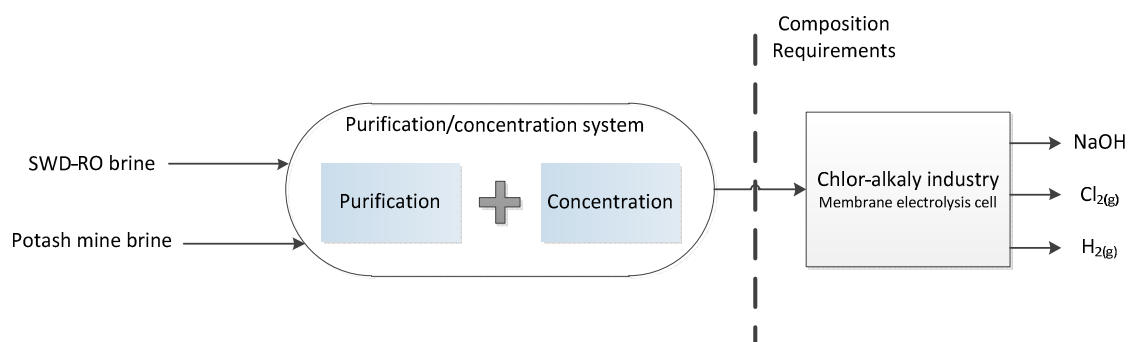
Figure 1.1 Scheme of the proposed reuse of brines in the chlor-alkali industry

1.1. Objectives

The main objective of this thesis is to assess the viability of both SWD-RO brine and potash mine brine reuse in the chlor-alkali industry. A sustainable treatment system is defined to reuse both brines in the electrolysis BAT, which is considered to be membrane cell electrolysis.

According to the general objective, the specific goals of this thesis are:

- To identify potential technologies for brines treatment.
- To characterize the two brines studied and determine the removal and concentration needs to meet the electrolysis requirements.
- To identify the best purification/concentration options for SWD-RO brine and potash mine brines studied, according to their composition.
- To evaluate experimentally at pilot sale the purification and concentration process using ED and NF to determine product quality and process consumptions.
- To optimize the alternative technologies chosen for brine concentration and purification.

1.2. Overview of the thesis

We organize this thesis as it follows:

Chapter 2 briefly describes the chlor-alkali process and usual and emerging brine purification/concentration technologies used in this industry.

Chapter 3 contains a state of the art of the different technologies and experiences carried out to reuse similar brines.

Chapter 4 introduces the brines studied and their chemical composition. Composition of the brines is compared to the electrolysis requirements and thus, purification and concentration needs to reuse these brines are defined.

Chapter 5 describes the experimental studies and validation of concentration assays carried out using electrodialysis in the ED pilot plant of Barcelona. This chapter also describes a mathematical model to predict the NaCl concentration reached in the ED process with SWD-RO brine.

Chapter 6 describes the experimental purification studies on brine nanofiltration technology with the two brines described in Chapter 4.

Chapter 7 presents the experimental studies on brine purification using precipitation with collector brine, SWD-RO brine and concentrated SWD-RO brine by electrodialysis.

Chapter 8 concludes on the results obtained in the different experiences carried out with the brines studied and gives recommendations for future works.

Chapter 2

Brine needs in the chlor-alkali industry

2.1. Chlor-alkali process.

Chlor-alkali industry produces chlorine (Cl_2 $_{(g)}$), hydrogen (H_2 $_{(g)}$) and sodium hydroxide (NaOH) or potassium hydroxide (KOH) by electrolysis of a nearly saturated salt solution. Chlorine is the main objective of the process as is the most valuable product obtained. Produced chlorine is commonly used to produce PVC or other chemical compounds that are widely used; more than 85% of all pharmaceuticals and more than half the products of the chemical industry depend on chlorine chemistry. With every tone of chlorine produced, 1,1 tones of caustic soda are also made. Caustic soda is mainly used in the chemical industry but can also be employed for soap production, water treatment, aluminum production or oil refining. Moreover, per ton of chlorine gas produced, 0,028 tone of hydrogen is generated. This hydrogen can be reused in the same chlor-alkali industry or as feed product in the food industry.

At the beginning of 2011, the European chlorine production reached 802.944 tones. The market for chlorine has reached maturity in Europe and, therefore, the increase in demand is expected to be in other countries with higher economic growth due to PVC production. The world chlorine demand is in constant growth (+ 5%/year) thanks to the PVC increasing demand (*Eurochlor, 2010*).

The main technologies used in the chlor-alkali industry to produce chlorine are mercury, diaphragm and membrane cell electrolysis. The diaphragm cell process and the mercury cell process were both introduced in the late 1800; the membrane cell

process was developed in 1970 (*IPPC, 2001*). Each of these processes represents a different method of keeping the produced chlorine separated from the other products of the electrolysis process (*Martinez, 2003*). The main characteristics of each technology are represented in Table 2.1. In Figure 2.1, the evolution of % of total production capacity of each of these technologies in Europe is represented. As can be seen, the membrane cell is the technology that gained more importance in the last years due to its environmental advantages and lower power consumptions

Table 2.1. Main characteristics of the different electrolysis technologies. (Ochoa, 1996)

	Mercury	*Diaphragm*	*Membrane*
Cell voltage (V)	3.9-4.2	2.9-3.5	3-3.6
Current density (kA/m²)	8-13	0.9-2.6	3-5
Current efficiency %	97	96	98.5
Power consumption (kWh/t NaOH 50%)	3560	3580	2970
Chlorine purity %	99.2	98	99.3
Hydrogen purity %	99.9	99.9	99.9
Purification grade needed	Low	Medium	High
Cell productivity (tons NaOH/year)	5000	1000	100
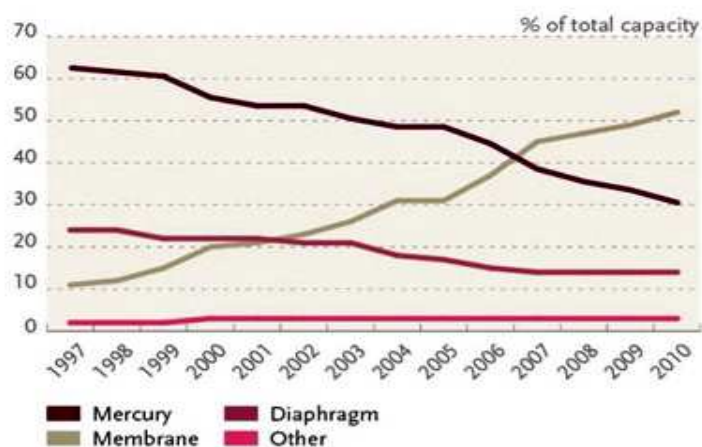
Fig. 2.1. Evolution of % total production capacity of different production routes in Europe (Eurochlor, 2010)

The membrane cell process has ecological advantages, as it does not use mercury or asbestos and is the most energy efficient process. Best Available Technology (BAT) for the production of chlor-alkali is considered to be membrane technology, although non-asbestos diaphragm technology could also be defined as BAT *(IPPC, 2001)*. Thus, according to European Directive 96/61/CE and the OSPAR Decision 90/3, it is expected that changes in technologies to BAT will occur before 2020 to reduce mercury pollution. Nevertheless, the change of technology to membrane cells is being been slow because most existing chlorine plants were installed in the 1970s and no need to redesign the plant has risen until now *(IPPC, 2001)*. Only three

mercury cell rooms were converted to membrane technology during 2009 in Europe, and another one was definitively shut down.

2.1.1. Membrane electrolysis

In membrane electrolysis cell, the anode and cathode are separated by a water-impermeable ion-conducting membrane that allows the pass of sodium and hydroxide ions. Therefore, sodium and hydroxide ions migrate from the anode, where brine is introduced, to the cathode, as is detailed in Figure 2.2. In the cathode, caustic soda and hydrogen are produced according to reaction 2.2. Caustic soda is typically brought to a concentration of 32-35% by continuously recirculating the solution in the cathode.

In the anode compartment, chloride ions are oxidized to chlorine gas according to reaction 2.1. Membrane prevents the migration of chloride ions in the cell; thus, the caustic soda produced does not contain salt and it has high quality compared to other production processes. Depleted brine is discharged from the anode compartment and saturated with salt.

Anode: $\qquad 2Cl^- + 2e^- \rightarrow Cl_{2\,(g)}\uparrow \qquad\qquad$ *(2.1)*

Cathode: $\qquad 2Na^+ + 2H_2O + 2e^- \rightarrow H_{2\,(g)}\uparrow + 2\,Na^+ + 2OH^- \qquad$ *(2.2)*

Global reaction: $\;2Na^+ + 2Cl^- + 2H_2O \rightarrow Cl_{2(g)} + H_{2\,(g)}\uparrow + 2\,Na^+ + 2OH^- \qquad$ *(2.3)*
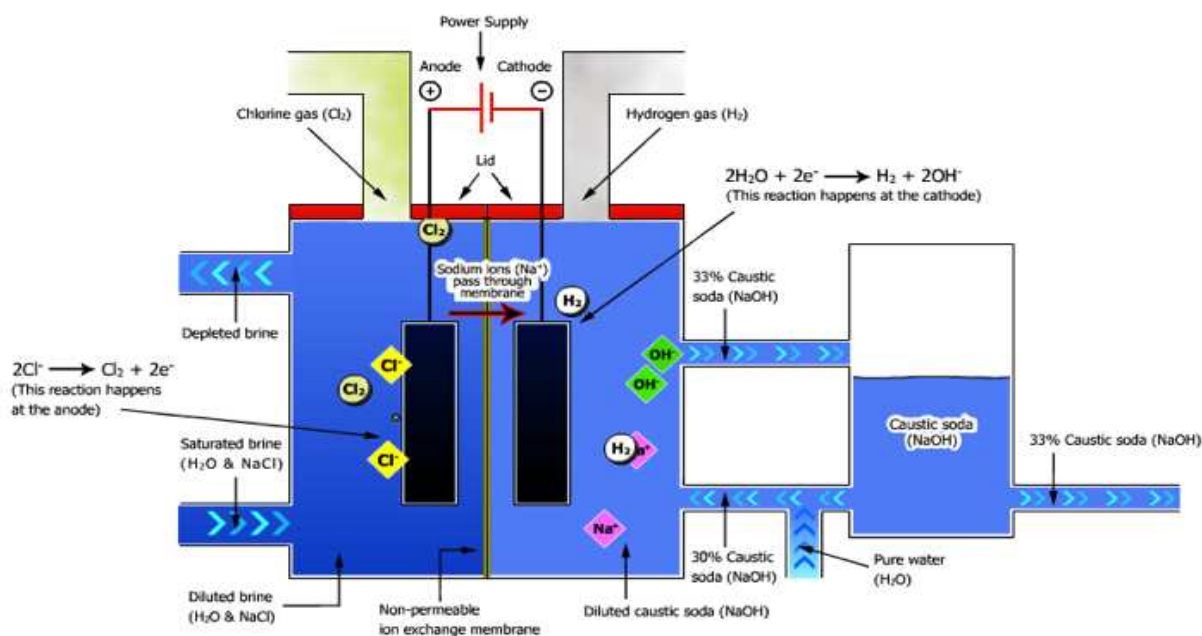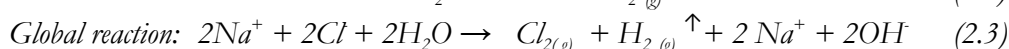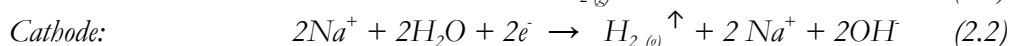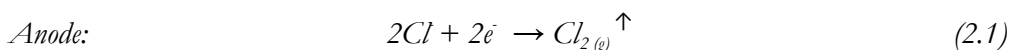
Fig.2.2. Diagram of a membrane electrolysis cell. (Eurochlor,2010)

Cathode material usually used is stainless steel or nickel, whereas the anodes used are metallic. The membranes used in the cell are commonly made of two layers of perfluorinated polymers. The cathodic adjacent layer consists of perfluorinated

polymer with substituted carboxylic groups and the anionic adjacent layer consists of perfluorinated polymer with substituted sulphonic groups. All the membranes used must be chemically resistant to the products obtained. To give the membrane mechanical strength, the membrane is generally reinforced with PTFE fibres *(IPPC, 2001)*. The general economic lifetime of chlor-alkali membranes is approximately three years, but ranges between 2-5 years, depending on the quality of the brine used *(IPPC, 2001)*. It is important to use high quality brine or to exhaustive purify the brine in order to extend the lifetime of the membranes.

2.1.2. Brine treatment in the chlor-alkali industry

The brine purification process for the chlor-alkali industry depends on the technology used. The requirements of the different technologies considered BAT are represented in Table 2.2. In Chapter 4, the requirements of the electrolysis cells are compared to the composition of the brines studied in this thesis. It can be observed from Table 2.2 that the brine needs to be highly concentrated on NaCl and impurities content must be very low.

Table 2.2. Composition requirements of the electrolysis process. Effects and control methods of each element (IPPC, 2001).

	Diaphragm cells	Membrane Cells		Effect	Control Method
		Limit $\leq 4kA/m2$	Limit $\geq 4kA/m2$		
Components					
Cl^-	151.7 g/kg	151.7 g/kg	151.7 g/kg		
Na^+	98.3 g/kg	98.3 g/kg	98.3 g/kg		
NaCl	250 g/kg	250 g/kg	250 g/kg		
Impurities					
Al^{3+}	-	100 ppb	100 ppb	Precipitates	Precipitation
$Fe^{2+.}\ Fe^{3+}$	0.5ppm	1 ppm	1 ppm	Covers the anode	
I^-		1 ppm	200 ppb	Precipitates	Purgue
Ba^{2+}	0.01ppm	< 1 ppm	< 500 ppb	Precipitates	Precipitation or ion exchange
Ca^{2+}	4 ppm	$\sum$ < 30 ppb	$\sum$ < 20 ppb	Reduces the efficiency	Precipitation, ion exchange or nanofiltration
Mg^{2+}	1 ppm				
Ni^{2+}	0.1ppm	0.01ppm	0.01ppm	Reduces the efficiency	Nanofiltration
SiO_2	15 ppm	<10 ppm	< 6ppm	Reduces the efficiency	Precipitation
SO_4^{2-}	5 g/L Na_2SO_4	< 10 g/L Na_2SO_4	<8g/L Na_2SO_4	Reduces the efficiency	Precipitation, Purgue or nanofiltration
Sr^{2+}		< 500 ppb	< 400 ppb	Reduces the efficiency	Ion exchange or nanofiltration

Membrane electrolysis requires exhaustive purifications, as its composition requirements are stricter than the other technologies. Elements that may precipitate on the membrane surface or reduce the efficiency of the process must be removed from the brine. Brine purification when membrane electrolysis is used generally consists of a primary treatment to remove major elements, such as calcium and magnesium, and a secondary treatment to finally soft the brine to ppb levels. Primary treatment usually consists of precipitation with Na_2CO_3 and NaOH whereas secondary treatment is usually carried out with ion exchange resins. The scheme of purification used in the membrane chlor-alkali industry can be found in Figure 2.3. For other technologies, primary treatment alone is usually enough to meet the requirements.

On the other hand, brine also needs to be concentrated close to saturation limit in order to maintain the efficiency of the electrolysis process in all kinds of technologies. This high concentration is usually reached by adding solid salt or by simply evaporating the brine. In the last years, several studies on alternative brine concentration have been carried out using different technologies such as membrane distillation, reverse osmosis or electrodialysis. These experiences are further explained in Chapter 4. Nevertheless, these alternative technologies have never been implemented in the chlor-alkali industry. Electrodialysis has been studied for seawater concentration to be used as feed brine in the chlor-alkali industry (*Blancke 2006, 2007*).
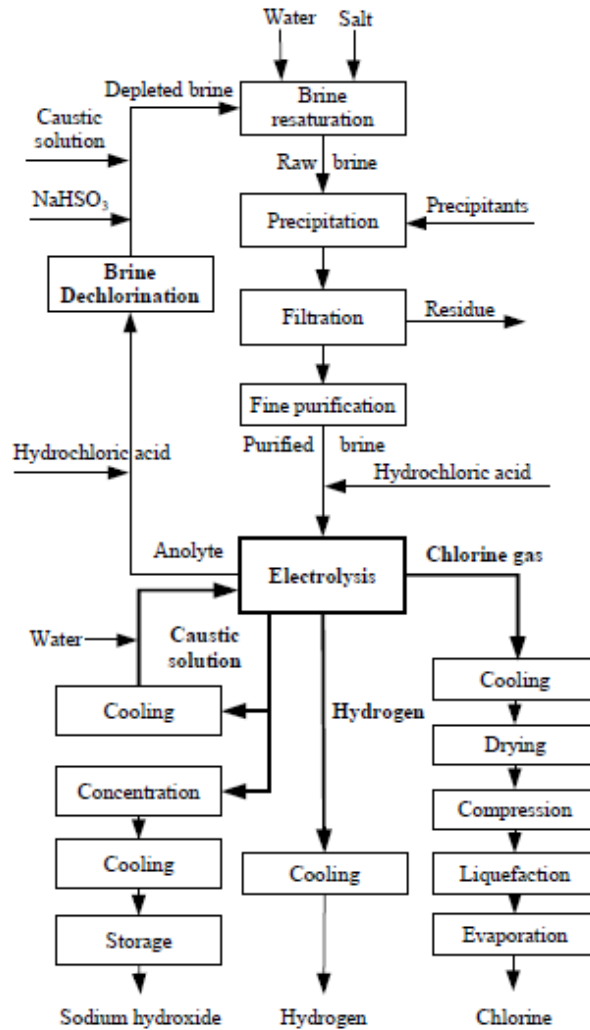
Fig. 2.3. Purification and process scheme of a membrane electrolysis process (IPPC, 2001)

2.1.2.1. Brine concentration by electrodialysis.

Concentration of brine up to saturation limits before electrolysis is necessary to guarantee the efficiency of the process. Usually this saturation is achieved by adding solid salt to the brine or by simply evaporating the brine. Nevertheless, several studies on alternative brine concentrations have been carried out in the last years despite they have not been industrially implemented. From the alternative technologies studied, ED was seen as advantageous technology for this project, as can intrinsically purify the brine with its selective membranes.

Electrodialysis is an electrochemical separation process in which electrically charged membranes and electrical potential difference are used to separate ionic species from aqueous solution.

Desalination of brackish water is the area of major application of electrodialysis, although it is also used to produce ultrapure water, remove salt from cheese whey or soy, concentrate solutions, produce energy through reverse electrodialysis or to produce acid-base solutions. The main characteristic of this technology is the ability to concentrate brines at higher concentration than evaporation with less energy consumption (*Pereira et al, 2006*). Nevertheless, electrodialysis is only considered to be economically advantageous for concentrating brines with less than 100kg/m³ of salts (*Turek et al, 1996*). Otherwise, electrodialysis is not used for concentrating solution to more than 20% of salts because energy consumption quickly increases from this point on because of diffusion phenomena that appear. Another advantage of electrodialysis is that it can be used to purify solutions when selective membranes are used. Selective membranes allow to selectively concentrate monovalent ions from the inlet solution.

Taking this into account, electrodialysis is used in Japan, Kuwait, Taiwan and South Korea to concentrate seawater up to 20% NaCl before evaporation to produce edible salt, as detailed in Figure 2.4 (*Pereira et al, 2006*). In addition, electrodialysis has been studied to produce solid salt from mine brine (*Turek, 2004, Turek et al, 2005a, 2005b*) or to recover salt from seawater and brackish water reverse osmosis brine (*University of South Carolina, 2006, Tanaka et al, 2003, Turek et al, 2002a, 2002b, Korngold et al, 2009*). Electrodialysis is also being studied as a concentration technology for seawater to feed chlor-alkali cells in Solvay (*Blancke 2006, Blancke 2007*).
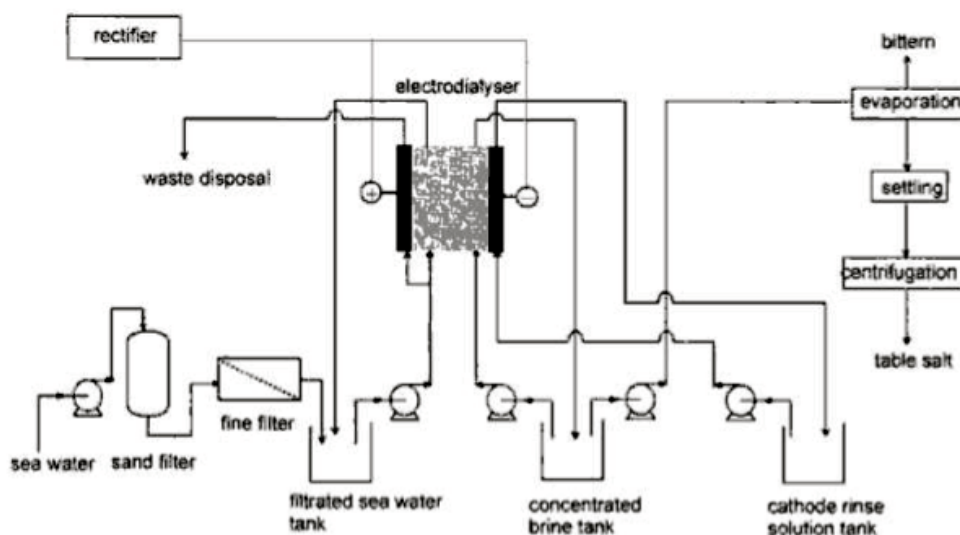
Fig. 2.4. Seawater concentration by ED in Japan (Tanaka, 2007)

Electrodialysis configuration and procedure

Electrodialysis membranes are disposed in a stack that has two electrodes and groups of cell pairs inside, as detailed in Figure 2.5. The number of cell pairs depends on the quality of product desired and the amount and composition of the solution to be

treated. Each cell pair consists of an anion permeable membrane, a cation permeable membrane and two spacers.
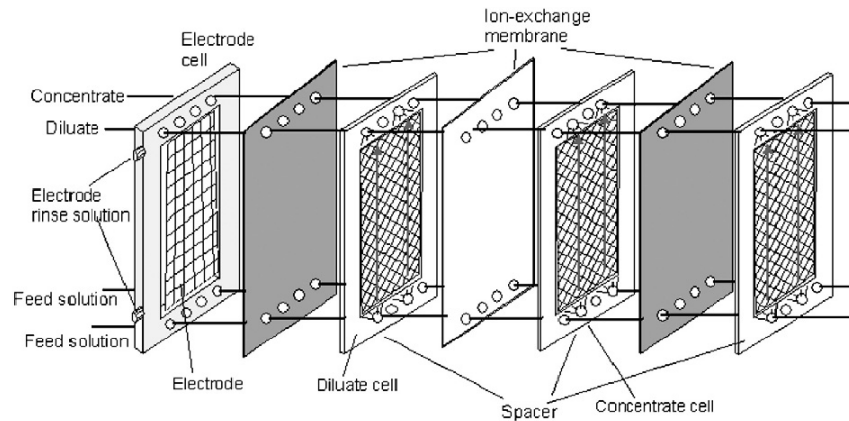
Fig. 2.5.Scheme of stack construction design (Strathmann 2010)

In Figure 2.5, electrodialysis stack is represented. Cation and anion membranes are disposed alternatively inside the stack, with a spacer between them. Two types of compartments are then formed: diluate and concentrate compartments. When electric potential difference is applied, ions migrate inside the stack passing through the selective membranes to a concentrate compartment. Anions can pass only through anionic membranes whereas cations can pass only through cationic membranes. Thus, membranes set up in concentrate compartment will prevent ions from moving further and will concentrate the solution in this compartment. In conclusion, the diluate compartment will be deconcentrated during operation and concentrate compartment will be concentrated. The solution in the cathode will be alkalized whereas in the anode it will be acidified according to the secondary reactions produced in these chambers .
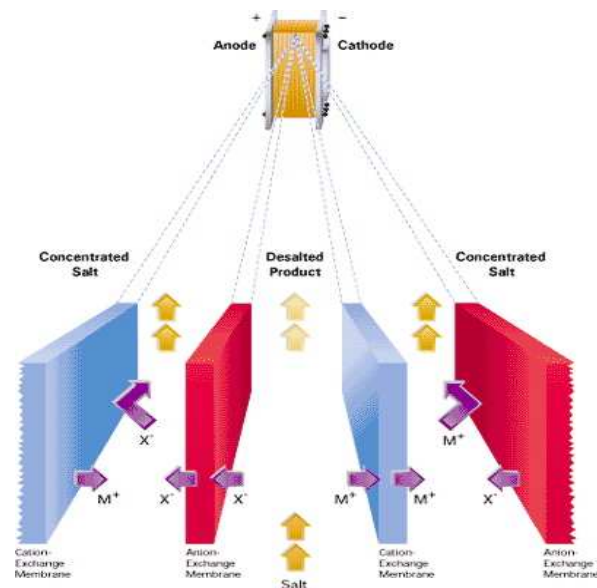
Fig. 2.5. Picture of a stack and operation principle diagram of ED process. (Source: Ameridia, 2011)

When brines with sodium chloride are used in the electrodes of the ED stack, chlorine is formed in the anode compartment and hydrogen in the cathode compartment according to reaction 2.4 and 2.5. Membranes in the electrodes must be chemical resistant and with enough mechanical strength to resist the formation of these byproducts.

$$2Cl^- \rightarrow Cl_{2\,(g)} + 2\,e^- \qquad (2.4)$$
$$2\,H_2O + 2\,e^- \rightarrow H_{2\,(g)} + 2OH^- \qquad (2.5)$$
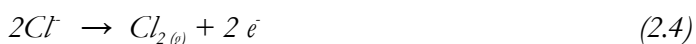
Membranes for electrodialysis are typically made of hydrocarbon films with ion-exchange functional groups. They are usually categorized as homogeneous or heterogeneous, depending on the production process. The heterogeneous membranes are made by grinding ion-exchange resins to a powder that is used to produce a reinforced polymer. The film-forming polymer is usually polyethylene or poly (vinylidene fluoride) (*Pereira et al, 2006*).

Homogeneous membranes have a polymer matrix of styrene crosslinked with divinylbenzene (DVB) and ion-exchange functional groups of sulfonic acid (for cationic membranes) or quaternary amines (for anionic membranes). Typically heterogeneous membranes are thick, opaque and mechanically strong, but they tend to have higher resistance and lower selectivity than homogeneous membranes. (*Pereira et al, 2006*).

Electrodialysis membranes are permselective (or ion selective) and can be tailored to inhibit the passage of polyvalent ions. Different membrane manufacturers can be found in the market offering several applications and membrane characteristics. In Table 2.3, main manufacturers of ion exchange membranes for electrodialysis and their commercialized brand can be found.

Table 2.3. Main manufacturers of electrodialysis membranes and commercial brand. (Valero et al. 2011)

Manufacturer	Country	Commercial brand
Asahi Chemical Industry Co.	Japan	Aciplex
Asahi Glass Col. Ltd.	Japan	Selemion
DuPont Co.	USA	Nafion
FuMA-Tech GmbH	Germany	Fumasep
GE Water & Process	USA	AR, CR...
LanXess Sybron Chemicals	Germany	Ionac
MEGA a.s.	Czech Republic	Ralex
PCA GmbH	Gernany	PC
Tianwei Membrane Co.Ltd.	China	TWAED
Tokuyama Co-Astom	Japan	Neosepta

In electrodialysis, the spacer defines the distance between the membranes and guides the fluid in a certain way inside the stack. The spacer is usually made of nonconducting and hydrophobic materials such as polyethylene, polypropylene, polyvinyl chloride and various elastomers. Conductive spacers have been studied lately to reduce the energy consumption and increase the operable current density (*Strathmann, 2010*). Different membranes profiles have also been studied in order to replace the spacers in future applications. Tortuous path spacers are most commonly used because they maximize the solution retention time inside the stack, both creating turbulence and maximizing the ion pass through the membranes. The usual velocity range inside the stack is comprised between 0.18 to 0.35 m/s, at less velocity polarization phenomena can be observed on the membrane, reducing the ion transport (*Valero et al. 2011*). Higher velocities can generate high pressure drops inside the stack. It is important to maintain the same pressure inside the stack in order not to damage the membranes, which are very sensitive to pressure differences between compartments.

The electrodes used in an electrodialysis stack must withstand the electrochemical reactions and the solutions that circulate in the electrode chambers. Titanium covered by platinum or by dioxide of manganese, ruthenium, iridium or other substances are most commonly used as anode. Stainless steel is commonly used as cathode. (*Pereira et al, 2006*)

One of the main operating parameters of ED is the current density applied, which determines the ion migration in the solution and the concentration obtained. This current density cannot be higher than the limiting current density (LCD) that is the current density where the solution electrolysis takes place (*Blancke, 2006*). Transport of hydroxyl ions can take place inside the stack at current densities higher than LCD and thus, precipitation of $Ca(OH)_{2\ (s)}$ and $Mg(OH)_{2\ (s)}$ can occur inside the stack, reducing the efficiency of the process and lifetime of the membranes. LCD must be determined experimentally for every solution according to the operating conditions of the stack. It is determined by monitoring the resistance of the cell over the intensity applied, LCD is obtained when a quick increase of resistance is registered (*Lee et al, 2006*).

Scaling and fouling are the major problems in ED. Scaling takes place when salts precipitate on the membrane surface whereas fouling is the biofilm formation on the membranes (*Pereira et al, 2006*). These two phenomena create an increase in the internal resistance of the stack and thus, an increase in total energy consumption. In order to avoid them, pretreatment of inlet solutions is commonly used. Electrodialysis reversal (EDR), where polarity of the stack is frequently changed and cleaning in place (CIP) with acid solutions can also be used (*Strathmann, 2010*).

The results obtained using ED depend on different transport phenomena such as migration or ion diffusion in the compartments. These phenomena are further explained in Chapter 5. Moreover, ion interactions and operation conditions of the

stack as well as stack design have to be taken into account to understand ED performance (*Sadrzadeh et al, 2007a*). Nevertheless, depending on the membranes used, different concentration factors (CF) can be reached according to the ions characteristics. Selective membranes are able to concentrate monovalent ions and obtain higher CF factors for NaCl (*Blancke, 2006*). In consequence, this method could be used to intrinsically purify and to concentrate the brine for the chlor-alkali industry; nevertheless, it is still in the study stage using seawater (*Blancke, 2006*).

2.1.2.2. Primary purification: selective precipitation.

The main goal of primary treatment is to remove the elements that will affect the performance of the stack or quality of the products obtained. Primary treatment usually consists of precipitation with sodium carbonate and sodium hydroxide to precipitate $CaCO_{3\,(s)}$ and $Mg(OH)_{2\,(s)}$ according to the reactions 2.6 to 2.9 (*Elliot, 1999*). Metals may also precipitate during this stage. The most important reactions during this treatment are 2.6, 2.7 and 2.9 as solubility of sulphate depends on temperature and NaCl concentration (*Elliot, 1999*). These reactions take place in two separated vessels. After that, the purified brine is filtrated, acidificated and heated up to 50°C to be finally introduced in the electrolysis cell, as is detailed in Figure 2.7.

$$CaSO_4 + Na_2CO_3 \leftrightarrows CaCO_{3\,(s)} + Na_2SO_4 \qquad (2.6)$$

$$MgSO_4 + 2\,NaOH \leftrightarrows Mg(OH)_{2\,(s)} + Na_2SO_4 \qquad (2.7)$$

$$CaCl_2 + Na_2CO_3 \leftrightarrows CaCO_{3\,(s)} + 2\,NaCl \qquad (2.8)$$

$$MgCl_2 + 2\,NaOH \leftrightarrows Mg(OH)_{2\,(s)} + 2\,NaCl \qquad (2.9)$$
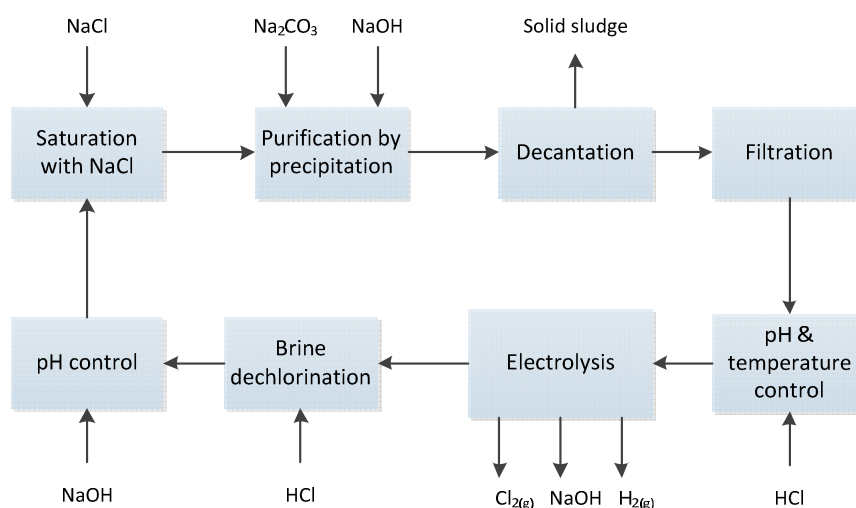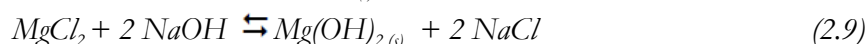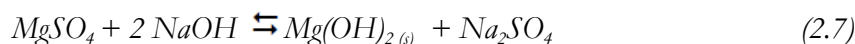
Fig. 2.7. Diagram of the brine loop in the chlor-alkali industry using a primary pretreatment.

Using stoichometric quantities, these purification reactions can take several hours to complete. To speed up the purification process, excess of chemicals and temperatures over 60°C are used in the chlor-alkali industry. These high temperatures are achieved by recirculating the brine in the electrolysis loop circuit, as detailed in

Figure 2.7, or can be reached using solar ponds (*Valderrama et al., 2008*). According to the literature reviewed, the excess of NaOH used should be from 0.1 to 0.5 g/L while Na_2CO_3 should be between 0.3 and 1.5 g/L. Reactant order addition effect can be neglected but it is improved when done in separate vessels (*Elliot, 1999*). As metals hydroxides can form when NaOH is added, it is recommended to add this reactant after carbonate in order to improve the settling time.

Sulphate can be controlled by adding calcium chloride or barium salts to precipitate calcium or barium sulphate respectively ($CaSO_{4(s)}$, $BaSO_{4\ (s)}$). As water soluble barium salts are highly toxic, other treatment processes have been studied. Sulphate can be controlled by bleeding part of the brine from the brine electrolysis loop, thus avoiding its accumulation in the brine. Nanofiltration (NF) has emerged as a membrane technology for sulphate removal, as mainly removes polyvalent ions without reducing the composition of monovalent ions. It has been tested to remove sulphates with high efficiency in the chlor-alkali industry *(Barr 2001)* and it is currently being studied as a primary treatment for calcium and magnesium removal from highly concentrated brines *(Madeni et al, 2007)*.

Solid salts obtained during this purification process through precipitation could be separated and reused as by-products if purity was adequate. Steinhauser (2008) studied the reuse of different products obtained during the Solvay process and concluded on different possible applications; nevertheless, the use of cleaner raw materials was recommended in order to obtain almost pure products.

Precipitation alone is not enough to reduce the levels of calcium and magnesium for the membrane electrolysis cell, so an additional softening is required. For other electrolysis technologies, ppm levels are enough to meet the requirements. Other technologies such as nanofiltration are being studied as primary purification methods for the electrolysis process.

2.1.2.3. Nanofiltration for brine purification

Nanofiltration is important for water softening and removal of organic contaminants. It is also used to selectively separate multivalent ions from monovalent ions or water. (*Yacubowicz et al, 2005*). It has also been studied for sulphate removal in the chlor-alkali industry and it is currently being studied for primary pufication. Recently, nanofiltration as seawater pretreatment for RO process has been studied.

Nanofiltration (NF) is a pressure driven separation process. The filtration process takes place on a selective separation layer formed by a charged membrane. The driving force of the separation process is the pressure difference between the feed and the filtrate (permeate) side at the separation layer of the membrane. Membranes are typically rated by molecular weight cut-off (MWCO) rather than nominal pore size. The MWCO is typically less than 1000 Daltons *(Baker, 2004)*.

Nanofiltration properties range somewhere between ultrafiltration (UF) and reverse osmosis (RO), thus nanofiltration can selectively reject charged ions and uncharged ions with molecular size higher than 1000 Dalton, as represented in Figure 2.8.
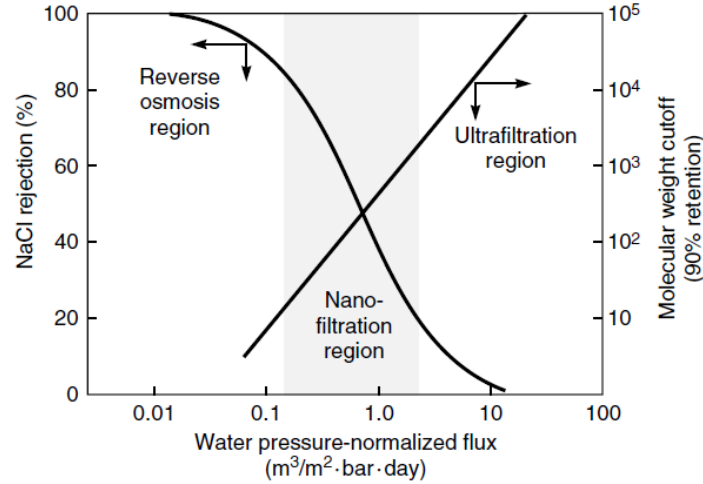
Fig.2.8. Nanofiltration permeability, molecular weight cut-off and rejection compared to other technologies. (Baker, 2004)

Nanofiltration is usually operated at 10-40 bar with spiral wound modules, although other different membrane configuration can be used. Some nanofiltration membranes are based on cellulose acetate but most of them are based on interfacial composite membranes. The preparation procedure used can result in acid or basic groups attached to the polymeric backbone (*Baker, 2004*). As a result, charged membranes are obtained.

Rejection in nanofiltration is calculated using equation 2.10. Water permeability through the membrane is calculated through equation 2.11.

$$R = \left(1 - \frac{C_p}{C_f}\right) \cdot 100 \qquad (2.10)$$

$$PWP = \frac{Q_{permeate}}{A_{membrane} \cdot P} \qquad (2.11)$$

Where C_p is the concentration of the permeate and C_f is the concentration of the feed solution. $Q_{permeate}$ is the permeate flow rate, $A_{membrane}$ is the area of the membrane used and P the pressure applied.

Nanofiltration has been used with highly concentrated brines in order to remove sulphates (*Barr 2001, Twardowski, 1996, Twardowski et al, 1999*) because of its ability to remove polyvalent ions without significantly rejecting monovalent ions. Sulphate

Removal System (SRS) was developed by Kvaerner Chemetics and commercialized for the chlor-alkali industry; this system could achieve 95% sulphate rejection in all cases studied, independently of the NaCl brine concentration. SRS was developed to work with sodium sulphate concentrations up to 120g/L with pressures from 30 to 40 bar (*Barr, 2001*). Rejection in SRS system versus initial sodium sulphate concentration is represented in Figure 2.10. Rejection diminishes when sulphate concentration increases due to both the polarization effect created on the membrane surface and the increase of the effective pore radius.
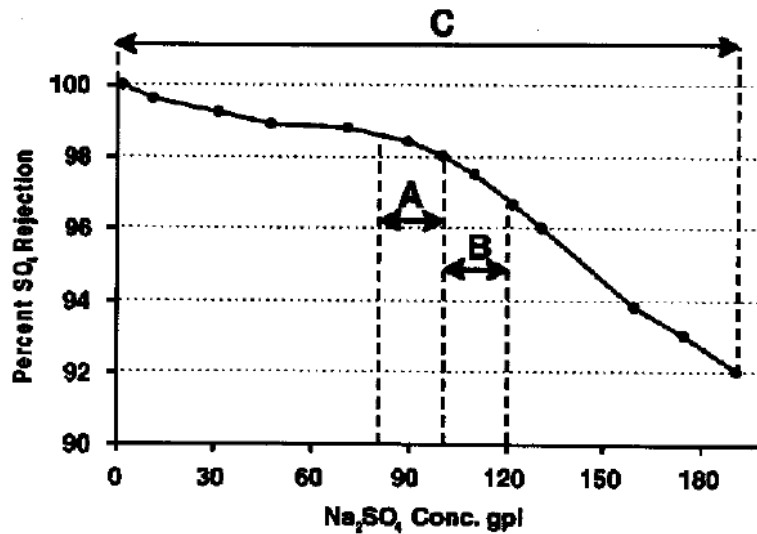
Fig. 2.10. Sulphate removal according to the inlet composition using SRS sytem (Barr, 2001)

Sulphate is highly rejected in SRS system because membranes used are negatively charged and tend to retain the anions in the concentrate. Therefore, sodium or other cations can pass through the membrane creating a positive charge in the permeate. In order to chemically balance the solution, chloride ions (which are smaller than sulphate ions) pass through the membrane according to the Donnan effect (*Krieg et al, 2004*). Thus, permeate can be concentrated in NaCl salt while sulphate is removed.

Recently, selective membranes for sulphate removal or with high permeabilities have been developed for brines (*Hong et al, 2006, Wang et al, 2007, Ahmad et al. 2004*) although they have not been yet commercialized. Nanofiltration for seawater pretreatment in RO process has been studied *(Hassan et al. 2000, Drioli et al. 2002, Eriksson et al. 2005, Abdullatef et al. 2007, Llansana et al. 2007)*. With these systems, scaling in RO process is minimized.

Nanofiltration has also been tested in the laboratory as primary treatment for calcium and magnesium removal from highly concentrated brines in the chlor-alkali industry (*Madeni et al, 2007*). Different commercial membranes, which are detailed in Table 2.4, were used in this study in a flat-sheet module.

Table 2.4. NF membranes tested with saturated brines. (Madeni et al, 2007)

Membrane	Material	Structrure	Thickness (μm)
PVD	Polyethylene terphetelete	Two layers	150
BW30	Polyethylene terphetelete	Two layers	150
TFC-SR	Polyvinyl alcohol	Three layers	150
3700	Polysulfone	Two layers	-
FT30	Polyamide	Two layers	160
NF45	Polyethylene terphetelete	Two layers	150
DOW-PS	Polysulfone	Two layers	150

The goal of the study was to determine the optimal membrane to obtain both high polyvalent ions removal and high permeate fluxes. Results obtained with highly concentrated brine showed that the optimal operation conditions were 40ºC and 8 bar using the PVD membrane. Results at 40ºC and 8 bar are represented in Table 2.5.

When pressure was increased, a maximum of rejection was reached at 8 bar and then it steadily decreased; on the other hand, permeate fluxes increased with pressure. When temperature was increased, mobility of ions was also increased and in consequence, concentration polarization was reduced. Moreover, at higher temperatures higher fluxes could be obtained due to viscosity reduction of the solutions.

Table 2.5. Flux and rejections obtained with the membranes detailed in Table 2.4 for brine purification. (Madeni et al. 2007)

Membrane	Final flux (L/m² h)	Rejection % S (VI)	Rejection % Fe (II)	Rejection % Mg (II)	Rejection % Ca²⁺ (II)	Rejection % NaCl
NF45	10	26	96	37	27	21
BW30	4	19	56	26	23	1
DOW-PS	171	28	35	29	16	1
FT30	3	15	14	30	29	1
TFC-SR	17	16	52	28	18	1
3700	300	15	29	27	17	1
PVD	16	20	60	40	32	1

In all the membranes studied by Madeni et al (2007), rejection was higher for polyvalent ions than monovalent ions, which is a constant for nanofiltration process. Sequence of rejection depends on initial ion concentration and hydrating radius. As highest is the radius and lower the concentration, higher rejections are obtained with one membrane *(Madeni et al, 2007)*.

In conclusion, nanofiltration is a useful technology for polyvalent ion purification. When applied to saturated brine, different operating parameters must be taken into

account in order to optimize the performance of the system, as the high ionic strength of the solution affects the results obtained.

2.1.2.4. Secondary treatment: ion exchange resins.

Ion exchange resins can be used to remove some ions from a diluted solution. In the chlor-alkali industry are mainly used as a secondary treatment to polish the brine for the membrane electrolysis *(IPPC, 2001)*.

Ion Exchange materials are insoluble substances containing ions which are able to be exchanged with other ions in solution. Ion exchangers are insoluble acid or bases which have salts that can be exchanged to other ions, as depicted in Figure 2.11. If they can be exchanged with positive ions, they are known as cationic exchangers whereas if the exchange is done with negative ions, they are known as anionic exchangers.

Ion Exchange resins are usually saturated after some time of operation and their removal efficiency drastically decreases. At that point, chemical treatment is necessary to recover the resin.
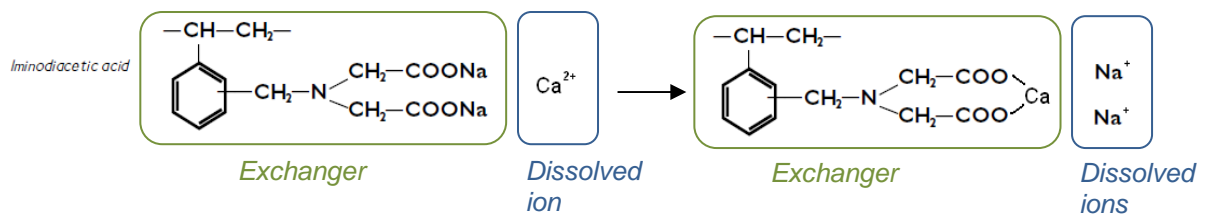
Fig.2.11. Operational method for ion exchange resins. Lewatit TP208 containing methylamino diacetate as functional group

Primary treatment of the membrane electrolysis process is not enough to reach the required composition, so an additional softening is required. Calcium, magnesium and other metallic elements can be finally removed to ppb levels by ion exchange resins.

Secondary treatment generally consists on a filtration step to remove suspended solids from the brine followed by ion exchange step *(IPPC, 2001)*. In the chlor-alkali industry, ion exchange resins must be frequently regenerated and it supposes important economic and operating cost. Different applications and type of resins can be found commercially; in Table 2.6. some resins and its main target can be found.

Table 2.6. Commercial ion exchange resins for brine treatment.

	ROOM & HAAS	LANXESS	DOW	ORICA
Element				
Al (III)	Amberlite IRC747	Lewatit TP208	DOWEX IDA-1	
Fe (II)			DOWEX IDA-1	*
I (-I)	Amberlite IRC747	Lewatit S6328A	DOWEX 1	
F (-I)			DOWEX 21K XLT	
Ba (II)	Amberlite IRC747		DOWEX RSC	
Ca (II)	Amberlite IRC747	Lewatit Monoplus TP208, Lewatit Monoplus TP260, Lewatit TP208, Lewatit TP260,	DOWEX MAC-3	*
Mg (II)	Amberlite IRC747	Lewatit Monoplus TP208, Lewatit Monoplus TP260, Lewatit TP208, Lewatit TP260,	DOWEX MAC-3	*
K (I)				
SiO$_2$	Amberlite IRC747	Lewatit TP208		
B (III)	Amberlite IRA743		DOWEX BSR-1	
Sr (II)	Amberlite IRC747		DOWEX IDA-1	
Ni (II)		Lewatit TP207	DOWEX IDA-1	
Hg (II)	Ambersep GT74	Lewatit Monoplus TP214	DOWEX IDA-1	*

There is one resin with this application.

Ion exchange resins removal efficiency depends on the element to be treated, the kind of resins and the initial concentration and volume of the solution to be treated (*Brown et al, 2000*). Operating and regeneration conditions of the resins are usually fixed by the supplier according to their own experience. Nevertheless, this purification method can only be applied for the removal of ions with low concentration, if not saturation of the resins can rapidly occur increasing the operating costs.

SWD-RO and mine brines reuses

3.1. Brine reuse in the chlor-alkali industry

3.1.1. Mine brine

Mine brine reuse in the chlor-alkali industry was first studied in Poland at the beginning of the 60s. High salinity was observed in Vistula River, which is one of the main water sources of the country, because of the coal mine brine reject disposal and reuse of these brines was then needed to reduce the salinity in the river. Due to the high salinity of the coal mine brines, its reuse in the chlor-alkali industry using mercury and diaphragm cells was studied (*Turek et al, 1995a*). Nevertheless, this reuse was not economically feasible as pretreatment was expensive. Turek *et al.* (*1995a*) proposed different pretreatments for this mine brine in order to study the economical viability reuse in the diaphragm cell. Therefore, pretreatments using precipitation methods were used to recover valuable salts and minimize treatment costs.

Mine brine treated by Turek *et al.* (*1995a*) had high content of calcium, magnesium, ammonium and sulphates. However, its NaCl content was lower than diaphragm cells required, concentration and purification treatment was then necessary for its reuse. Firstly, concentration and purification trials were done adding solid salt to saturate the brine and sodium hydroxide and sodium carbonateto remove calcium and magnesium at 40ºC. Sedimentation rates were very low and this process was considered unuseful for

its industrial application. In consequence, preliminary magnesium removal was studied to improve the sedimentation rate (*Turek et al, 1995b*) and different concentration/purification systems were redesigned, as detailed in Figure 3.1.
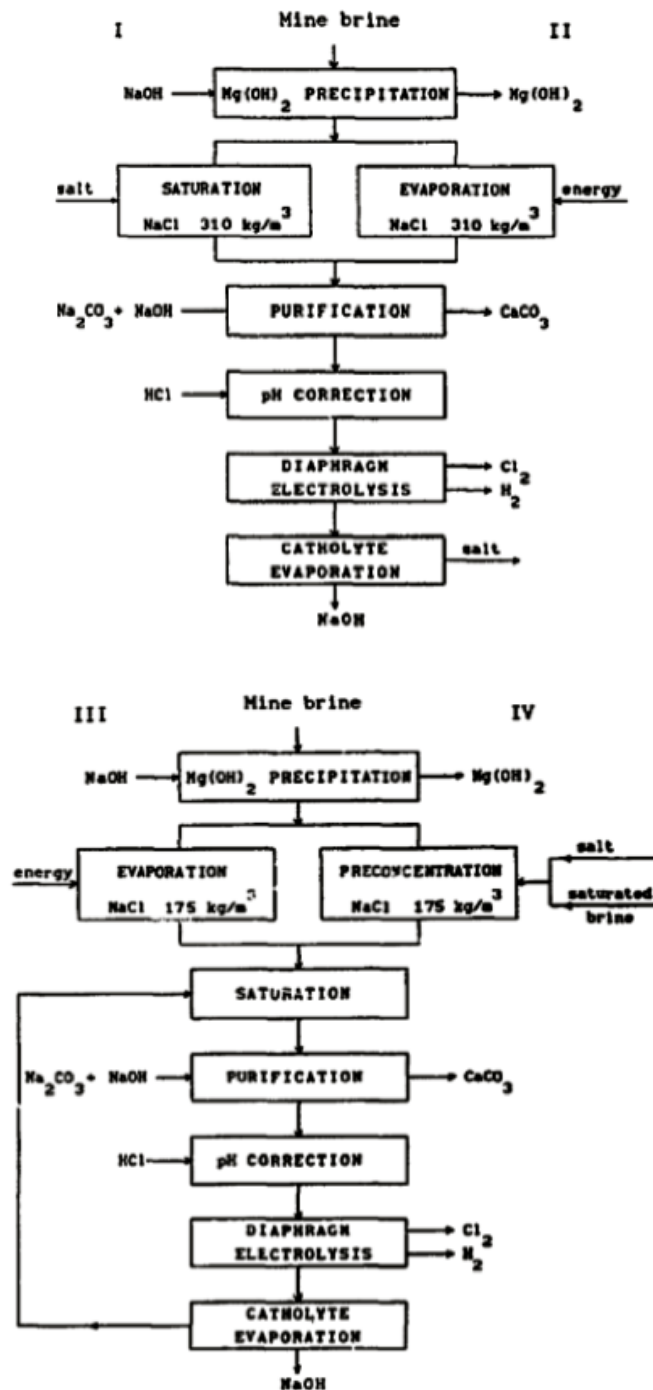
Fig. 3.1. Four options proposed to reuse coal mine brine in the electrolysis process (Turek et al, 1995a)

In option I, brine was saturated with solid salt whereas in option II evaporation was used. In options III and IV brines were concentrated up to approx. 175 g/L using either solid salt addition or evaporation and it was finally saturated with the evaporated catholyte brine outgoing the diaphragm cell. It was determined that option III was the most economical and feasible system to reuse the brine, as consumed less energy and no

external solid salt additions were needed. In consequence, this option was further studied in the laboratory.
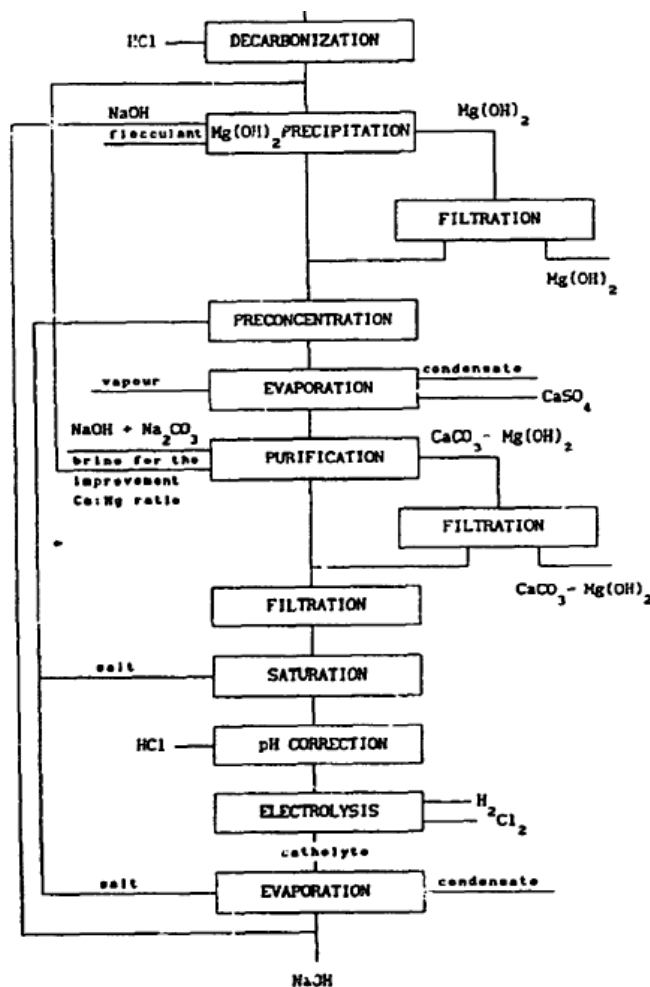
Fig.3.2. Variations on option III to purify the coal mine brine for the electrolysis process (Turek et al, 1995a)

In the laboratory, the option III was improved with more detailed treatment, as can be seen in Figure 3.2. Firstly, decarbonation of brine with HCl and air was carried out, then prepurification of magnesium with NaOH addition was done because the brine had higher content of magnesium than calcium and that difficulted the usual precipitation procedure. Brine was then concentrated up to 315 g/L NaCl using evaporation at 45ºC for 6h; sulphates precipitated during this stage as $CaSO_{4(s)}$. Concentrated brine was treated with sodium carbonate and sodium hydroxide to remove calcium and magnesium remaining in the brine and was finally saturated with the evaporated catholyte brine. pH adjustment was needed to introduce the brine in the electrolysis cell.

Using the proposed treatment, the brine was concentrated up to saturation limits and calcium, sulphate and magnesium were removed up to ppm levels. In addition, valuable salts were obtained and the economically feasibility of reusing the mine brine in the diaphragm cell was demonstrated. Nevertheless, diaphragm cell requirements are less

strict than membrane cell's, and in consequence, more research on brine treatment should be carried out to reuse this kind of brines in the membrane cell of the chlor-alkali industry.

3.1.2. Seawater

Use of seawater as feed brine for the chlor-alkali industry was previously studied by Solvay, the chlor-alkali manufacturer leading this reuse project (*Blancke 2006, 2007*). In order to use seawater in a membrane electrolysis cell, the brine was first ultrafiltrated to remove suspended solids and organic matter and was then concentrated using electrodialysis. Concentrated seawater was saturated with solid salt and purified using precipitation and ion exchange resins. Concentrated brine was also acidified to remove CO_2 before getting into the membrane electrolysis cell, as detailed in Figure 3.3.
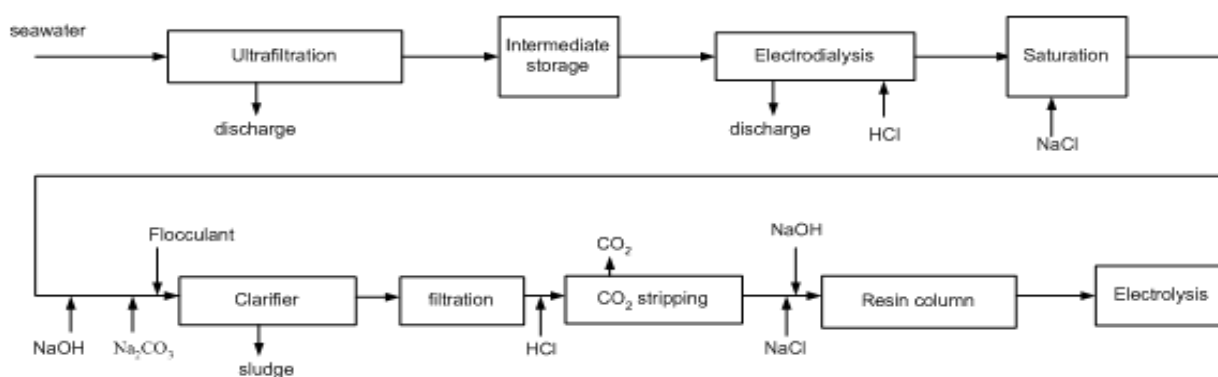
Fig. 3.3. Seawater treatment process for its reuse in the chlor-alkali industry (Blancke, 2007)

Electrodialysis of brine was carried out at CH-O Ashahi micropilot stack with Selemion membranes, described in Table 3.1. LCD was determined with seawater at 0.37 kA/m² (operating conditions: 20ºC and linear velocity of 6cm/s); in consequence, the micropilot was operated at 0.3 kA/m² in order to avoid concentration polarization. A change in operating parameters (seawater temperature, chloride concentration, linear velocity of the feeds, etc.) will change the limiting current density and so, it has to be determined experimentally in every plant.

Using the operation conditions described before, brine concentration of 190 g/L was reached. Power consumption was between 0.12-0.17 kWh /kg NaCl according to the inlet seawater temperature (20-36ºC). This power consumption is in the range of the ones obtained in the solid salt production in Japan by electrodialysis, where 174 g/L are reached at 0.27 kA/m² with power consumption of 0.16 kWh/kg (*Tanaka 2010a*). Nevertheless, technical target for brine concentration by electrodialysis is to obtain a concentration higher than 200 g/L NaCl with energy consumption lower than 0.12 kWh/kg NaCl (*Fujita, 2009*) and so, further research is needed.

Table 3.1. Electrodialysis stack characteristics used for seawater concentration (Blancke, 2006)

Model	CH-0
Membrane Type	Selemion
Dimensions of a membrane	160 mm x 280 mm
Space between membranes	0,75 mm
Effective dimension of a membrane	120 mm x 175 mm
Effective area of a membrane	0.021 m²
Number of membrane pairs	10

Brine composition during all the purification and concentration process is detailed in Table 3.2. It can be seen that ED mainly concentrated monovalent ions.

Table 3.2. Brine composition after different stages for seawater reuse. (Blancke, 2007)

		Seawater UF	Concentrated brine by ED	Purified brine
Components				
Cl (-I)	g/kg	[11-13.3]	[108-124]	149
Na (I)	g/kg	[5.7-8]	[68-70]	96
NaCl	g/kg	[16.7-21.3]	[176-194]	245
Impurities				
Al (III)	mg/kg	< 0.1	< 0.1	< 0,1
Fe (III), Fe (II)	mg/kg	< 0.1	< 0.1	< 0.1
I (-I)	mg/kg	< 0.1	< 0.1	< 0.1
F (-I)	mg/kg	< 5	< 5	< 0.1
Ba (II)	mg/kg	< 0.1	< 0.1	< 0.1
Br (-I)	mg/kg	[29.1-31.3]	[50.0-52.0]	200
Ca (II)	g/kg	[0- 0.80]	[0.55-2.50]	$\sum$ < 20 ppb
Mg (II)	g/kg	[0-1.87]	[1.10-3]	
K (I)	g/kg	[0-1.4]	[2.9-4.8]	4.01
SiO$_2$	mg/kg	[0-1.5]	[0-1.4]	< 0.5
S (VI)	g/kg	[0.2-2.5]	[0-1.3]	0.3
B (III)	mg/kg	[1-3.7]	[1-1.2]	1.66
Sr (II)	mg/kg	[2.2 -4.8]	[18.5-20.2]	0.2
TOC	mg/kg	16	< 1	< 5

The performance of Seawater electrodialysis (SWED) concentration was studied varying different operating parameters (*Blancke 2006*). Diluate concentration and inlet temperature effects on concentration, production flux and power consumption were studied. It was observed that at concentrations lower than approx. 9 g/L of chloride in the diluate cell, the voltage of the stack, and consequently the power consumption, drastically increased. It was also observed that at higher seawater temperatures, lower power consumptions and higher production flows were obtained but less concentration in the brines could be reached. This fact should be taken into account when designing an industrial plant in order to get steady production. Some precipitates of calcium

sulphate were observed after some time of operation due to not regulating the pH in the stack; antiscalants addition or pH control should be done to avoid this problem.

Electrolysis with membrane cell was carried out using the treated seawater brine; no significant difference in the results obtained was observed compared to usual brines. Power consumption and current intensity efficiency were maintained from previous experiments with usual brine. Therefore, the use of seawater in the chlor-alkali industry was demonstrated to be technically feasible but exhaustive pretreatment could be a disadvantage for its high capital and operating costs (*Blancke, 2007*). Moreover, as the brine contained potassium, it was concentrated in the electrodialysis process and final product quality was affected: 4-5 g/kg of potassium hydroxide (32%) could be found in the sodium hydroxide produced. The same occurred with bromide: bromine concentration in the chlorine stream was approximately 600 mg Br_2 /kg Cl_2, which was 10 ten times higher than the bromine obtained using brine from solid salt. In consequence, the purity of the products obtained could be a disadvantage for brine reuse in the chlor-alkali industry. Nevertheless, other uses of the products obtained during the electrolysis that not required high purities could be studied.

3.2 . SWD-RO reject reuses

Possible reuses of RO reject have been fully reviewed by Kim (2011) and Van der Bruggen *et al.* (2003). Usually, these brines are used to produce solid salt and recover water through different concentration/separation technologies such as evaporation, electrodialysis, membrane distillation, solar ponds, selective precipitation or eutectic freezing crystallization, among others. When precipitation is used to recover salts, antiscalants used in the RO process can reduce the precipitating rate of several salts and so, different studies on antiscalant removal to increase precipitation has been carried out recently (*Greenlee et al, 2010a , 2010b , Greenlee et al. 2011, Rahardianto et al 2010*). Zero Liquid Discharge (ZLD) systems combining several concentration/separation technologies are seen as a promising methodology for inland desalination, where disposal of brine is usually problematic and solid by-products can be obtained and further reused. However, these systems are usually expensive and high energy demanding, so are only partially implemented. RO brine has also been treated to obtain acid and bases solutions using bipolar membranes and chlorine with electrolyzers (*Badruzzaman et al, 2009*) or to recover water from RO concentrate by electrodialysis (*Korngold et al, 2009, Turek et al. 2009, Oren et al. 2010, Zhang et al. 2010*).

SWD-RO reject is usually drained back to the sea because it is the cheapest disposal option. Even so, solid salt production and water recovery has been studied as a disposal alternative. Reuse of this brines for talasoteraphy, as cooling fluid or wetlands recovery have also been recently studied, although it has never been implemented (*Canaragua, 2010*). SWD-RO brine has been studied for Na_2CO_3 production through modified Solvay process involving ammonia (*El-Naas et al. 2010*). In this process, CO_2 was captured and used for the production process, standing for both a beneficial reuse of this brine and CO_2 emissions reduction.

In Kuwait, SWD-RO reject is selectively concentrated up to 200 g/L NaCl by electrodialysis and it is further concentrated by evaporation until saturation to recover NaCl to be reused in the chlor-alkali industry (*Pereira et al, 2006*). SWD-RO selective concentration by ED and evaporation has also been studied by other authors to recover NaCl salt (*Hayashi et al, 2000, Tanaka et al, 2003*). Electrodialysis has demonstrated to be an advantageous concentration method for brine concentration up to 200g/L, because it mainly concentrates monovalent ions that can be further recovered as valuable salts. For concentration higher than 200g/L NaCl , ED power consumptions increase and other technologies can be more efficient.

ED and evaporation of SWD-RO combined with selective precipitation and chlorine injection have also been studied by The University of South Carolina (2006) to recover NaCl, $Mg(OH)_2$ and Br_2 , as detailed in Figure 3.4. This system was called Zero Desalination Discharge (ZDD) and was patented in 2009 by Veolia Water. ZDD consisted on selectively concentrating the SWD-RO brine by electrodialysis with monovalent ion selective membranes. The diluate of ED, enriched with polyvalent ions, was treated with NaOH to recover $Mg(OH)_2$ and was further concentrated by evaporation until road salt was obtained. The concentrate of ED was further concentrated by evaporation, obtaining NaCl, and was finally treated with $Cl_{2\,(g)}$ to recover $Br_{2(g)}$.
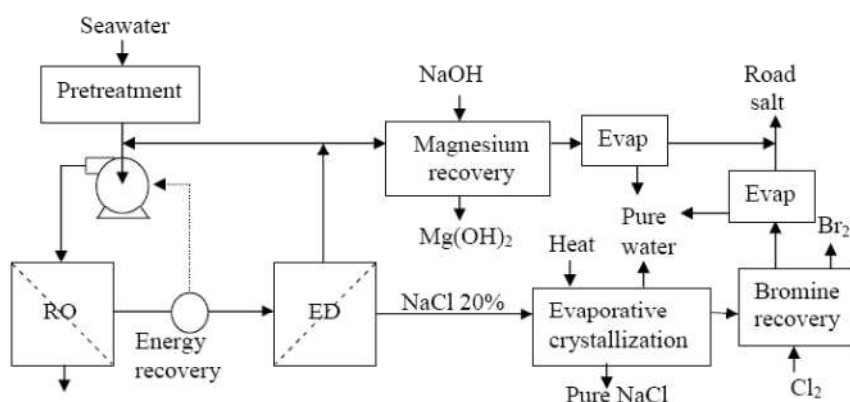
Fig.3.4. ZDD scheme. (University of South Carolina, 2006)

The bromine production was obtained by injecting $Cl_2(g)$ into the brine according to the reaction 3.1, and stripping the product to the air in a system detailed in Figure 3.5. Other systems such as membrane contactors could be used to inject chlorine; they have been tested for chlorine dioxide injection in potable water (*Muttoo et al. 2001*).

$$2Br^- \; + \; Cl_{2\,(g)} \rightarrow Br_{2\,(g)} \; + \; 2Cl^- \qquad\qquad (3.1)$$
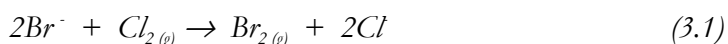
It was necessary to control pH and temperature of the process so $Br_{2(g)}$ could be effectively formed and removed from the brine
.
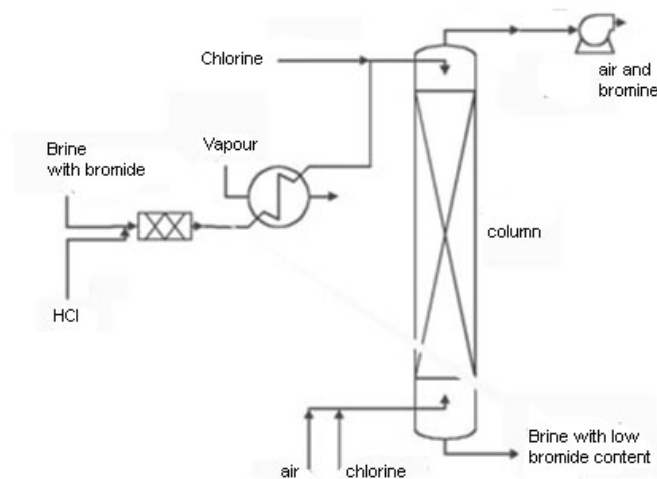
Fig. 3.5. Scheme of a bromide removal system (Pastacaldi 2001)

Aquatec (*2010*) developed a patent to recover NaCl from SWD-RO brines by combination of evaporation, fisico-chemical precipitation with NaOH and Na_2CO_3, ion exchange resins and crystallization. With this process high purity NaCl could be obtained. Nanofiltration was used before SWD-RO in order to remove most of the polyvalent ions present in the brines so, the pretreated SWD-RO reject has low content of impurities compared to the traditional SWD-RO system. Turek (2002 a) and M'nif *et al.* (2007) also used nanofiltration as seawater pretreament for RO system; Turek (2002b) treated rejected brine using distillation and crystallization to obtain reusable salts.

Membrane distillation (MD) has also been studied as concentration method for SWD-RO reject (*Mericq et al, 2010*) and it has also been used combined with crystallization systems to recover salts (*Turek 2002a, Drioli et al. 2002, Ji et al. 2010*). This MD and Mcr system was studied among other different configurations for seawater desalination (*Macedonio et al, 2006*) and was developed in a lab scale obtaining valuable salts, mainly NaCl (*Macedonio et al, 2007*). Macedonio *et al.* (2006) concluded that conversion was increased from 40% to 92,8% combining NF/OI/MCr; on the other hand, energy requirements were risen up to 5 times.

Ohya *et al* (2001) concentrated SWD-RO brine in a ED system combined with evaporators or crystallizations to finally obtain Li, K, Br, B, V, Se or Mo through ion exchange resins. Metal extraction from SWD-RO brine has also been studied by Jeppesen *et al.* (2009) and Le Dirach *et al* (2005) using different chemical extractions such as liquid-liquid extraction, precipitation, lixiviation, hydrolysis or ion exchange resins, depending on the element to be recovered. Gibert *et al.* (2010) studied the recovery of Cs, Rb, Li and U from SWD-RO brines using ion exchange resins. Resins get quickly saturated when high concentrations of ions are used, so they might be very selective to the ion to be removed and they also might be resistant to high ionic strength of the SWD-RO brine.

RO brine is used in Eilat (Israel) mixed with seawater to produce solid salt through solar ponds (*Ravizki et al, 2007*). Usually solar ponds have been used for RO brine disposal in

inland areas, but some applications with SWD-RO or seawater can be found (*Ahmed et al, 2000; Valderrama et al, 2008, Li et al, 2010*). Brines can also be used in solar ponds to recover energy through heat exchangers (*Leblanc et al, 2007*, *Velmurugan et al, 2008*). Salinity gradients are created inside the solar ponds because of the solution heating up. In consequence energy can be stored, provided that the brine is not mixed and temperature is maintained. When a heat exchanger is introduced into a solar pond, energy can be obtained in a regular basis.

For contraposition to the idea of solar ponds, where heat is used to produce salts, RO brine has also been used to recover salts and water by eutectic freeze crystallization *(Reedy et al. 2010, Randall et al. 2011)*. This technology has proven to be effective, as its energetic cost is lower than evaporative crystallization. High purity salts (more than 96%) and water can be obtained. This technology has only been studied in a small scale and it has never been implemented industrially. Moreover, it has only been tested with BWRO reject with contents of salt up to 3.5 g/L NaCl and with synthetic brine of 117 g/L.

The summary of the five applications of SWD-RO brine reuses reviewed in this Chapter can be found in Table 3.3. It can be seen that the general reuse trend is to produce solid salt by different concentration methods.

Table 3.3. Summary of SWD-RO brine reuses reviewed.

Reuse of SWD-RO brine	*Reference*	**Method**
Solid salt production	University of South Carolina, 2006	ED + Evaporation/precipitation
	Hayashi et al, 2000 Tanaka et al, 2003	ED + Evaporation
	Aquatech, 2010	Evaporation + Precipitation+ IEX + Crystallization
	Ohya et al, 2001	Evaporation + Crystallization + IEX
	Ji *et al.* 2010	Membrane Distillation- Crystallization
	Drioli et al, 2002 Macedonio et al, 2007 Turek 2002a	Evaporation + MCr MD + MCr MD + Crystallization
	Macedonio et al, 2006	NF + MCr
	Mericq et al, 2010	MD
	El-Naas *et al.* 2010	Modified Solvay process
	Ravizki et al, 2007	Solar pond
	Reedy *et al.* 2010, Randall *et al.* 2011	Eutectic freeze crystallization
Metal recovery	Gibert *et al.* 2010	IEX
	Jeppesen et al, 2009 Le Dirach 2005	Liquid-Liquid extraction, hydrolysis, lixiviation, IEX.
Thalassotherapy	Canaragua, 2010	Use in spas, health treatments

Reuse of SWD-RO brine	Reference	Method
Wetlands	Canaragua, 2010	Recovery of wetlands
Energy recovery	Valderrama *et al.* 2008	Solar pond
	Canaragua, 2010	Brine as cooling solution

3.3. Mine brine reuse

Mine brines are mainly reused to recover valuable solid salts through different concentration/separation processes. Usually, these brines need an exhaustive pretreatment to remove some elements that will affect the quality of salt produced and so, its reuse becomes expensive.

In Poland, mine brines have been studied to produce NaCl through evaporation. Usually these brines have been concentrated by evaporation until precipitation occurred. Ericsson *et al* (1996) tested OI as a concentration method, followed by evaporation as is detailed in Figure 3.6. With this system, 99.5% pure salt was obtained with an energy consumption of 50kWh/m^3 of inlet brine.
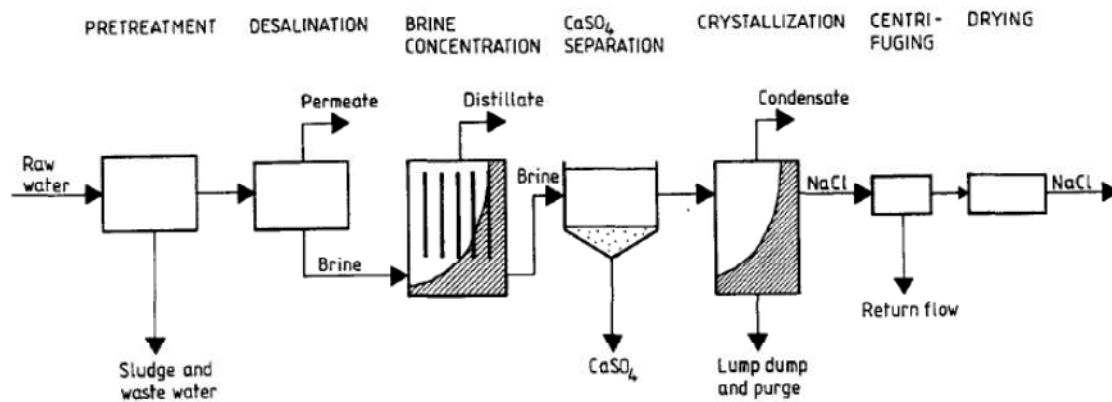
Fig. 3.6. Scheme used by Ericsson et al. (1996) to recover NaCl from mine brine.

In order to reduce the cost of salt production with brines with less than 130 g/L of salt, Turek *et al.* (1996) studied the application of different membrane technologies to concentrate brines. Purification with these membrane technologies was also expected for mine brines in order to obtain higher salt purities. ED and RO were tested for mine brine concentration but further evaporation was needed in both cases to reach the 300 g/L. It was concluded that membranes were useful for brine concentration of brines with less that 100 g/L salts, with higher salt concentration evaporation was economically advantageous unless sulphates were present. In order to avoid sulphate precipitation during concentration, nanofiltration could be used as pretreatment stage.

Turek *et al.* (*Turek 2004, Turek et al, 2005a*) tested different membrane technologies in order to concentrate mine brine with less than 100 g/L of salts, to further evaporate it and recover NaCl. ED was combined with EDR, as depicted in Figure 3.7, to obtain higher concentration brines (up to 290 g/L NaCl) avoiding evaporation step. EDR was useful to remove magnesium and sulphate and so, to obtain higher recovery rates. Magnesium and sulphate could be precipitated from the concentrated EDR reject and further reused.
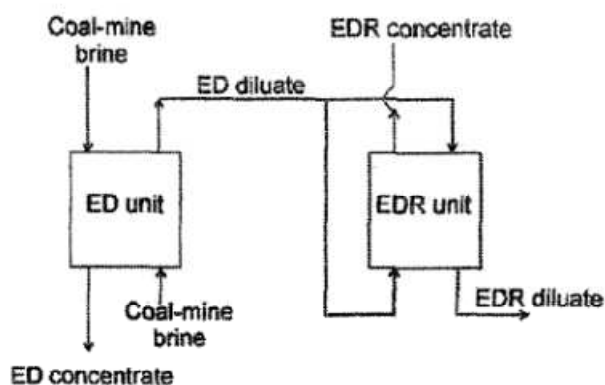
Fig.3.7. ED and EDR coupling for coal mine brine concentration. (Turek et al, 2005a)

Total energy consumption for brine concentration with ED+EDR system was around 0,35 kWh/kg NaCl, This energy consumption was low compared to the energy needed to evaporate this brine (0.73 kWh/kg). Furthermore, the quality of the salt produced was higher than the one obtained by the conventional method that made this reuse extremely encouraging.

Following this study, Turek *et al.* (2005b) proposed the reuse of Wesola mine to produce solid salt. Two different concentrated brines were tested and two different concentration methods were studied: evaporation and ED concentration. Nanofiltration was needed as pretreatment in order to avoid sulphate precipitation in the evaporation step. Same reuse study was carried out for Debiensko coal mines. In this case NF followed by evaporation and crystallization system was studied (*Turek et al. 2008 a*). Different commercial NF membranes were tested, proving their ability to reject polyvalent ions and purify the brines for its next concentration step. With this pretreatment system, the energy requirements were reduced by 0.5 kWh/kg salt compared to the requirements of evaporation alone. Nanofiltration was also studied for sulphate removal from Paradox Valley brine*(Bader, 2008)*, which contained more than 260 g/L NaCl with more than 90% rejection of sulphate with less than 10% rejection of NaCl.

Mine brines have also been studied for energy production through EDR (*Turek et al. 2008b*). Brines are mixed with low salinity waters in a EDR stack and voltage is produced due to the ion migration caused by the gradient of concentrations. Maximum energy obtained depends on current density, flow velocity and membranes resistance.

This technology is still under development and due to its high investment costs; it has not been industrially applied.

In Table 3.4. a summary of the mine brines reuses reviewed can be found. It can be seen that the most used application for this brines is the production of solid salts.

Table 3.4. Summary of the mine brine reuses reviewed

Brine reuse	Reference	Method
Solid salt production	Bader 2008	NF
	Turek *et al*, 1996	ED or Evaporation
	Turek, 2004 Turek *et al*, 2005a	ED-EDR
	Turek *et al*, 2005b	ED/NF+ evaporation + crystallization
	Turek *et al*, 2008a	NF + evaporation + crystallization
	Ericsson *et al*, 1996	OI + evaporation + crystallization
Energy recovery	Turek *et al*, 2008b	Reversal ED

Chemical characterization of potash mine and SWD-RO brines

Chlor-alkali industry usually uses saturated NaCl brine as a raw material to produce chlorine gas, hydrogen gas and sodium hydroxide through electrolysis. Commonly, this raw brine comes as a solid salt such as rock or solar salt, and the feed brine is prepared by dissolving it (*Elliot, 1999*). However, other sources have been studied lately as alternative feed brine for the chlor-alkali industry but have not been implemented due to high economic cost or product quality limitations.

Two different brines are studied in this thesis in order to be reused in the chlor-alkali industry and reduce the environmental impact they produce when are drained: reverse osmosis reject from seawater desalination plants and the rejects of potash mines. Both brines have been characterized in order to study its reuse and define a treatment system.

The rejects from the potash mines located in Cardona, Súria and Sallent (El Bages, Barcelona) are currently drained to the sea through a pipe of more than 80km long that collects all the drainages from different points of the mines, as can be seen in Figure 4.1. This pipe also collects the brine disposal of the chlor-alkali factory of Solvay in Martorell. Other sources of brine coming from different industries or from water treatment plants, as the Abrera drinking Water potabilization plant, could be discharged into a new pipe constructed between 2008-2009. The drainages from the minse can be diluted due to rain effects and so, the composition of the brine in the

collecting pipe can suffer some variations depending on the weather conditions and drains of the industries connected. This fact can be a disadvantage when designing a treatment system because of produced brine quality variability. Contrary, the brine produced on a seawater desalination plants have a constant composition as the recovery ration of the RO process is nearly constant.

The Llobregat brine collector was built up in the 80s, when the concentration of chloride in the Llobregat river drastically increased due to the direct drainage of the potash mines rejects *(Martin-Alonso 2006, Rovira et al. 2006)*. After the building of this brine collector, the levels of NaCl were restored but the environmental problem was moved to the Mediterranean Sea. This pipe currently leads approx. 100L/s of highly concentrated brine.
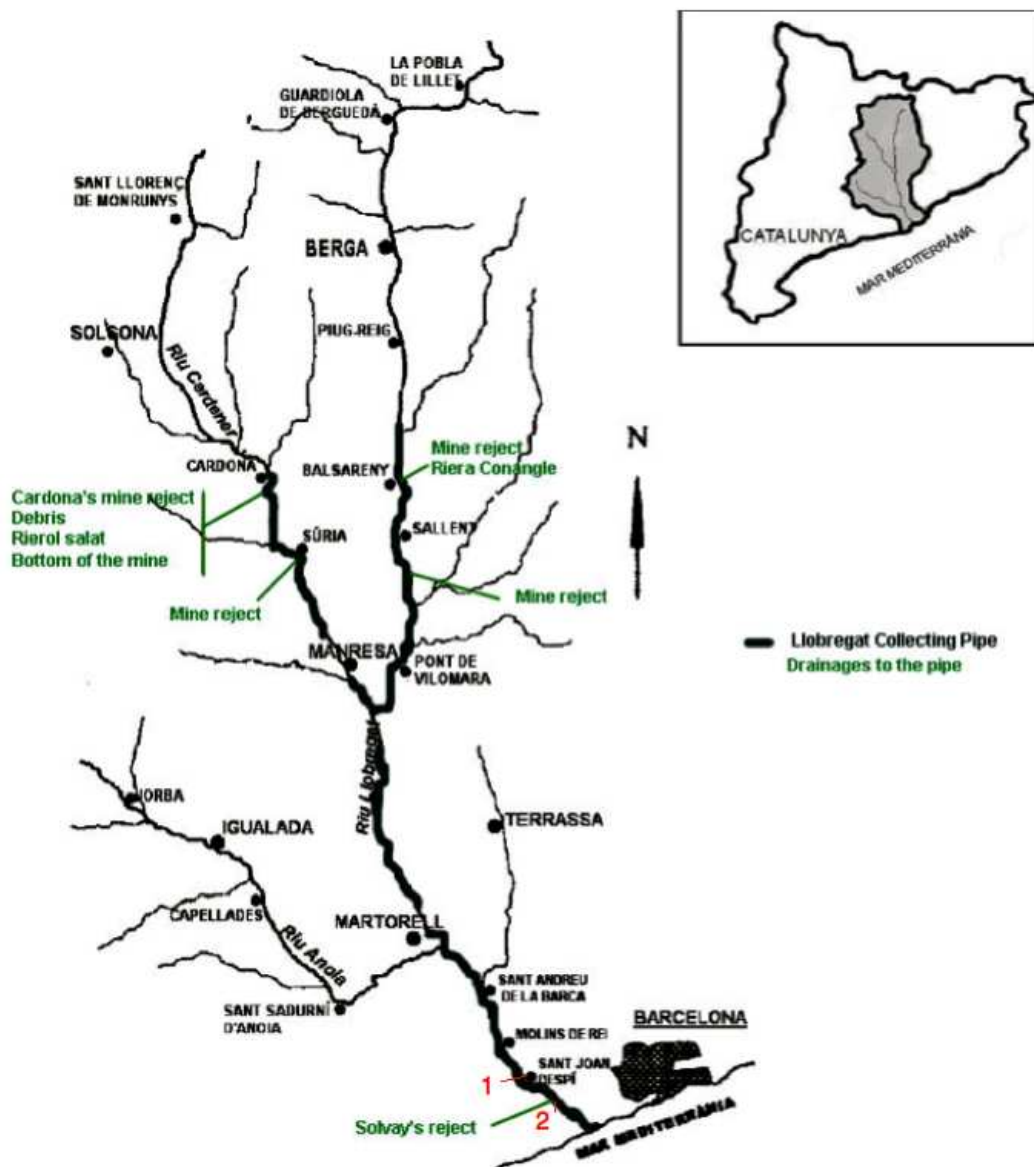
Fig 4.1 Scheme of the brine discharges and route of the Llobregat collecting pipe (Rovira, 2008)

4.1. Experimental methodology.

Samples from different points of the Llobregat brine pipe are being continuously analyzed by the water laboratory of Agbar, however in this thesis, only the brine circulating at the end of the collecting pipe in St. Joan Despí (point 1 in Figure 4.1) (before Solvay's factory reject, point 2 in Figure 4.1.) was considered for its reuse because of its high salinity content and proximity to Solvay's factory. Collector brine samples were taken weekly from this point during one year in order to characterize this brine and to determine the variation of concentration due to seasonal effects or industrial discharges.

The SWD-RO brines compositions were obtained from two different research RO pilot plants located in the Sostaqua Research Desalination Platform in El Prat (Barcelona) (www.sostaqua.com) that were operating according to industrial parameters used in the Barcelona desalination plant. One of them was operating with high recoveries and so, brine composition was higher in all the elements analyzed. Different pretreatments were studied and differenced both brines. Samples during one year were taken and analyzed periodically.

Collector brine was pretreated to remove particulate matter by acidification, heating and filtration. SWD-RO brine samples were analyzed directly after dilution, as no particulate matter could be observed. Chloride from all samples was determined potentiometrically through precipitation with $AgNO_3$ in a METHROM 721 potenciometer with a silver chloride electrode. Sulphate and bromide were determined by ionic chromatography using a 761 Compact IC Methrom equipped with an Anion Dual 2-6.1006.100 column. Trace metals and sodium, potassium, calcium and magnesium were determined by different methodologies, according to their concentration, using ICP-OES Variant 725.

4.2. Brine composition

The general composition of both brines studied in this thesis can be found in Table 4.1. As collector brine presented some variability, maximum, minimum and average compositions obtained during the year analyzed are represented. SWD-RO brine had a constant composition and so only the average is represented. It can be observed that collector brine is more concentrated than SWD-RO brine; nevertheless it has also more impurities than can be a drawback when reusing this brine.

Table 4.1. Composition of the brines studied.

			Collector Brine		SWD-RO Brine	
		Max	**Average**	**Min**	**1**	**2**
Components						
Cl (-I)	g/L	150	120.5	50	48.1	38.8
Na (I)	g/L	71	65	57	23.9	20.8
NaCl	g/L		165			
Impurities						
Al (III)	mg/L	-	0.03	-		<0.5
Fe (II, III)	mg/L	-	39.87	-		< 0.2
Ba (II)	mg/L	-	0.01	-		< 0.2
Br (-I)	mg/L	380	270	140		130
Ca (II)	mg/L	1,200	860	690	962	830
Mg (II)	mg/L	12,000	5,110	520	3,640	2,640
K (I)	mg/L	25,000	17,500	2,500	878	750
Ni (II)	mg/L	-	0.003	-		0.07
Mn (II)	mg/L		0.9			0.01
Cu (II)	mg/L		0.2			0.03
Cr (III)	mg/L		0.01			0.007
SiO_2	mg/L					<1
S (VI)	g/L	6.5	5.48	4.7	6.70	5.41
Sr (II)	mg/L	24	1.20	0		16

The composition of the SWD-RO brine is considered to be more or less steady over the time as the operating parameters are kept constant. SWD-RO Brine 2 had approximately the same composition of the RO brine currently discharged by the Barcelona desalination plant and that was finally used in most of the experiments.

Collector brine presented concentration differences according to the period of the year where the sample was taken. When rainfall increased, lower concentrations could be observed in the brine and the opposite occurred during summer time. Collector brine mainly comes from the brine rejects of the potash mines that are kept constant all over the year; however, approximately 20% of its composition depends on the drainages coming from the mine tailings that are currently drained to the collector. In Table 4.1, the variations in the composition of Na (I), Cl (-I) and Sr (II) over a part of the year analyzed can be found. As can be observed, brine composition is not steady all over the year and so, it can difficult the design of a treatment system to reuse it.
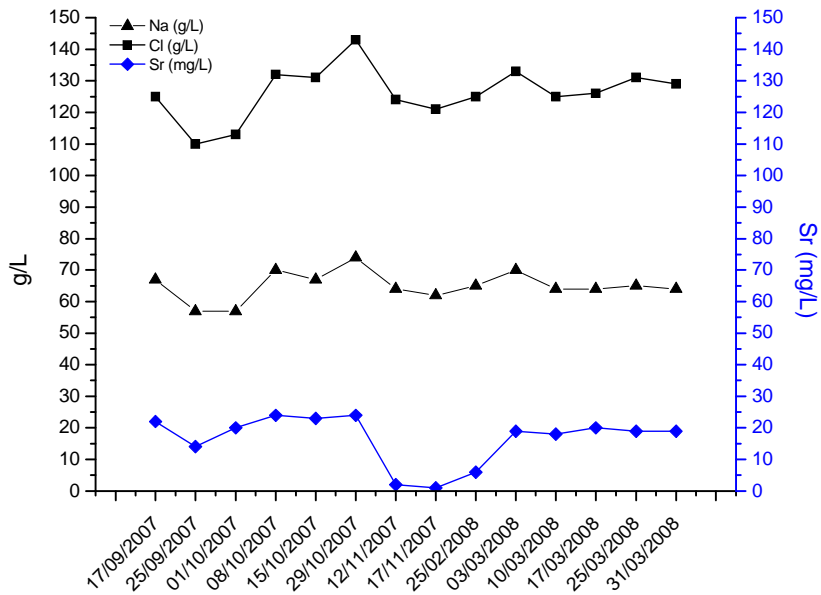
Fig 4.2 Variation of Na (I),Cl (-I) and Sr (II) concencentration on the collector brine during a part of the year analyzed

4.3. Chlor-alkali process requirements.

The brine requirements for the electrolysis process depend on the technology used and the current intensity applied. In the next future, membrane electrolysis cell is expected to be the predominant technology due to its lower environmental impact and energy consumption compared to other available technologies. In addition, a resolution from the Industry Ministery of Spain accorded to replace mercury involving technologies by 2020 and membrane and diaphragm cell are considered the best available technologies (BAT) (*IPPC, 2001*) .A complete description of membrane electrolysis cell and chlor-alkali industry have been described in Chapter 2.

The composition requirements of the chlor-alkali industry using membrane and diaphragm cells are detailed in Table 4.2. As can be seen from the composition requirements, the inlet brine needs to be concentrated up to 300 g/L NaCl in all cases and it has to be highly purified from polyvalent ions in order not to damage the cell or contaminate the final product.

Usually purification of the feed brine in the membrane cells is done in two steps, as the required final compositions are very strict. In the diaphragm cells only the first step is necessary. The first purification step consists of precipitation with sodium carbonate and sodium hydroxide to reduce the amount of calcium and magnesium in the brine and, at the same time, precipitate some metals. In the second step, ion-exchange resins are used to polish the brine from the traces of other elements remaining. This treatment must be modified according to the brine composition inlet.

In Table 4.2, studied brines are compared to the stricter electrolysis composition requirements (membrane cell requirements). It can be noticed that both brines needed a concentration step to meet the NaCl electrolysis requirements of 300 g/L NaCl, proximal to saturation limit. Collector brine has higher NaCl concentration (and so, saturation could be reached by simply adding a small amount of solid salt. This concentration method was considered the most advantageous for this mine brine, as treatment costs would be reduced. Therefore, only purification systems were studied for this brine.

In Table 4.2, impurities to be treated in both brines to meet the electrolysis requirements are highlighted. Several polyvalent ions such as strontium, calcium, magnesium, barium and aluminium have to be removed from both brines. The concentration of all these ions is much higher than the membrane cell's requirement, and an exhaustive purification is needed. Other ions, such as potassium and bromine do not have any composition requirement but they must be controlled to avoid contaminating the final product. Bromide can contaminate the chlorine produced with bromine whereas potassium can add potassium hydroxide to the sodium hydroxide produced. It can be observed from Table 4.2 that the potash mine brine had a high content of potassium.

Table 4.2. Membrane cell composition requirements and collector abd SWD-RO brine compositions.

		Collector Brine	SWD-RO Brine		Membrane cells requirements
		Average	1	2	
Components					
Cl (-I)	g/L	120.5	48.1	41.5	182.0
Na (I)	g/L	65.0	23.9	22.8	117.9
NaCl	g/L	165	61	59	300
Impurities					
Al (III)	mg/L	0.03		**<0.5**	0.1
Fe (II, III)	mg/L	**39.87**		< 0.2	1
Ba (II)	mg/L	0.01		< 0.2	< 0.5
Br (-I)	mg/L	270		130	-
Ca (II)	mg/L	**860**	962	830	-
Mg (II)	mg/L	**5,110**	3,640	2,640	$\sum$ < 20 ppb
K (I)	mg/L	17.500	878	750	-
Ni (II)	mg/L	0.003		**0.07**	0.01
Mn (II)	mg/L	**0.9**		0.01	0.1
Cu (II)	mg/L	0.2		**0.03**	0.03
Cr (III)	mg/L	0.01		0.007	1
SiO$_2$	mg/L			<1	< 6
S (VI)	g/L	5.50	6.70	5.40	<8
Sr (II)	mg/L	**1.20**		**16**	< 0.4

4.4. Conclusions

In order to reuse SWD-RO and the Llobregat collector brines in the chlor-alkali industry using BAT, both brines need a purification step to remove polyvalent ions as well as a concentration step to reach NaCl saturation.

Collector brine presents composition and flowrate variations due to the runoffs that are discharged into the pipe. This could be a disadvantage when designing a treatment system, as steady production and quality could not be assured. In addition, collector brine has high potassium content that will contaminate the final NaOH produced with KOH; this fact will limit its application in the pharmaceutical industry.

Several polyvalent elements such as strontium, nickel, calcium, manganese, cupper, magnesium, barium and aluminium have to be removed. Iron must be specially removed from the collector brine. Both brines need NaCl concentration in order to reach saturation limits, especially SWD-RO brine.

According to the literature reviewed in Chapter 3, electrodialysis was chosen as the best technology for SWD-RO brine concentration because it is able to intrinsically purify the brine with selective membranes. Collector brine has a high NaCl concentration and addition of solid salt was considered the best option to reach saturation. In consequence, concentration of collector brine was not studied in this thesis.

Chapter 5

Selective NaCl concentration of SWD-RO brine by Electrodialysis

Electrodialysis (ED) was evaluated as a selective concentration method for SWD-RO brines. Experimental evaluations were carried out in a ED pilot plant (500L/h), using ion-exchange selective membranes (Neosepta ACS and CIMS) for NaCl concentration.

The fundamentals of ED brine concentration and the state of the art of brine concentration by ED were reviewed in Chapter 2 and 3. In general terms, when electrical potential is applied, different mass transport phenomena take place inside the stack. First of all, the charged species in the solution are transported to the cathode or anode through the ion-exchange membranes. This phenomenon is called ion migration flux. Moreover, due to the current intensity applied, water solvating the ions also migrates through the ion-exchange membranes to produce what is known as electro-osmosis flux or water migration flux. In addition, after a period of operation, when a gradient of concentration appears between the diluate and concentrate compartments, two mass transport phenomena take place: diffusion and osmosis. Diffusion flux is considered the migration of ions from the concentrate compartment to the diluate compartment, which is also known as back diffusion. Water is also transported from the diluate compartment to the concentrate to produce what is known as osmosis flux.

As a result, the maximum concentration achieved is determined by the combination of these four principal mass transport phenomena taking place inside the stack. However, parameters such as temperature and brine concentration or current density used will also determine the performance of the pilot plant and should be taken into account.

Ion transport velocity is mainly limited by the diffusion phenomena through the membranes. Thus, usually there is an increase in the number of ions on the surface of the membranes during electrodialysis. This phenomenon is known as concentration polarization. The magnitude of concentration polarization taking place on the membrane surface depends on different parameters such as current density, feed stream velocity, cell design and membrane properties (*Lee et al., 2006*).

When the ion concentration in the bulk solution approaches zero, the current density approaches the maximum value in the process, which is defined as the limiting current density (LCD). Electrolysis of the brine occurs at the LCD level, thus increasing the pH and drastically increasing the solution's electrical resistance. Consequently, precipitation of $Mg(OH)_{2(s)}$ and $Ca(OH)_{2\,(s)}$ could take place and process efficiency is reduced (*Baker, 2004*). In general, electrodialysis uses less current when it is operated above the LCD level (*Lee et al. 2006*). The LCD is therefore an important parameter to determine before starting operation.

Parameters such as inlet temperature and concentration can affect the performance of the process in some extend. When higher inlet temperatures are used, lower concentrations can be reached due to changes in brine density and, in consequence, an increment of water migration flux can be observed. Nevertheless, slightly low energy consumptions can be obtained at higher temperatures, due to the voltage reduction in the stack (*Blancke, 2007*). At temperatures lower than 25ºC, higher concentrations can be reached but higher energy consumptions are obtained. This fact should be taken into account when operating continuously, as day-night effect could affect the quality and quantity of the product obtained.

Inlet concentration also determines the maximum concentration reached in the tank. Inlet concentration determines the maximum current density that can be used without producing the electrolysis of water, and then, the maximum concentration reached. When inlet concentration is high, higher current densities can be used and lower voltages can be obtained in the stack (*Blancke, 2007*). The final composition is also determined by the configuration of the pilot plant. That fact can be an advantage when using SWD-RO brine, as lower energy consumptions could be obtained due to its high concentration. When using seawater, some organic algae contamination could be found on the membrane surface (*Tanaka, 2010a)* and should be also taken into account when using SWD-RO brine. In addition, pH is necessary to be controlled to avoid some precipitations in the stack, and so, to reduce the effective membrane surface and efficiency of the process.

Finally, in this thesis ED is evaluated for SWD-RO brine selective NaCl concentration. Experiments using different current densities and inlet temperatures were evaluated to optimize the concentration process and determine its technical viability. Selectivity and energy consumption of the concentration process is also evaluated. A mathematical model to predict the performance of the plant and design future experiments was carried out.

5.1. Materials and methods.

5.1.1. SWD-RO brines and ion-exchange membranes used

The ED pilot plant could be fed with two different SWD-RO brines detailed in Chapter 4. The membranes used in the stack to selectively concentrate NaCl were anionic Neosepta ACS and cationic Neosepta CIMS. Characteristics of these membranes are detailed in Table 5.1. In the electrodes, Neosepta CMB and AHA were used as present high mechanical strength to resist the gas formation in these chambers.

Table 5.1. Main characteristics of the membranes used in the pilot plant

	ACS	CIMS
Type	Strongly basic anion permeable	Strongly acidic cation permeable
Characteristics	Mono-anion permselective (Cl- form)	Monocation permselective (Na-form)
Electric resistance* (ohm-cm$_2$)	3.8	1.8
Burst strength** (MPa)	0.15	0.10
Thickness (mm)	0.18	0.15
Usual application	Purification of pharmaceutical products, nitrate removal from groundwater, desalination of aminoacid, vinegar and soy-sauce	Deacidification of metal solutions

* Equilibrated with 0.5N NaCl solution at 25ºC
** Measured by a Mullen Burst Strenght Device

5.1.2. ED pilot plant description and operation

Due to the unlimited acces to SWD-RO brines, the ED pilot plant was designed using one single pass for the diluate and electrode streams. With this design, the operating process was simplified and so, the pilot plant was able to operate at higher current densities and to obtain higher NaCl concentrations.

The ED pilot plant was fed with SWD-RO brines coming from El Prat desalination plants. The ED pilot plant structure is shown in Figure 5.1. The ED stack used was a EURODIA AQUALIZER SV-10 with 50 cell pairs made up of Neosepta cation-exchange membranes (CIMS) and anion-exchange membranes (ACS) (1000 cm^2

active surface area per membrane). The membranes used in the electrolyte chambers were Neosepta CMB and AHA, which had high mechanical strength to resist the gas formation.

The brine flow rate through the ED stack was 500 L/h in the concentrate and diluate compartments and 150 L/h in the electrolyte chambers. Because the ED plant had unlimited access to the feed brines the circuits of diluate and electrolytes had a single-pass design, as shown in Figure 5.1. This made it possible to operate at higher current densities so problems such as temperature increases in the cell and the precipitation of calcium sulphate in the diluate compartments were minimized. The concentrate flow was recirculated until the maximum concentration was reached. The hydrogen gas that formed in the catholyte chamber during operation was removed by means of ventilation, whereas the chlorine gas that formed in the anolyte chamber was treated through neutralization with sodium bisulphite. Reuse of this chlorine produced was also studied for water potabilization in a lab scale, but this study was not included in this thesis. The main characteristics of the pilot plant and stack used can be found in Table 5.2.
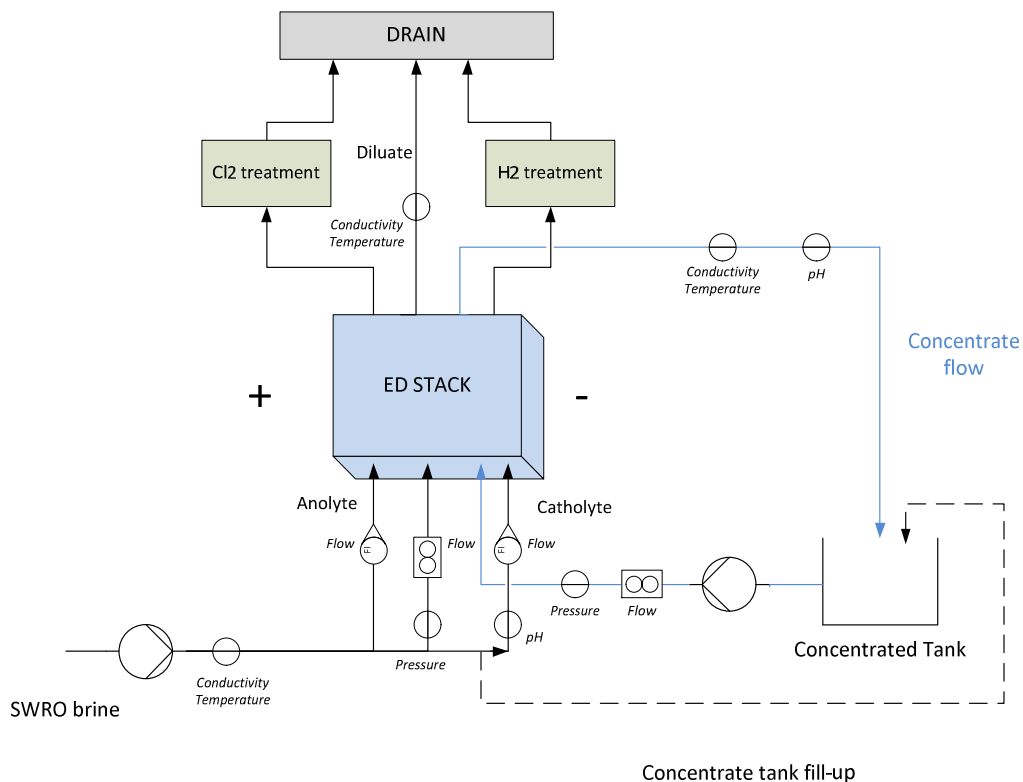
Figure 5.1. Diagram of the main components of the ED pilot plant and parameters monitorized.

Table 5.2. Main characteristics of the ED pilot plant in El Prat (Barcelona).

Feed flow rate	500 L/h
Electrode flow rate	150 L/h each
Concentrate flow rate	500 L/h
Tank volume	1000 L - 250 L – 100 L
Stack	SV10-50 Eurodia Aqualizer(c)
Membranes	Neosepta ACS, CIMS
Effective membrane area	1000 cm² each
Number of cells	50
Power consumption	400V at 50 Hz Total: 2.5 kW
Dimensions	620 x 450 x 313 mm

Figure 5.2. Picture of the ED pilot plant located at the El Prat Seawater Desalination Plant.

The volume of the feed (SWD-RO brine) container was 1000 L and that of the concentrate product container was 1000 L, 250 L or 100 L depending on the experiment. For all cases, the overflow of the concentrate tank was measured when the maximum concentration of NaCl was reached.

Hydrochloric acid was added at different points to keep the pH of all the streams between pH 3 and 5.5 depending on the characteristics of the circuit. The pH was maintained at around 7 in the diluate, 5.5 in the concentrate streams and at around 3 in the cathodic stream to avoid precipitations. Different current densities were evaluated in the range of 0.30 to 0.60 kA/m². Inlet and outlet temperatures were monitored during all the experiments carried out.

The concentration process was monitored by in line measurements of conductivity, temperature, pH, flow-rate, pressure, current intensity and voltage. Sensors positions are indicated in Figure 5.1. Values of these sensors were used for the automatization of the plant and, in some cases, were used as alarm values to stop plant operation.

The maximum operating current intensity using SWD-RO brine was established at the ED pilot plant by monitoring voltage and current intensity to determine the increase in resistance. The operating conditions were an inlet feed stream of 500 L/h at 12.8ºC when the SWD-RO Brine 2, detailed in Chapter 4, was used.
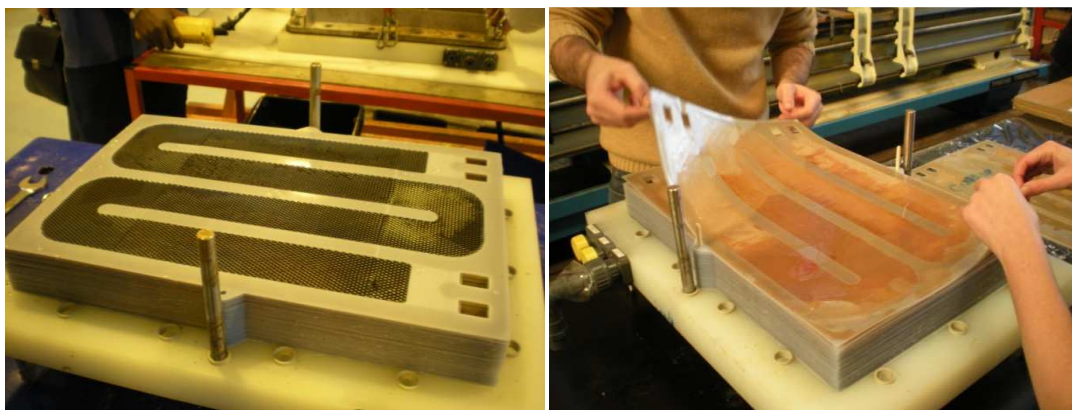
Figure 5.3. Picture of the spacers and membranes used.

5.1.3 Analytical methodologies and chemical analysis.

Samples were taken from the concentrate tank, the inlet brine, and the diluate and concentrate streams leaving the stack every 2 hours. The sodium chloride, sulphate, calcium and magnesium levels in the samples were analyzed using different analytical methods. Chloride was determined potentiometrically through precipitation with $AgNO_3$ at a METHROM 721 potenciometer using a silver chloride electrode as end-point indicator. Calcium and magnesium were determined by Atomic Absorption Spectrophotometry using Analyst 300 Perkin Elmer. Sulphate was determined by ionic chromatography using a 761 Compact IC Methrom equipped with an Anion Dual 2-6.1006.100 column. Trace metals like aluminium, copper, iron, nickel and strontium were determined using ICP-OES Variant 725. Potassium was determined also with ICP-OES. Detection limits determined were: 0.0225 mg/L of aluminium, 0.007 mg/L of copper, 0.0011 mg/L of potassium, 0.0150 mg/L of nickel, 0.0075 mg/L of strontium and 0.0011 mg/L of potassium.

Finally, sodium chloride was determined by charge balance of the major ions of the solution. Conductivity and temperature of diluate and concentrate streams were monitored during operation to ensure the concentration process was successful.

Along the ED experiments, the membrane stack was open for membrane maintenance. Membrane surfaces, especially those close to both electrodes, were examined by SEM-EDS using a JEOL 3400® Scanning Electron Microscopy with Energy Dispersive System.

5.1.4. Data analysis. Determination of concentration factors (CF), membrane ions selectivity (S^A_B), current efficiency (η) and electrical consumption (EC).

Concentration factors (CF) were calculated according to equation 5.1 to determine the process performance.

$$CF_A = \frac{C_A(t)}{C_{A,0}}$$

(5.1)

Where $C_A(t)$ is the concentration of ion A at time t and $C_{A,0}$ is the initial concentration of ion A in the solution. Membrane selectivity (S^A_B) was calculated by the method described by Van der Bruggen (2004) and represented as:

$$S^A_B = \frac{CF_A - CF_B}{(1 - CF_A) + (1 - CF_B)}$$

(5.2)

If ion A is transported slower than B, the S^A_B value will be positive; S^A_B will be negative the other way round, when B would be transported slower.

Current efficiency of ion A (η) was calculated through the results obtained in the diluate stream in a continuous mode. To determine the current efficiency, equation 5.3 was used.

$$\eta_A = \frac{z \cdot F \cdot Q_d \cdot (C_{A,f} - C_{A,o})}{n \cdot I} \cdot 100 (\%)$$

(5.3)

Where z is the charge number of ion A, F is the Faraday constant, I is the applied current, Q_d is the diluate flow rate through the stack, $C_{A,f}$ and $C_{A,o}$ is the diluate and feed concentration respectively and n is the number of cell pairs in the ED stack.

Electrical consumption (EC) was calculated in two different ways, depending on the operating procedure. On one hand, electrical consumption regarding the energy necessary to increase the NaCl concentration in the tank was calculated according to equation 5.4. This consumption is related to a batch process, where only the concentrate tank volume is used. On the other hand, electrical consumption based on the concentrate tank overflow obtained was calculated when the maximum NaCl was reached. At that point, the overflow and NaCl composition of the concentrate tank were measured and stack potential and current intensity were monitored. This consumption was related to a continuous process, where the overflow was considered to be the product. It was calculated using equation 5.5, where cell consumption is divided by the amount of salt overflowing from the concentrate tank.

$$EC_{batch} = \frac{Mean\ membrane\ stack\ potential\ (V) \cdot I(A) \cdot operated\ hours\ (h)}{V_{tank}\ (L) \cdot C_{NaCl}(\frac{g}{L})}$$

(5.4)

$$EC_{continuous} = \frac{Membrane\ stack\ potential\ (V) \cdot I(A)}{Production\ overflow\ (\frac{g\ NaCl}{h})}$$

(5.5)

5.2. Evaluation of brine concentration capacity of ED

5.2.1. Brines saturation thresholds.

The average compositions of the main components of the SWD-RO brines are shown in Table 4.2. of Chapter 4. As brines are concentrated along the ED process, an evaluation of the potential precipitation of brines components was estimated. The saturation index of minerals whose precipitation could limit the concentration step was calculated with the PHREEQC code (*Parkhurst, 1995*) using the PITZER equilibrium data based. Saturation index of inlet brines and the evolution as a function of the concentration phenomena occurring on the concentrate circuit are collected in Table 5.3.

Table 5.3. Variation of Saturation Indexes as a function of concentration factors of the brine when calculated using PhreeqC with Pitzer database at pH 7.

	Concentration factor (CF) for univalent ions (CF/2 for polyvalent ions)				
	Initial	**2**	**3**	**4**	**5**
NaCl	-1.89	-1.08	-0.63	-0.12	0.42
KCl	-2.95	-2.30	-1.83	-1.42	-1.02
$MgCl_2 \cdot 6H_2O$	-6.36	-5.53	-4.66	-3.84	-3.03
$CaSO_4 \cdot 2H_2O$	-0.27	-0.31	0.12	0.58	1.11
$SrSO_4$	-0.27	-0.30	0.16	0.69	1.34
$CaCO_3$	0.59	1.09	1.64	2.04	2.24
$MgCO_3$	0.80	1.34	1.96	2.43	2.72
$CaMg(CO_3)_2$	2.24	3.27	4.44	5.32	5.80

Initial inlet brines were oversaturated with calcium carbonate, magnesium carbonate and calcium magnesium carbonate, as shown in Table 5.3 (initial concentration). Additionally, the evolution of the saturation index for NaCl, KCl, , $MgCl_2 \cdot 6H_2O$, $CaSO_4 \cdot 2H_2O$, $SrSO_4$, $CaCO_3$, $MgCO_3$ and $CaMg(CO_3)_2$ as a function of the concentration process indicates that the brine could be concentrated up to 4 times (approximately 280 g/L NaCl) without NaCl precipitation risk. Because the brines contained the antiscalants from the RO process, precipitation of carbonate and sulphate salts did not take place easily despite their oversaturation, thus benefiting the ED process. The antiscalants used in the RO process were mainly super-threshold agents that were able to stabilize supersaturated salt solutions preventing precipitation of carbonate and sulphate salts mainly. Antiscaling dosing provided from the RO operation protocols indicated the use 1-2.5 mg/L of Permatreat 191. Moreover, HCl was added in different points of the concentrate in order to maintain it at 5.5 and ensure that most of the inorganic carbon was present as bicarbonate, which will not cause scaling. This anti-scaling decarbonation has been fully described by Zhang *et al.* (2010). In consequence, 280g/L NaCl was considered the value threshold for this study.

5.2.2. Determination of limiting current density (LCD)

The maximum operating current intensity using SWD-RO brine was established at the ED pilot plant by monitoring voltage and current intensity to determine the increase in resistance under given experimental conditions previously detailed. The results on variation of resistance of the solution (R) versus current density (I_d) are shown in Figure 5.4. Comparison of values with the results obtained by Blancke (2006) using seawater in a CH-0 Ashahi micropilot cell with Selemion membranes and with the data obtained by Fidaleo *et al.* (2011) using 1.2 M NaCl in EUR2 cell with Neosepta CMX and AMX membranes is also represented in Figure 5.4.
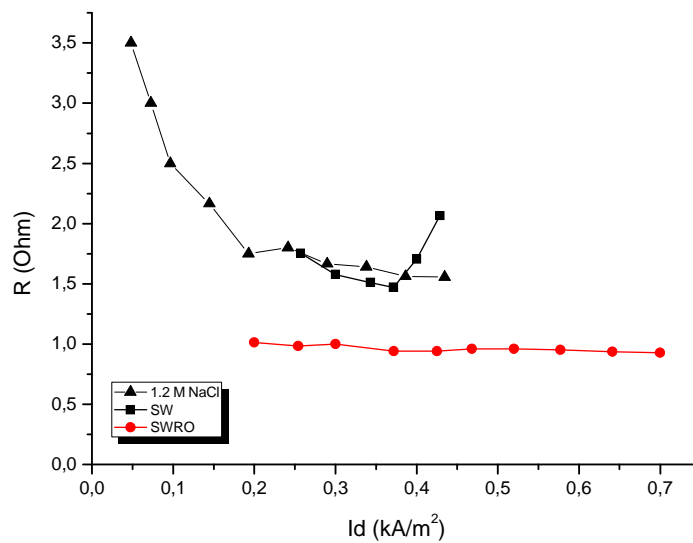
Figure 5.4. Determination of LCD at the pilot plant. Resistance of the solution R *(ohm) versus current density* I_d *(kA/m_2) at 500 L/h at 12.8ºC and comparison with the values obtained with seawater by Blancke (2006) at 20ºC and the ones obtained by Fidaleo et al. (2011) using 1.2 M NaCl*

Resistance from SWD-RO brine was much lower than the one recorded by seawater or by prepared NaCl solutions due to concentration and membranes differences mainly. Operation conditions such as inlet velocity and temperature can also affect the LCD obtained, so this value must be determined experimentally in all cases. It can be seen than, although SWD-RO and synthetic NaCl solutions had approximately the same NaCl composition, voltage differences observed were due to membrane resistance differences, other ions present in the brines, inlet temperature and stack configuration. The lower voltages obtained with SWD-RO brines would be a benefit for its concentration and further reuse, as energy consumption will be well under the usual value obtained with seawater.

LCD for seawater was determined at 0.36 kA/m^2 by Blancke (2006) which is proximal to the operational value used in salt production industries in Japan. In the voltage range studied with SWD-RO, no increase of resistance was observed and the

LCD could not be determined. This confirmed the fact that, thanks to the single-pass configuration of the pilot plant and the high concentration of the solution, the LCD would never be reached. According to the manufacturer, the maximum voltage applicable to the stack was 65V, which corresponds to a maximum current density of 0.70 kA/ m^2, so this current density was considered the maximum operative current of the pilot plant. Nevertheless, some operational problems regarding hydrogen removal were observed above 0.60 kA/ m^2 and higher current densities could not be evaluated.

5.3. Evaluation of ED performance on NaCl concentration from SWD-RO brines.

5.3.1. Identification of optimum plant operation conditions

An experiment at 30 A (0.3 kA/m^2) with SWD-RO brine 1 inlet in the concentrate tank and SWD-RO brine 2 as a feed stream at 26ºC was carried out to determine the optimum plant operation conditions. The volume of the concentrate tank was 1000 L, so it took more than 80 hours to reach 180 g/L NaCl approx. The concentrated tank concentration profile is shown in Figure 5.5. The diluate produced in the ED pilot had a composition between the 50-60 g/L throughout the experiment due to the single-pass configuration. However, the composition of this diluate was not totally constant because the variations in RO pilot plant operations generated variations in the inlet brine composition. Moreover, differences in the concentrate tank composition during the experiment were due to operational stops and start-up of the ED plant. Initially difficulties on pH control on the circuits showed the formation of precipitates in the concentrate compartment, thus increasing the voltage, , and consequently shutting down the plant. The increase on an appropriate HCl dosing in the circuits avoided this problem in later experiments. Finally, the concentrate tank was reduced to 250 L to speed up the concentration process.
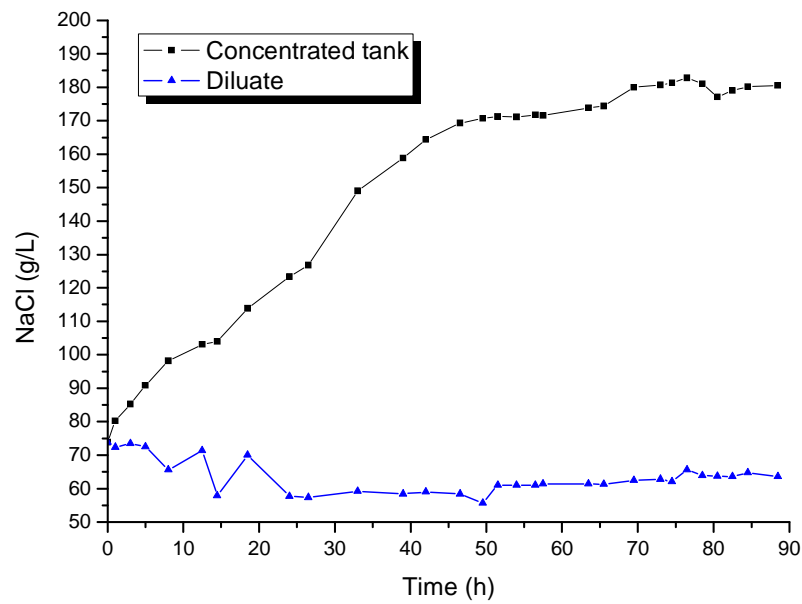
Figure 5.5. Profile of NaCl concentration (g/L) in the tank and diluate concentration in the experiment at 0.30 kA/ m^2, 26ºC and a 1000 L concentrate tank. NaCl approximate composition in this experiment was determined considering that all Cl ions were in form of this salt.

5.3.2. Concentration performance.

Two experiments were carried out at 40 A (0.4 kA/ m^2) and 30 A (0.3 kA/ m^2) with a tank of 250L and SWD-RO brine 2 at low temperatures (10-14 ºC). Other experiments with a 100L tank were carried out at 35A (0.35 kA/ m^2), 50A (0.5 kA/ m^2) and 60A (0.6 kA/ m^2) at temperatures of 28ºC. The concentration results obtained in these experiments are shown in Table 5.4. In Table 5.4 only minor elements that were over the membrane cell requirements determined in Chapter 4 are represented, all other minor elements analyzed with ICP-OES fulfilled the requirements of the membrane electrolysis cell represented in Chapter 2.

Table 5.4. Composition results, concentration factors (CF) and time necessary to reach the maximum NaCl concentration during the experiment at 30A (0.3 kA/ m²) and 40A (0.4 kA/ m²) at 14°C and 10°C, and at 35A (0.35 kA/ m²) , 50A (0.5 kA/ m²) and 60A (0.6 kA/ m²) at 28° Inlet SWD-RO brine 2.

	0.30 kA/m² (14ºC)			0.40 kA/m² (10ºC)			0.35 kA/m² (28ºC)			0.50 kA/m² (28ºC)			0.60 kA/m² (28ºC)		
g/L	C_0	C_f	CF	C_0	C_f	CF	C_0	C_f	CF	C_0	C_f	CF	C_0	C_f	CF
NaCl	71.5	239	3.3	57.7	264	4.5	65	210	3.2	65	244	3.8	65.1	261	4
K(I)	0.89	3.33	3.7	0.68	3.55	5.2	0.70	3.10	4.4	0.77	3.2	4.2	0.74	3.50	4.7
Mg (II)	2.5	1.3	0.5	2.5	1.2	0.5	2.2	1.1	0.5	2.3	1.3	0.6	2.3	1.2	0.5
Ca (II)	0.8	0.7	0.9	0.8	0.7	0.9	0.6	0.4	0.6	0.7	0.3	0.4	0.7	0.3	0.4
S (VI)	4.7	1.4	0.3	4.9	1.0	0.2	5.4	1.7	0.3						
mg/L															
Al (III)	0.05	DL	-	0.03	DL	-	0.28	0.17	0.6	0.11	0.10	1	0.08	DL	-
Ni (II)	0.06	0.14	2.3	0.05	0.12	2.4	0.06	0.11	1.8	0.06	0.20	3.3	0.06	0.12	2.0
Sr (II)	15.0	12.7	0.9	14.7	10.7	0.7	13.2	13.2	1.0	14.0	14.0	1.0	13.6	13.0	0.9
Cu (II)	0.02	0.03	1.5	0.03	0.04	1.3	0.02	0.2	10	0.03	0.2	6.6	0.02	0.13	6.5
Time (h)	35			38			15			14			13		

*DL : Detection limit

Membranes used in the pilot plant were selective for the transport of univalent ions, so higher concentration factors were obtained for these ions, as can be seen in Table 5.3. Concentration factors and final NaCl concentration reached was dependent on inlet temperature, at higher inlet temperatures brine densities changed and lower NaCl concentrations could be reached due to larger osmosis flux through the membranes. Nevertheless, lower energy consumptions could be obtained due to large overflow produced. This fact was previously reported by Blancke (2007) who recommended operating at high temperatures in order to obtain larger production flows. Table 5.4 also shows that higher NaCl concentrations were reached at higher current densities due to the effect of water and ion migration that increase with the intensity applied. However, the concentrations reached in these experiments were not high enough to meet the membrane electrolysis requirements (300g/L NaCl), which meant that further concentration is needed.

It can be seen from Table 5.4 that polyvalent ions in the concentrate tank of the pilot plant were diluted or were kept constant, reaching similar CF in the experiments at the same temperature. Nickel and copper did not follow the general trend; its concentration was increased in all the experiments. It can be observed from Figure 5.6 and Figure 5.7 that, in the pH range studied (4-7), major ionic form of nickel and copper are $NiCl^+$ and $CuCl^+$, which are univalent and so, can pass through the membrane and get concentrated on the brine produced. Concentration factor of copper is from 2 to 5 times higher than the concentration factor of nickel, depending

on the temperature and current density used. It can be observed in the speciation diagrams of Figures 5.6 and 5.7, that the fraction of $CuCl^+$ in the brine is up to 3 times higher than the fraction of $NiCl^+$, in consequence, it can obtain higher concentration factors as more copper is available to be transported. Moreover, some copper in the brine could be originated by the degradation of the copper wires used to measure the potential drop inside the cell. This factor is going to be evaluated when the stack will be opened.

$[Ca^{2+}]_{TOT}$ =	20.00 mM	$[Sr^{2+}]_{TOT}$ =	0.20 mM
$[Mg^{2+}]_{TOT}$ =	100.00 mM	$[Cu^{2+}]_{TOT}$ =	0.50 µM
$[K^+]_{TOT}$ =	10.00 mM	$[Ni^{2+}]_{TOT}$ =	1.20 µM
$[Cl^-]_{TOT}$ =	1.20 M	$[Al^{3+}]_{TOT}$ =	2.00 µM
$[Na^+]_{TOT}$ =	1.00 M	$[SO_4^{2-}]_{TOT}$ =	50.00 mM
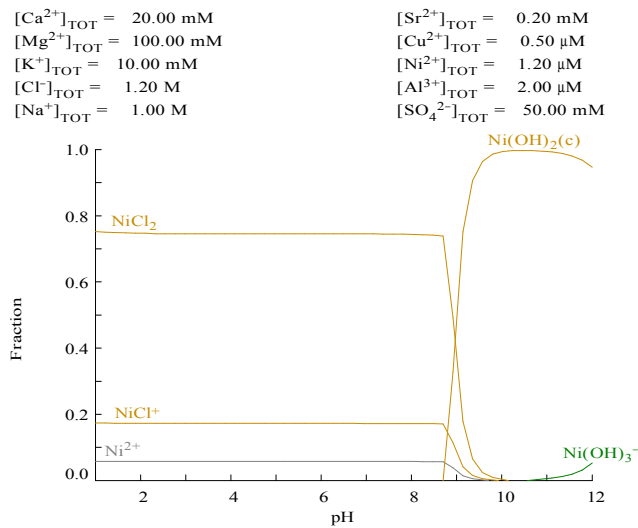
Fig. 5.6. Speciation of Ni (II) (fraction porcentage) in the brine as a function of the pH

$[Ca^{2+}]_{TOT}$ =	20.00 mM	$[Sr^{2+}]_{TOT}$ =	0.20 mM
$[Mg^{2+}]_{TOT}$ =	100.00 mM	$[Cu^{2+}]_{TOT}$ =	0.50 µM
$[K^+]_{TOT}$ =	10.00 mM	$[Ni^{2+}]_{TOT}$ =	1.20 µM
$[Cl^-]_{TOT}$ =	1.20 M	$[Al^{3+}]_{TOT}$ =	2.00 µM
$[Na^+]_{TOT}$ =	1.00 M	$[SO_4^{2-}]_{TOT}$ =	50.00 mM
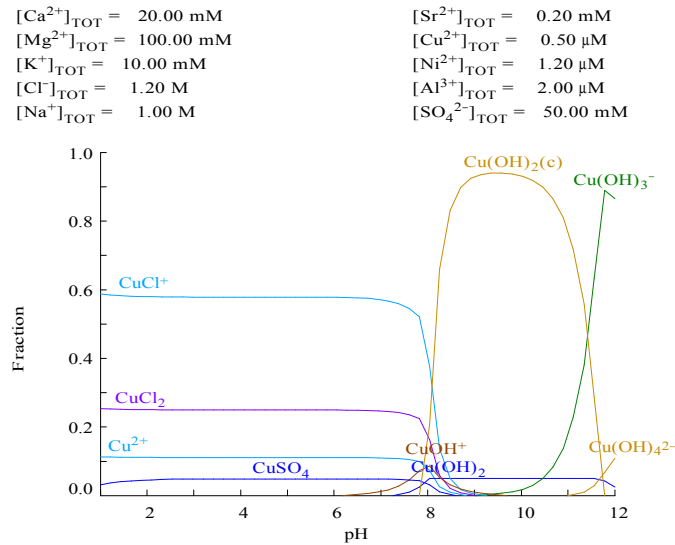
Fig. 5.7. Speciation of Cu (II) (fraction porcentage) in the brine as a function of the pH

The major cation concentration order when using SWD-RO brine was K(I) > Na (I) > Ca (II)> Mg (II); as Ca^{2+} has lower hydrating ionic radii than Mg^{2+} (stokes radius of 0.349 over 0.429 nm), it can move faster and so, slightly higher CF can be obtained compared to magnesium. The minor cation concentration order was Cu

(II) > Ni (II) > Sr (II) > Al (III). It can be concluded that concentration order of polyvalent ions was highly dependent on electric charge and ionic radii, polyvalent ions with lower electric charge got more concentrated in all the experiments. Migration of polyvalent ions was not a primary phenomenon and their final composition was mainly determined by the osmosis and electro-osmosis fluxes.

In Table 5.5, CF and selectivities of ACS and CIMS membranes operated at 0.3 kA/m^2 at 14ºC with SWD-RO brines are compared to the values reported in the literature. The first work is a seawater electrolyzer reported by Yamane *et al.* (1969) when using CLS-25T and AVS-4T Neosepta membranes for salt production at 0.2 kA/m^2, the second work is seawater concentration results with Selemion ASA and CMA membranes at 0.3 kA/m^2 (Blancke, 2006), the third one is the results obtained by Turek *et al.*(2009) when using BWRO brine with Selemion CMV and AMV membranes and the last one, the results obtained by Korngold *et al.* (2009) with BWRO brine and Selemion CMT and AMT Ashahi Glass desalination membranes. It can be seen that concentration factors were higher in the experiences reviewed because the initial concentration was lower. CFs obtained by Turek *et al.* (2009) were specially high because the brine was treated using batch EDR. Nevertheless, ACS and CIMS membranes were proved to be highly selective to univalents ions, as its selectivity relation was the highest in all cases reviewed.

Table 5.4.Concentration factors (CF) and selectivities obtained at 0.3 kA/m^2 at 14ºC with SWD-RO brines and CIMS/AMS membranes compared with the data from three different previous experiences reported in the literature.

	CIMS /ACS	CLS-25T /AVS-4T (Yamane *et al.* 1969)	ASA /CMA (Blancke, 2006)	CMV /AMV (Turek *et al.* 2009)	CMT /AMT (Korngold *et al.* 2009)
Feed inlet	SWD-RO brine	SW	SW	BWRO brine	BWRO brine
Na (I)	3.2	5.7	9.7	11.1	-
Ca (II)	0.8	7.6	6.3	10.4	1.1
Mg (II)	0.5	6.0	2.7	10.8	1.8
Cl (I)	3.2	5.7	11.5	11.1	1.4
S (VI)	0.3	0.6	0.2	10.3	1.3
S_{Ca}^{Na}	-1.2	0.2	-0.2	0.0	-
S_{Mg}^{Na}	-1.6	0.0	-0.7	0.0	-
S_{SO4}^{Cl}	-1.9	-1.2	-1.2	0.0	-0.1

Diluate production from the cell was constant in all experiments at about 50-60 g NaCl/L, which means that only 6-8 g/L of NaCl were removed in each pass, depending on the current density applied. Current efficiency of chloride ion was

calculated in all experiments using the diluate concentration (in one-single pass configuration), results showed that chloride transported more than 80% of the current in the stack when temperatures were low, as is detailed in Figure 5.8. When inlet temperatures were high, this value was reduced due to higher water flux in the stack, reaching around 50% of the transport. Current efficiency of chloride ion was improved after cleanings (CIP) of the membranes, reaching more than 92% of current transport at low inlet temperatures.
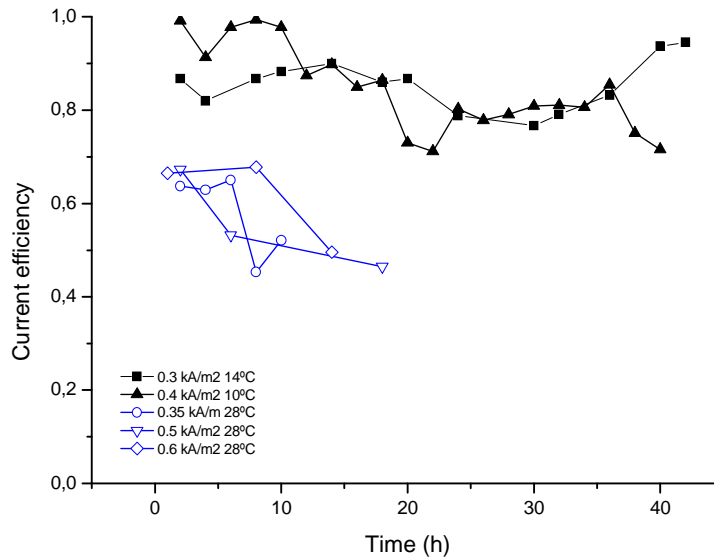
Figure 5.8. Current efficiency for chloride ions as a function of time at different inlet temperatures.

The sulphate, calcium and magnesium concentrations in the diluate were similar to the inlet brine composition, given that the circuit had a single-pass design. This confirmed the fact that polyvalent ions in the concentrate tank were mainly diluted by water transport inside the cell and that the migration of these ions was not significant.

In Table 5.6 brine obtained at the end of the experiments is compared to the membrane electrolysis requirements. Elements that do not meet electrolysis requirements are highlighted. It can be seen than in all cases the brine should be further concentrated to reach saturation limit. This could be done by adding a small amount of solid salt (between 90 and 40 g/L NaCl). Moreover the brine would also need a purification step to remove calcium, magnesium, copper, nickel and strontium in all cases studied.

Table 5.6. Comparison of concentrated brines obtained with ED and membrane cell requirements.

	0.30 kA/m² (14ºC)	0.40 kA/m² (10ºC)	0.35 kA/m² (28ºC)	0.50 kA/m² (28ºC)	0.60 kA/m² (28ºC)	Membrane cell requiremens
g/L						
NaCl	239	264	210	244	261	300
K(I)	3.33	3.55	3.10	3.20	3.50	-
Ca (II)	**0.6**	**0.7**	**0.4**	0.3	0.3	20 ppb
Mg (II)	**1.3**	**1.2**	**1.1**	1.3	1.2	
S (VI)	1.4	1.0	1.7			8
mg/L						
Al (III)	**DL**	**DL**	**0.17**	**0.1**	**DL**	0.1
Ni (II)	**0.14**	**0.12**	**0.11**	**0.2**	**0.12**	0.01
Sr (II)	**12.7**	**10.7**	**13.2**	**14.0**	**13.0**	0.4
Cu (II)	**0.03**	**0.04**	**0.2**	**0.2**	**0.1**	0.01

5.3.3. Electrical Energy Consumption

Energy consumption could be calculated in two ways, depending on the operating procedure of the pilot plant. Batch operation energy consumption was calculated when the full concentrated tank was considered the product obtained, whereas continuous operation energy consumption was calculated when the overflow of the tank when the maximum concentration was reached was considered the product.

Energy consumptions needed to increase the concentration in the tank (batch operation) over the concentration reached at different current densities are represented in Figure 5.9. In Table 5.7, the energy consumption calculated according to equation 5.5 can be found. In industrial cells, the electrode potentials are not considered because the voltage produced is low compared to that produced by the total number of cells. However, in pilot plants, electrode potential significantly increases energy consumption and must be taken into account.

Electrode potentials were measured in the experiments carried out at higher temperatures using a datalogger which monitorized the potential between membranes. Nevertheless, electrode potentials could not be experimentally determined in the experiments at low temperatures because datalogger was not already installed, and, in those cases, stack potential was reduced by 10V following the stack supplier's instructions.
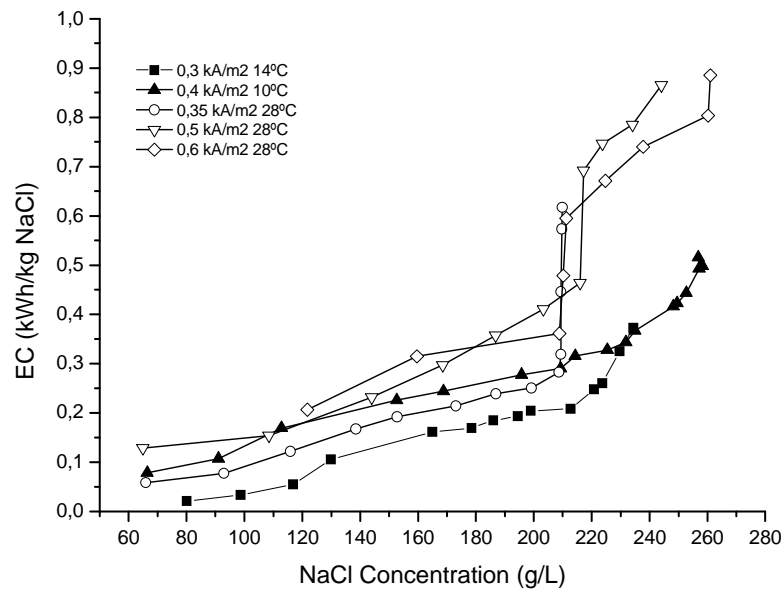
Figure 5.9. Batch energy consumption as a function of NaCl concentration in the tank and current density applied at different inlet temperatures.

As can be seen in Figure 5.9 batch energy consumption rises gradually in all the experiences until the concentration in the tank reached 210 g/L NaCl approximately. From this point on, the consumption increases dramatically because osmosis and ion diffusion fluxes inside the stack reach a maximum due to the concentration gradient between diluate and concentrate compartments, as is further explained in section 5.4.4. In consequence, NaCl concentration in the tank increases very slowly from this point on. At that point, the energy applied is used to slowly increase NaCl concentration of the tank and so, specific energy consumption increases. If the process needs to be operated in a batch mode, the optimum of energy consumption-concentration would be obtained around 200 g/L NaCl at 0.2-0.3 kWh/kg NaCl in the range of 0.3-0.4 kA/m^2, depending on the current density applied and feed inlet temperature.

Table 5.7. Energy consumption when operated in a continuous mode in experiments carried out in the pilot plant.

I (A)	Stack potential (V)	Stack potential without electrodes (V)	Maximum NaCl (g/L)	Overflow (L/h)	Production (NaCl g/h m²)	Inlet temperature (ºC)	Energy consumption (kWh/kg NaCl)
30	28.3	18.3*	239	9	2,15	14	0.25
40	28.4	18.4*	264	12	3,16	10	0.23
35	22.0	15.2	210	15	3,15	28	0.17
50	26.5	17.0	244	18	5,36	28	0.16
60	31.7	21.7	261	19	4,95	28	0.26

Electrode potential was considered to be 10V

When energy consumption based on product obtained or overflow (continuous operation) was calculated (see Table 5.7), it was observed that was similar experiments, but this consumption depended on the intensity applied and the temperature. The energy consumption sharply increased from 0.5 to 0.6 kA/m^2 at 28ºC, so 0.5 kA/m^2 was considered the maximum operable point at higher inlet temperatures. It was observed that at higher inlet temperatures, stack voltage decreased, as did energy consumption due to conductivity brine changes. The temperature can also affect the product flow rate because it causes changes in brine density, given that lower flow rates are obtained at higher temperatures.

Technical targets when operating electrodialyzers to produce solid salt from seawater in Japan are obtaining a concentration higher than 200 g/L NaCl with an energy consumption lower than 0.12 kWh/kg NaCl (*Fujita, 2009*). This value was nearly obtained with SWD-RO when operating the plant in a continuous mode. More than 200 g/L NaCl were obtained at 28ºC with an EC of 0.16 kWh/kg when operated at 0.50 kA/m^2.

A comparison of the performance of an industrial electrodialyzer to obtain solid salt from seawater and the results obtained in the pilot plant in Barcelona in continuous operation and batch mode can be found in Table 5.8. The values obtained in the pilot plant were within the range of the industrial process in all cases studied, although these values could be further optimized. Higher concentrations were reached in the pilot plant with slightly higher current densities and energy consumptions.

Table 5.8. Comparison of the performance of an industrial electrodialyzer using seawater in Japan and the pilot plant using SWD-RO brine in Barcelona.

	I_d (kA/m^2)	Inlet temperature (ºC)	Maximum NaCl (g/L m^2)	Energy consumption (kWh/kg NaCl)
Industrial cell (*Tanaka 2010a*)	0.27	23.5	174	0.16
Pilot Plant Batch mode	0.30	14.0	199	0.20
	0.40	10.0	209	0.30
	0.35	28.0	208	0.29
	0.50	28.0	186	0.35
	0.60	28.0	208	0.38
Pilot Plant Continuous mode	0.30	14.0	226	0.25
	0.40	10.0	252	0.23
	0.35	28.0	210	0.17
	0.50	28.0	244	0.16
	0.60	28.0	261	0.26

Other comparisons with literature can be done even though the operating methods and solutions used are different. Fidaleo *et al.* (2005) studied energy consumption with NaCl solutions up to approximately 100 g/L NaCl in a lab cell. The consumption obtained was between 0.18 and 0.33 kWh/kg with 80% solute recovery and current densities of 0.20 to 0.30 kA/ m². As can be seen, the energy consumption values obtained were in the range of the ones presented in the literature, but more research is needed to obtain data on energy consumption under different operating conditions so that the energy consumption of the pilot plant can be reduced and optimal NaCl concentrations can be reached.

5.3.4. Membranes evaluation after operation

After some months of operation, the stack was opened in order to analyze membranes integrity. Membranes were examined by SEM-EDS and no precipitates were observed in their surface. The absence of precipitates of magnesium, calcium and carbonates support the deduction provided in section 5.2.1.

Exhaustive cleanings in place (CIP) with HCl were performed frequently to recover the flow rate and pressure of the stack that was affected due to scaling. Despite CIPs, some organic matter and diatoms could be found on the membranes, as is depicted in Figure 5.10. These organic matter and diatoms were present in the SWD-RO brines, where the TOC content was around 1.4 mg C/L. Nevertheless, no consequences were observed in the concentration process performance.
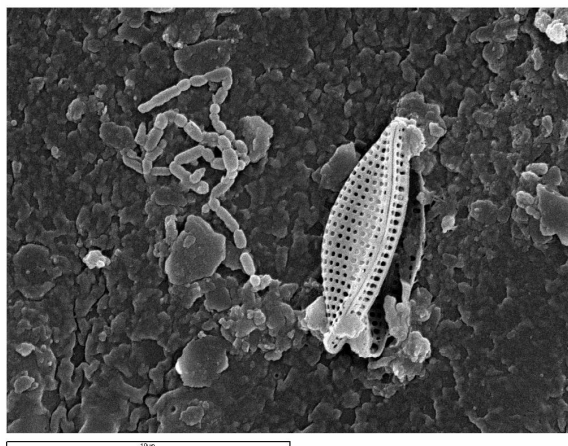

Figure 5.10. Organic matter and diatoms detected on the membranes surface by SEM-EDS after some months of operation.

Some clogging could be observed in the inlet channel of the membranes caused by particulate matter that could pass the inlet filter. This generated an overpressure on the stack and consequently stopped the pilot plant. This clogging was manually

cleaned and then the filter was substituted to minimize this problem in future experiments.

5.4. Modelling of SWD-RO brine concentration process using ED

ED modeling for water desalination has been widely studied in the last years. Modeling is important in order to predict the behavior of the process for experimental designs and to optimize its operation. It can be an useful tool to reduce experimental time and costs.

Models for ED process were reviewed by Rohman *et al.* (2008). Mathematical models are mainly focused on the different mass transfer phenomena that take place through the membranes or in the boundary layers. Other models theoretically study the ion and water flux in 2D or 3D; however, they are very complex and are not commonly used in the modeling of ED systems.

In consequence, different types of models are available to describe the ED process. The most used are based on irreversible thermodynamic (IT) approach with describe transport of ions and water through the membranes, treating them as black boxes. IT approach completely considers the cross effects of all flows through the membrane.

Nernst-Planck (NP) equations are considered a reduced form of IT equations where only diffusion and electro-migration are taken into account, considering that convective flux can be neglected. Nernst-Planck is used for solutions with one salt and which are diluted, so ion interactions are not taken into account (*Fidaleo et al. 2005*). Nernst-Planck equations can be coupled with other equations describing hydrodynamics conditions and ion transport in the surrounding solutions, chemical reactions and other conditions, creating a more effective model. Nerst-Einstein equations can be applied simultaneously to Nernst-Planck equations to relate diffusion coefficients with molar conductivities. Thus, Nernst-Planck extended will be formed including the velocity of the solution.

Maxwell-Stefan (MS) equation is also widely used for multi component solutions. MS takes into account the electrical potential in the stack and the activity and pressure gradients to describe the transport in membranes. Moreover, these equations take into account the diffusivity or friction coefficient for each pair of components as transport coefficients. MS equations do not have restrictions and are convenient for membrane characterization. Nevertheless, they are complicated because of high number of transport coefficients required.

In the recent years, different works on seawater or high salinity brines modeling have been implemented (*Tanaka 2003, 2005, 2010a, Fidaleo et al. 2011, Fidaleo et al. 2005, Sadrzadeh et al.2007b, Moon et al. 2004*). Sadrzadeh, *et al.* (*2007b*) modeled an one-pass flow process using mass balances and obtained concentration in the diluate compartment for various voltage, flow rates and feed concentration. Moon *et al.*

(*2004*) studied the ionic transport across the membranes using a 2D or 3D continuous model. Tanaka also studied coupled models where current density distribution, mass transport, cells voltage and energy consumption are taken into account. These models have been applied to different ED configurations (*Tanaka 2009, 2010b*) and lately; it has been applied for seawater concentration modeling by electrodialysis. Nevertheless, this model required several experimental parameters that should be determined previously and difficult its application.

Fidaleo *et al.* (*2005, 2011*) studied mass transfer, mass balance and potential drop and limiting current density based on Nernst-Planck equation. In their work, steps to determine the different parameters needed for the model are fully described. Fidaleo et al (*2005, 2011*) concluded that NP equations could be applied to solutions with high content of a strong electrolyte such as NaCl.

A simple model based on Nernst-Plank (NP) equations was developed in thesis and was used to predict the evolution of the NaCl concentration process taking place at the ED pilot plant. The model was considered valid for the prediction of pilot plant's performance in general terms.

5.4.1. Model assumptions

To design an ED process several parameters must be taken into account: stack and spacer configuration, membranes type, operating conditions, intensity and voltage applied, feed concentration and flow rates, etc. In order to simplify the ED modelling, different ideal assumptions were made:

a) Nernst-Planck mass transport equations were assumed. Consequently, no interaction between ions was taken into account and the activity coefficients of all ions were assumed to be 1, despite the solution's high ionic strength. Moreover, transport due to convection was not considered.

b) The model focused only on sodium and chloride. Other ions were not taken into account.

c) Feed and concentrate flow rates were assumed to be constant during the entire operation. Moreover, inlet flow composition was considered to be constant, as was the temperature at around 25°C.

d) It was assumed there were no hydraulic or electric leaks in the stack or in the circuits.

e) The operating current density was lower than the limiting current density (LCD) and was constant throughout the experiment.

f) All stack compartments had the same geometry. All the concentrate compartments had the same hydrodynamic conditions; the same was assumed for the diluate compartments. However, in real conditions viscosity

increases when higher concentrations are reached and different hydrodynamic conditions are experienced that can affect the thickness of the boundary layer.

g) The solutions in the stack compartments and the concentrate tank were considered perfectly mixed.

h) Fouling and scaling phenomena in the stack were not studied.

i) The cationic membranes used in the stack were considered permeable only to cations and the anionic membranes were considered permeable only to anions. Thus, the diffusion of counter ions was not taken into account. This assumption considers the membranes to be ideal; this can be far from real behavior, as membranes can lose their permselectivity at high concentrations.

j) The electrode compartments were not modelled.

k) The diffusion coefficients were assumed to be constant throughout the experiment.

l) The mass transfer coefficients of the ions studied were understood to be equal in all compartments

5.4.2. Model equations

In order to model the process and establish the system inputs and outputs for the mass balances, a control volume was used consisting of two compartments of the stack and the concentrate tank. This control volume and the flow rates and concentrations involved in the model equation are shown in Figure 5.11. Figure 5.11 shows the flow diagram for the ED plant together with the simplified concentration profiles in an ED cell pair.

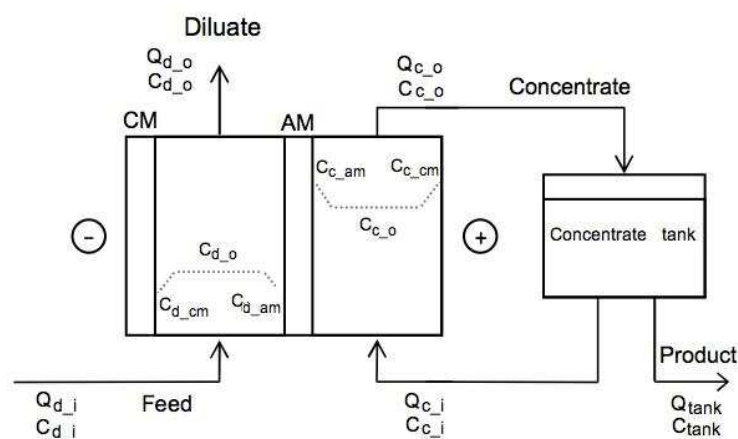*Fig. 5.11. Diagram of the flows and concentrations used in the model.*
Qd_o diluate stream outlet flow rate; Cd_o outlet NaCl concentration of the diluate stream; Qd_i diluate stream inlet flow rate; Cd_i inlet NaCl concentration of the diluate stream; Qc_o concentrate stream outlet flow rate; Cc_o outlet NaCl concentration of the concentrate stream; Qc_i

concentrate stream inlet flow rate; Cc_i inlet NaCl concentration of the concentrate stream; Cd_cm NaCl concentration on the cation membranes in the diluate compartment; Cd_am NaCl concentration on the anion membranes in the diluate compartment; Cc_cm NaCl concentration on the cation membranes in the concentrate compartment; Cc_am NaCl concentration on the anion membranes in the concentrate compartment

When current is applied, different mass transport phenomena take place inside the stack. First of all, the charged species in the solution are transported to the cathode or anode through the ion exchange membranes. This phenomenon is called ion migration flux (M). In the model it was represented using equation 5.6, which, in this case, only considered NaCl migration (mol NaCl/h). This equation takes into account the efficiency of the process (η), which is calculated using equation 5.7, the total number of cells in the stack (N) and the current applied (I).

$$M = \frac{\eta \cdot I}{F} \cdot N$$

$$(5.6)$$

$$\eta = t_{Cl^-am} + t_{Na^+cm} - 1$$

$$(5.7)$$

The efficiency of the process, takes two parameters into account: the transport number of chloride ions in the anionic membrane ($t_{Cl\text{-}am}$) and the transport number of sodium ions in the cationic membrane ($t_{Na+\ cm}$).

In this thesis one of the assumptions used to simplify the model was that the membranes were ideal and counter ion transport was considered negligible (see assumption i). Thus, the efficiency of the process was considered to be 100% according to equation 5.7. At high concentrations membranes can lose part of their selectivity and the efficiency will be reduced. However, this assumption was necessary to develop an initial approach to model the results obtained in the pilot plant.

Due to the current intensity applied, water also migrates through the ion exchange membranes to produce what is known as electro-osmosis flux (Mw), as shown in equation 5.8 (mol H$_2$O/h). This equation is similar to the NaCl migration equation but takes into account the transport number of water (t_w) of the membranes used.

$$M_w = t_w \cdot \frac{\eta \cdot I}{F} \cdot N$$

$$(5.8)$$

The transport number of water (t_w) is considered to be the sum of the number of water molecules migrating with chloride ions (h_{Cl^-}) and the number of water molecules migrating with sodium ions (h_{Na^+}) when current intensity is applied, as represented in equation 5.9.

$$t_w = h_{Cl^-} + h_{Na^+}$$

$$(5.9)$$

In addition, after a period of operation, when a gradient of concentration appears between the diluate and concentrate compartments, two mass transport phenomena take place: diffusion and osmosis. In this model, diffusion flux (D) was the migration

of sodium chloride from the concentrate compartment to the diluate compartment (mol NaCl/h), as represented in equation 5.10. This equation takes into account several membrane parameters such as ion diffusion coefficients (D_{Cl_am}, D_{Na_cm}), area (S) and membrane thickness (σ), as well as the NaCl concentration on the membrane surface (C_{c_am}. C_{d_am} C_{c_cm} and C_{d_cm})

$$D = \frac{D_{Cl\_am} \cdot S}{\sigma_{am}} \cdot \left(C_{c\_am} - C_{d\_am} \right) N + \frac{D_{Na\_cm} \cdot S}{\sigma_{cm}} \cdot \left(C_{c\_cm} - C_{d\_cm} \right) N \tag{5.10}$$

Moreover, water is also transported from the diluate compartment to the concentrate due to the gradient of concentration, thus producing what is known as osmosis flux (D_w) (mol H_2O/h). This equation 5.11 is similar to the diffusion one, but the diffusion parameters are specific to water permeability (D_{w_am}, D_{w_cm}).

$$D_w = \frac{D_{w\_am} \cdot S}{\sigma_{am}} \cdot \left(C_{c\_am} - C_{d\_am} \right) N + \frac{D_{w\_cm} \cdot S}{\sigma_{cm}} \cdot \left(C_{c\_cm} - C_{d\_cm} \right) N \tag{5.11}$$

As mentioned above, the membrane surface concentration is needed to solve the diffusion and osmosis flux equations. These concentrations can be calculated using the equations proposed by Ortiz *et al.* (2005), which take into account the transport number of the ion (t_{Cl}^{-} or t_{Na}^{+}), the membrane area (S), the mass transport coefficient (k_m), the efficiency of the process (η) and the current intensity applied (I).

The model was completed using all these mass transport equations in the different NaCl balances of all the compartments and the concentrate tank of the pilot plant, as shown in equations 5.16 to 5.22.

- ▪ Concentrate compartment

Flow balance

$$Q_{c\_i} + Q_W = Q_{c\_o} \tag{5.16}$$

$$Q_W = (M_w + D_w) \cdot \frac{Mw_w}{\rho_w} \tag{5.17}$$

NaCl balance

$$C_{c\_i} \cdot Q_{c\_i} + M = C_{c\_o} \cdot Q_{c\_o} + N \cdot V_{cell} \cdot \frac{dC_{c\_o}(t)}{dt} + D \approx C_{c\_o} \cdot Q_{c\_o} + N \cdot V_{cell} \cdot \frac{C_{c\_o}(t) - C_{c\_o}(t - dt)}{dt} + D \tag{5.18}$$

- ▪ Diluate compartment

Flow balance

$$Q_{d\_i} = Q_W + Q_{c\_o} \tag{5.19}$$

NaCl balance

$$C_{d\_i} \cdot Q_{d\_i} + D = C_{d\_o} \cdot Q_{d\_o} + N \cdot V_{cell} \cdot \frac{dC_{d\_o}(t)}{dt} + M \approx C_{d\_o} \cdot Q_{d\_o} + N \cdot V_{cell} \cdot \frac{C_{d\_o}(t) - C_{d\_o}(t - dt)}{dt} + M \quad (5.20)$$

- ▪ Concentrate tank

Flow balance

$$Q_{\tan k} = Q_w \quad (5.21)$$

NaCl balance

$$C_{c\_o} \cdot Q_{c\_o} = C_{c\_i} \cdot Q_{c\_i} + C_{c\_i} \cdot Q_{\tan k} + V_{\tan k} \cdot \frac{dC_{c\_i}(t)}{dt} \approx C_{c\_i} \cdot Q_{c\_i} + C_{c\_i} \cdot Q_{\tan k} + V_{\tan k} \cdot \frac{C_{c\_i}(t) - C_{c\_i}(t - dt)}{dt} \quad (5.22)$$

The NaCl concentration, the time required to reach maximum concentration and flow production can be calculated at all times using a solver. Matlab, the solver used, was able to deal with the 17 equations and 17 variables each time.

Table 5.9. Summary of the equations in the model.

Equation	
$M = \dfrac{\eta \cdot I}{F} \cdot N$	5.6
$\eta = t_{Cl\ am} + t_{Na^*cm} - 1$	5.7
$M_w = t_w \cdot \dfrac{\eta \cdot I}{F} \cdot N$	5.8
$t_w = h_{Cl^-} + h_{Na^+}$	5.9
$D = \dfrac{D_{Cl\_am} \cdot S}{\sigma_{am}} \cdot \left(C_{c\_am} - C_{d\_am} \right) N + \dfrac{D_{Na\_cm} \cdot S}{\sigma_{cm}} \cdot \left(C_{c\_cm} - C_{d\_cm} \right) N$	5.10
$D_w = \dfrac{D_{w\_am} \cdot S}{\sigma_{am}} \cdot \left(C_{c\_am} - C_{d\_am} \right) N + \dfrac{D_{w\_cm} \cdot S}{\sigma_{cm}} \cdot \left(C_{c\_cm} - C_{d\_cm} \right) N$	5.11
$C_{d\_am} = C_{d\_o} - \dfrac{(1 - t_{Cl^-}) \cdot \eta \cdot I}{F \cdot k_m \cdot S}$	5.12
$C_{c\_am} = C_{c\_o} + \dfrac{(1 - t_{Cl^-}) \cdot \eta \cdot I}{F \cdot k_m \cdot S}$	5.13
$C_{d\_cm} = C_{d\_o} - \dfrac{(1 - t_{Na^+}) \cdot \eta \cdot I}{F \cdot k_m \cdot S}$	5.14

Equation	
$$C_{c\_cm} = C_{c\_o} + \frac{(1 - t_{Na^+}) \cdot \eta \cdot I}{F \cdot k_m \cdot S}$$	5.15
$$Q_{c\_i} + Q_W = Q_{c\_o}$$	5.16
$$Q_W = (M_w + D_w) \cdot \frac{Mw_w}{\rho_w}$$	5.17
$$C_{c\_i} \cdot Q_{c\_i} + M = C_{c\_o} \cdot Q_{c\_o} + N \cdot V_{cell} \cdot \frac{dC_{c\_o}(t)}{dt} + D \approx C_{c\_o} \cdot Q_{c\_o} + N \cdot V_{cell} \cdot \frac{C_{c\_o}(t) - C_{c\_o}(t - dt)}{dt} + D$$	5.18
$$Q_{d\_i} = Q_W + Q_{c\_o}$$	5.19
$$C_{d\_i} \cdot Q_{d\_i} + D = C_{d\_o} \cdot Q_{d\_o} + N \cdot V_{cell} \cdot \frac{dC_{d\_o}(t)}{dt} + M \approx C_{d\_o} \cdot Q_{d\_o} + N \cdot V_{cell} \cdot \frac{C_{d\_o}(t) - C_{d\_o}(t - dt)}{dt} + M$$	5.20
$$Q_{\tan k} = Q_w$$	5.21
$$C_{c\_o} \cdot Q_{c\_o} = C_{c\_i} \cdot Q_{c\_i} + C_{c\_i} \cdot Q_{\tan k} + V_{\tan k} \cdot \frac{dC_{c\_i}(t)}{dt} \approx C_{c\_i} \cdot Q_{c\_i} + C_{c\_i} \cdot Q_{\tan k} + V_{\tan k} \cdot \frac{C_{c\_i}(t) - C_{c\_i}(t - dt)}{dt}$$	5.22

5.4.3. Model calculations.

Matlab was used in order to solve the equation described in section 5.4.2. Migration and Electro-osmosis fluxes (equations 5.6 and 5.7) were independent of the rest of equations and were constant during the run of the model. These equations were directly implemented in the code.

NaCl balance equations inside the stack (equations 5.18, 5.20 and 5.22) are polynomial whereas the rest of equations used in the model are linear, in consequence a solver for non-linear equations is needed to run the model. The function fsolve was used for this purpose. When this function reached a convergent solution, the solution was recorded in a matrix and the time differential was increased by 5min to recalculate the variables and start the calculation process over again. With this process, the profile of NaCl concentration in function of the time could be determined. The model stopped when the concentration in the tank did not increase more than 5%.

5.4.4. Model parameters, variables and inputs

everal parameters such as diffusion coefficients and transport numbers in the membranes depend on the concentration of the solution or operating conditions. However, as the stack was difficult to handle and it was impossible to obtain some of the required experimental values, values obtained in the literature were used as a first approach (*Marcus 1997, Fidaleo et al. 2005, Firadaous et al. 2005, Ortiz et al. 2005*). Moreover, the ideal nature of the membranes was assumed to reduce the number of parameters needed (see assumption i). The list of all the parameters, inputs and

variables used in this work, as well as their value and the original source are shown in Table 5.10.

Table 5.10 .Inputs, variables and parameters of the model.

		Value	Reference
C_{d_i}	Input	Defined by user	
$C_{c\_i}(t=0)$	Input	Defined by user	
C_{d_o}	Variable	Calculated	
C_{c_i}	Variable	Calculated	
C_{c_o}	Variable	Calculated	
C_{d_cm}	Variable	Calculated	
C_{d_am}	Variable	Calculated	
C_{c_cm}	Variable	Calculated	
C_{c_am}	Variable	Calculated	
$C_{NaCl}^{sat}(25^0C)$	Parameter	359 g/L	
D	Variable	Calculated	
$D_{Cl^-\_am}$	Parameter	$6.52 \cdot 10^{-6}$ dm²/h	*Firdaous et al. 2005*
$D_{Na^+\_cm}$	Parameter	$4.93 \cdot 10^{-6}$ dm²/h	*Firdaous et al. 2005*
D_w	Variable	Calculated	
D_{w_am}	Parameter	$8.39 \cdot 10^{-5}$ dm²/h	*Firdaous et al. 2005*
D_{w_cm}	Parameter	$7.60 \cdot 10^{-5}$ dm²/h	*Firdaous et al. 2005*
F	Parameter	96,485 C/mol e-	
h_{Cl^-}	Parameter	3	*Marcus 1997*
h_{Na^+}	Parameter	4	*Marcus 1997*
I	Input	Defined by user	
k_m	Parameter	$7.7 \cdot 10^{-3}$ dm/s	*Ortiz et al. 2005*
M	Variable	Calculated	
M_w	Variable	Calculated	
Mw_{NaCl}	Parameter	58.5 g/mol	
Mw_{H_2O}	Parameter	18 g/mol	
N	Parameter	50	
Q_{d_i}	Input	Defined by user	
Q_{d_o}	Variable	Calculated	
Q_{c_i}	Input	Defined by user	
Q_{c_o}	Variable	Calculated	
$Q_{\tan k}$	Variable	Calculated	
Q_w	Variable	Calculated	
S	Parameter	10 dm²	
t_{Cl^-}	Parameter	0.603	*Fidaleo et al. 2005*
t_{Na^+}	Parameter	0.397	*Fidaleo et al. 2005*
t_{Cl^-am}	Parameter	1	
t_{Na^+cm}	Parameter	1	
t_f	Input	Defined by user	
t_w	Variable	Calculated	
V_{cell}	Parameter	Calculated	
$V_{\tan k}$	Parameter	250L – 100 L	
$\rho_{NaCl}^{sat}(25^oC)$	Parameter	1,198 g/L	
ρ_w	Parameter	1,000 g/L	
σ_{cm}	Parameter	$1.55 \cdot 10^{-3}$ dm	
σ_{am}	Parameter	$1.55 \cdot 10^{-3}$ dm	
η	Variable		

5.4.4. Results and discussion

As an initial step, the equations and solver used were shown to be stable and sensitive to variations in the parameters defined in Table 5.10. To do so, the model was run with the input values slightly modified and comparing the results, which did not show considerable deviations. Thus, the model was considered to be robust and able to be further validated with the experimental results obtained in the pilot plant

Two experiments were carried out to validate the model at the pilot plant at 40A (0.4 kA/m^2) and 30A (0.3 kA/m^2) with SWD-RO brine 2 as the feed solution at low inlet temperatures and 250L tank. The model was run using the same initial experimental input values in order to compare the results. The input values of the model (current density, inlet NaCl concentration, initial tank NaCl concentration, feed flow rate, concentrate flow rate and final time for the model) in the two cases are shown in Table 5.11.

As shown in Table 5.11, besides the current density used, the main difference between the two experiments carried out to validate the model was that the initial NaCl concentrations in the tank. After the first experiment at 40A, the concentrate tank could not be completely emptied and part of the concentrated brine remained in the tank, thus affecting the initial NaCl concentration of the experiment at 30A where this value was close to 80 g/L NaCl.

Table 5.11 Inputs of the model in the two runs at low inlet temperature (lower than 15ºC).

Parameter		Run at 40A	Run at 30A
Current density	kA/m²	0.40	0.30
Inlet NaCl concentration*	g/L	64.6	65.7
Initial tank NaCl concentration*	g/L	66.4	80.1
Feed flow rate	L/h	500	500
Concentrate flow rate	L/h	411	417
Final time for the model	h	40	45

* Approximate NaCl concentrations calculated based on the chloride ions present in the brine.

The experimental results and the predicted NaCl concentration in the tank are shown in Figure 5.12 and Figure 5.13. Although the model was designed in a very ideal basis and had several limitations, the predicted results accurately described the experimental values. In the second essay at 30A, some minor deviations were seen due to operating difficulties, which made it necessary to clean the cells frequently and stop and restart the process several times, thus slightly diluting the tank concentration. Nevertheless, the relative error between the predicted results and measured values was less than 2 % when low temperatures were used. Relative error of 10% was measured when inlet temperatures were 28ºC due to parameters deviation.
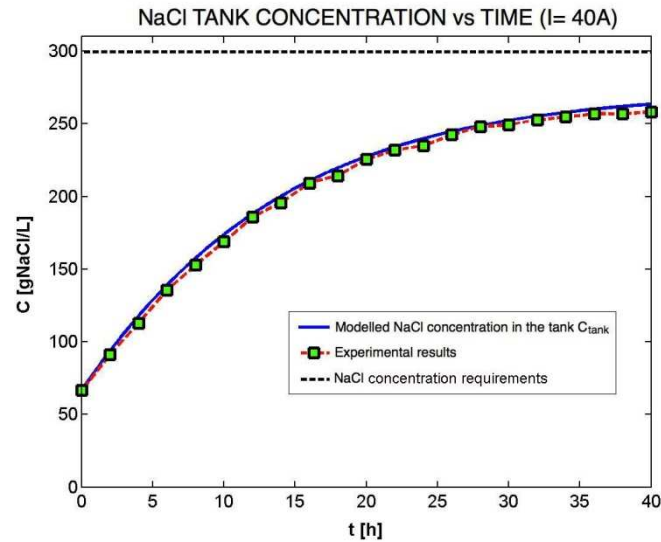
Figure 5.12. Experimental result and modelled tank concentration obtained at 40A (0.4 kA/m²)
and 10ºC
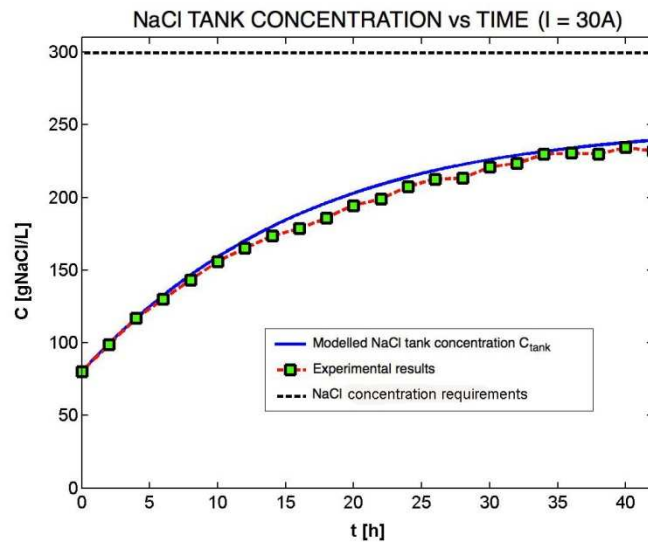
Figure 5.13. Experimental result and modelled tank concentration obtained at 30A (0.3 kA/m²)
and 14ºC.

The predicted results and experimental values obtained when the maximum NaCl concentration was reached in the tank at different current intensities evaluated are shown in Table 5.12. It can be seen that the predicted values are close to the experimental results, especially at low inlet temperatures. At inlet temperatures of 28ºC, higher concentration deviation can be observed, but time required to reach the maximum concentration and production obtained accurately fitted the experimental values. The minor deviations observed could have been due to the limitations of the ideal model assumptions made, specially the one considering the maximum efficiency of the process, and the parameter values used that were not measured experimentally. Scaling problems in the pilot plant, and temperature differences between modelled

and experimental values might have also caused these deviations. Fouling of the membranes was discarded after checking the membranes surface. This model was considered robust and useful to predict the performance of the NaCl concentration process in the pilot plant as well as the production overflow and time required to reach the maximum concentration. Nevertheless, this model could be further optimized by using experimental parameters to determine the performance at different temperatures and adjust concentration predictions..

Table 5.12. Comparison of experimental results and predictions of the mathematical model for SWD-RO brine concentration at a) low temperatures and b) high inlet temperatures

		a) Low temperature			
Parameter		**0.40 kA/m² (10ºC)**		**0.30 kA/m² (14ºC)**	
		Exp.	**Model**	**Exp.**	**Model**
Maximum NaCl concentration reached	g/L	258	264	234	239
Time required to reach maximum concentration	h	35	36	38	41
Production Qtank	L/h	13	12	9	10

		b) High temperature					
Parameter		**0.35 kA/m² (28ºC)**		**0.50 kA/m² (28ºC)**		**0.60 kA/m² (28ºC)**	
		Exp.	**Model**	**Exp.**	**Model**	**Exp.**	**Model**
Maximum NaCl concentration reached	g/L	210	247	244	274	261	288
Time required to reach maximum concentration	h	15	15	14	13	13	11
Production Qtank	L/h	15	12	18	16	19	18

The effects of ion diffusion and water osmosis in the concentration step were evaluated by using the model equations. Current intensities in the range of 30-40A were used as operating conditions, as are the usual values at the salt production plants of Japan.

As shown in Figure 5.14, the maximum concentration reached is limited by ion diffusion and water osmosis, given that the other phenomena remain constant during the concentrating process. Osmosis becomes more intense as the process goes on because the difference in concentration between the compartments increases until it reaches a maximum and then remains constant. When this maximum osmosis flux is reached, the maximum NaCl concentration in the tank is reached, as the total mass phenomena inside the stack reaches a steady state.
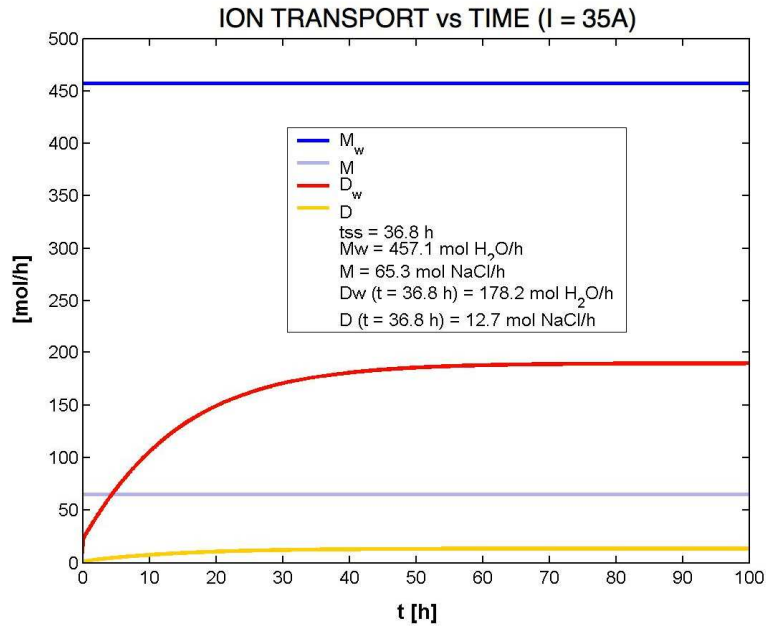
Figure 5.14. Modelled ion transport according to the different mass transfer phenomena taking place in the stack at 0.35 kA/m² when 250L tank is used. Inputs: Inlet NaCl concentration Cd_i = 65 g/L NaCl; Initial NaCl concentration in the concentrate tank Cc_i (t=0h)= 70 g/L NaCl; Diluate inlet flow rate Qd_i = 500 L/h; Concentrate inlet flow rate Qc_i = 410 L/h; Current intensity I = 35A; Final model timetf = 100 h). Mw: electrosmosis flux ; M: NaCl migration flux; Dw: osmosis flux; D: NaCl diffusion flux.

Finally, the effect of current intensities on the operating parameters that should be used in the pilot plant to reach the NaCl concentration requirements of the chlor-alkali industry (300g/L NaCl) was evaluated. The predicted tank concentration and time required to reach the maximum concentrations at different current intensities when 250L tank is used are shown in Figure 5.13.

As shown in Figure 5.15, the model predicted that between 60A and 70A (0.6-0.7 kA/m²) the NaCl requirement of 300 g/L NaCl would be reached after 25-28 h of operation with a 250L tank, this corresponded to 11h with 100L tank.. When 60A were used in the pilot plant, only 260 g/L of NaCl could be reached due to temperature limitations. Higher current densities could be evaluated in future works to obtain the threshold value of 300g/L NaCl.
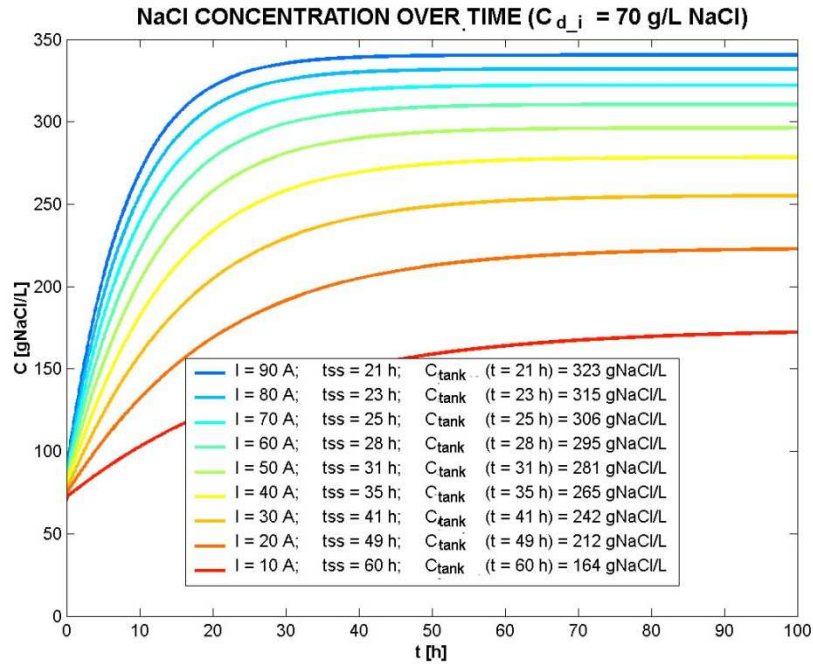
Figure 5.15. Modelled tank concentration and time required to reach the maximum concentration at different intensities when operating with 250L tank. Inputs: Inlet NaCl concentration Cd_i = 70 g/L NaCl; Initial concentrate NaCl concentration Cc_i (t=0h)= 70 g/L NaCl; Diluate inlet flow rate Qd_i = 500 L/h; Concentrate inlet flow rate Qc_i = 500 L/h; Final model time tf = 100h). I: current intensity; tss; time to reach the stationary state; Ctank: NaCl concentration in the concentrate tank

It can be observed that at higher intensities, the time required to reach the maximum concentration diminished and higher maximum concentrations were reached. This can be explained by the fact that the migration phenomenon is dependent on the current intensity applied, as shown in equation 5.6 and, as a result, at higher current densities more NaCl is transported. At the same time, more water is also transported and higher production flows are obtained. Nevertheless, due to the higher intensity used, energy consumption is also higher.

5.5. Conclusions

The experimental work done in the ED pilot plant shows that ED is a feasible membrane technology for concentration of SWD-RO brines. NaCl brines up to 244 g/L were achieved at 0.5 kA/m²with a energy consumption of 0.16 kW/kg NaCl at 28ºC when calculated in a continuous mode.

The single-pass configuration in the diluate and electrolytes circuits made it possible to work at higher current densities without reaching the LCD of the solution. Voltages obtained with SWD-RO brines were smaller than the ones reviewed in the literature, in consequence it was expected that energy consumption could be lower

when the plant will be totally optimized. Maximum operative current density was established by the stack manufacturer at 0.7 kA/m^2, however some operating problems occurred at current densities higher than 0.6 kA/m^2.

The ED membrane stack with selective Neosepta membranes made it possible to concentrate mainly NaCl in the concentration tank. CIMS and ACS membranes were proved to be highly selective to univalent ions. Higher NaCl concentrations could be reached at low inlet temperatures because, at higher inlet temperatures, brine densities changed and larger osmosis flux through the membranes could be obtained that slightly diluted the tank. Polyvalent ions in the tank were mainly diluted due to electro-osmosis and osmosis fluxes in the stack, reaching similar CFs in all the experiments carried out. Nickel and copper were an exception and got concentrated in all the experiences carried out because at the pHs evaluated, these ions were in form of univalent compounds. The brine obtained after the ED process needed further NaCl concentration (between 40-90 g/L NaCl should be added) and purification of calcium, magnesium, aluminium, copper, strontium and nickel.

It was necessary to maintain an acid pH in all circuits to avoid precipitation and consequently increase voltage and specific energy consumption. Decarbonation of concentrate tank was reached by lowering the pH to 5.5. Acid cleanings were done frequently to recover the flow rate and pressure of the stack that was reduced due to scaling.

The stack electrical potential depended on the inlet brine temperature. At higher temperatures, the voltage was reduced so energy consumption was also reduced. It was concluded that higher inlet temperatures were advantageous for brine concentration and that operation in a batch mode generated higher energy consumptions. In consequence, it was advisable to operate in a continuous mode at high temperatures to optimize the process.

The energy consumption of the pilot plant was in the range of the one generated by an industrial electrodialyzer to obtain solid salt from seawater and the values detailed in the literature. Nevertheless, higher NaCl concentrations were reached in the pilot plant. Additional research on energy consumption reduction is needed to optimize the process and meet the technical targets of 200 g/L NaCl with less than 0.12 kWh/kg.

The model developed using NERNST-PLANCK equations accurately predicted the maximum NaCl concentration when temperatures were lower than 25ºC, the time required to reach it, the production flow rate and the diluate concentration when inputs such as feed flow, feed concentration and intensity were given. The model was considered an useful tool to design future experiments. When temperatures were 28ºC, some deviations on the final concentration reached could be found but all other parameters were accurately predicted.

Nernst-Plank equations were simple and useful for determining the mass transfer phenomena inside the stack when SWD-RO brine was concentrated. Several assumptions were needed to simplify the equations used and some ideal conditions were considered to develop a very simple model.

Parameters taken from the literature were useful for the characterization of mass transfer. However, parameters should be determined experimentally to accurately fit the model at other temperatures and conditions.

The model was validated using data experimentally obtained in the concentration experiments at the pilot plant. Minor deviations in the modelled concentrations from the experimental points were caused by ideal assumptions in the model, differences in the parameters extracted from the literature, temperature differences, and/or scaling problems during operation. However, the model was considered valid to determine the NaCl concentration during all the experiments carried out at the pilot plant, given that the relative error was less than 2% at low temperatures and 10% at temperatures of 28ºC.

According to the model, when operating at a constant current intensity, the maximum concentration reached will be determined by ion diffusion and osmosis flux, given that the other mass transport phenomena remain constant during the experiment. When the maximum diffusion and osmosis are reached, the total mass phenomenon inside the stack reaches a steady state and the maximum NaCl concentration in the tank is reached.

At higher current densities, higher NaCl concentrations and flow productions can be reached because ion and water migration are only dependent on the intensity. However, higher energy consumption is required when working at higher current densities.

The model can be improved by determining experimental parameters according to our operating conditions, adding energy consumption calculations and considering other major ion interactions such as calcium and magnesium and possible precipitation phenomena.

Chapter 6

Brines purification by nanofiltration

Nanofiltration (NF) was tested in both types of brines described in Chapter 4 in order to remove polyvalent ions. The removal process of polyvalent ions from brines using nanofiltration is complex and it is still under debate. It depends on membrane characteristics and system operating conditions as well as electrostatic interaction between membrane and ions, ion size, pore size, diffusion fluxes, concentration gradients, solubility and dielectric repulsion (*Hilal et al, 2004*).

The main operating parameters that determine the results and rejections obtained in a nanofiltration process are (*Yacubowicz et al, 2005*):

• Pressure: it is the driving force responsible for NF process. The effective pressure is the supplied hydraulic pressure less the osmotic pressure applied on the membrane. NF is usually operated at 10 bar or higher.

• Temperature: Increasing temperature increases the permeate flux due to viscosity reduction. The rejection is not highly affected by temperature. At temperatures higher than 30C, some slight increase on rejection has been observed on highly concentrated brine nanofiltration due to concentration polarization reduction (*Madaeni et al. 2007*)

• Crossflow velocity: Increasing the crossflow velocity increases the permeate flux due to removal of fouling layer from the membrane surface. However, the maximum crossflow velocity is defined by the membrane construction.

• pH: In general, membrane can lose part of their charge at acidic pH as they are usually negatively charged. Moreover, pH can generate changes in the feed solution such as solubility or dissociation rate.

• Salinity: the increase of salinity will generate an increase of the effective pore radius of the membrane. Therefore, the rejection of monovalent ions will decrease as their concentration in the feed solution increases. The rejection of divalent ions will be less affected.

The major problems in nanofiltration are fouling and scaling due to microorganism adsorption or calcium precipitates on the membrane surface (*Hilal et al, 2004*). In order to avoid these problems, antiscalants can be added to the feed solution or cross-flow can be controlled to diminish these phenomena. Another problem when nanofiltration is used is concentration polarization on the surface of the membrane. Concentration polarization can be defined as the phenomenon that occurs when an ion is highly rejected by the membrane and covers its surface, creating a concentration gradient and reducing the pass of other ions due to the electric interactions. To minimize this phenomenon, high turbulent flow may be created on the membrane surface in order to remove the ions. Drawbacks of nanofiltration and its limitations when industrially applied have been described by Van der Bruggen *et al.* (2008).

Finally, nanofiltration was evaluated to remove polyvalent ions from SWD-RO and mine brines. Selectivity and removal efficiency of nanofiltration was evaluated using both a pilot plant and laboratory equipment. Different inlet pressures were evaluated in order to optimize the removal process and to obtain the highest production capacity. Energy consumption was also evaluated in the pilot plant.

6.1. Potash mine brine nanofiltration using flat-sheet membranes

6.1.1. Materials and methods. Laboratory equipment.

Nanofiltration experiments in the lab were carried out to determine if at low pressures some useful purification could be reached when using collector brine. In order to test the purification of brines by nanofiltration, a NF lab device was used in the Technologic Center of Manresa (CTM). The nanofiltration system consisted of a GE SEPA CF II flat module of 140 cm^2 of active area fed with Hydracell G03X pump that provided continuous inlet flow. The solution was pumped from a refrigerated tank of 25L were all the currents were recirculated, as can be seen in Figure 6.1. The feed solution was maintained around 25ºC throughout the experiments and mixing was assured by continuously stirring the feed solution. Pressure, flow rate, conductivity and pH were continuously recorded from different streams in order to determine the performance of the system. The pressure of the system was manually fixed using the valve in the concentrated stream; pressures in

the range of 10-30 bar were tested. Samples from the permeate stream were taken periodically when the conductivity was steady and were analyzed using ionic chromatography Dionex ICS1000 AS23 and CS16. In Figure 6.2 some pictures of the NF system used can be found.
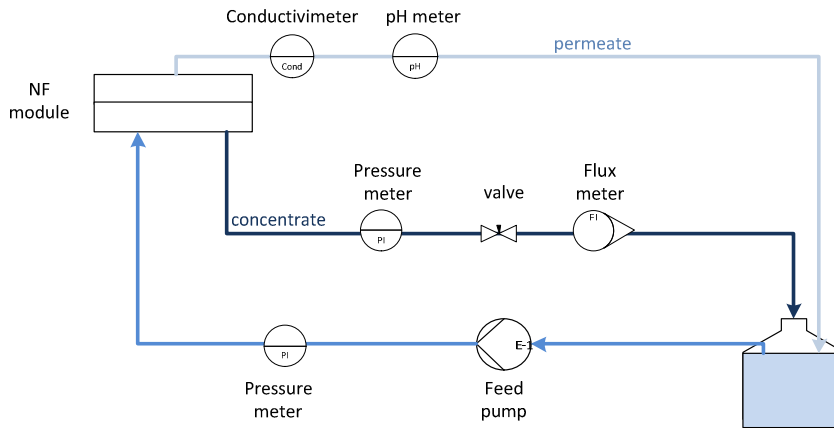
Fig. 6.1. Scheme of the flat-sheet NF membrane laboratory set-up.
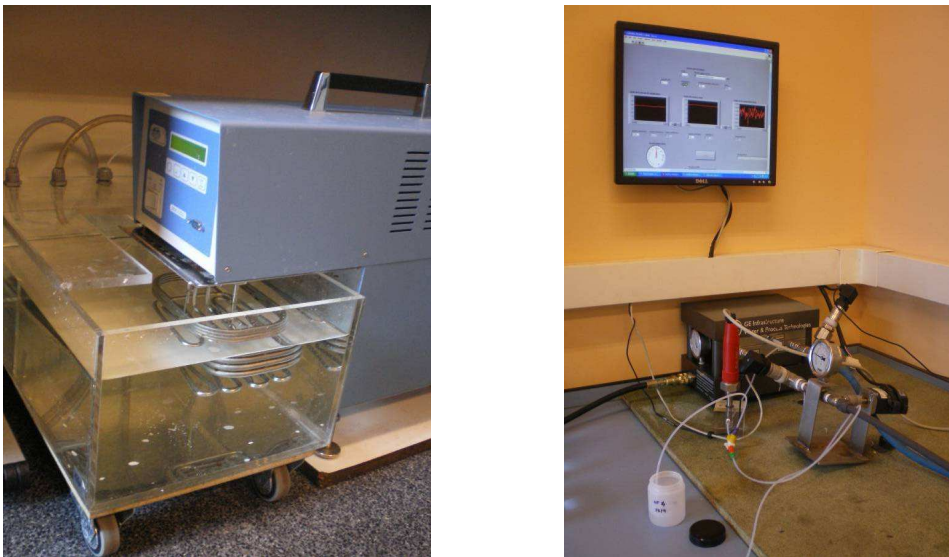
Fig. 6.2. Pictures of the flat-sheet NF membrane laboratory set-up used

The NF module was assembled according to the scheme of Figure 6.3. A spacer of 47 mil was used to improve the mass transfer on the membrane surface by creating turbulence. No shim was needed in the experiments carried out. The shim is a metallic piece used to fill the empty space between the cell bottom and the membrane, so inlet flux gets introduced tangentially on the membrane. Inlet flow was tested from 300 L/h (21.4 m^3/m^2h) to 540 L/h (34.3 m^3/m^2h), which corresponded to a superficial velocity (cross-flow) on the membrane surface of 1.25 to 1.75 m/s approximately.

NF270 and experimental (XUS) membranes kindly supplied by DOW were used in the experiments carried out to purify the brines. NF270 is membrane composed of a semiaromatic piperazine-based polyamide layer on top of a polysulfone microporous support reinforced with nonwoven polyester (*Pereira, 2006*). It is commonly used in the removal of organics from surface and ground waters, and presents medium rejection of calcium and magnesium but low rejection of sodium chloride. XUS membrane was an experimental membrane for seawater pretreatment and in consequence, it was designed for high ionic strength solutions and high calcium and magnesium rejection. Composition of XUS membranes was not provided.
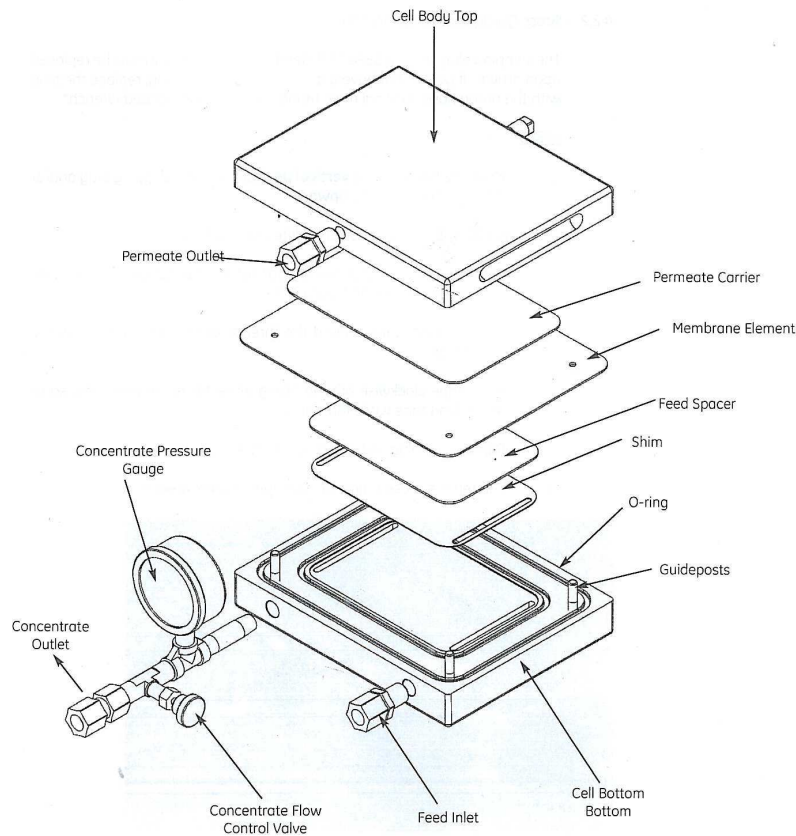
Fig. 6.3. Assembling diagram of the flat-sheet NF module. (source: GE)

6.1.2. Data analysis. Determination of permeate flow rate, reject and selectivity.

Permeate flow rate (PFR) was manually calculated considering the active area of the membrane and using the equation 6.1.

$$PFR = \frac{V_{permeate}}{t \cdot A_{membrane} \cdot P} \tag{6.1}$$

Where $V_{permeate}$ is the volume of permeate recollected during the time (t), $A_{membrane}$ is the active area of the membrane and P is the pressure of the system in bar.

Reject (R) and selectivity (α) of the membranes to a solute A were calculated using the equations.

$$R = \left(1 - \frac{C_{permeate}}{C_{feed}}\right) \cdot 100 \tag{6.2}$$

$$\alpha_{A/B} = \frac{100 - R_A}{100 - R_B} \tag{6.3}$$

6.1.3. Experimental results for flat-sheet membranes

Nanofiltration was tested using two membranes NF270 and XUS from DOW on the mine brine detailed in Chapter 4 to determine its purification viability. No pH correction or antiscalant additions were done to the sample used, which was pH 7.5. The results obtained when stationary state was reached in the different operating conditions can be found in Table 6.1 and Table 6.2. It can be observed from these tables that nanofiltration mainly removed polyvalent ions, as expected, and that it was not necessary to operate at high pressures to obtain high rejections. No fouling or scaling was observed in the membranes after the experiment; however, longer operation times should be tested in order to evaluate these phenomena at higher scales.

Table.6.1 Results obtained with the NF270 membrane using different operation conditions.

NF270	Transmembrane Pressure (bar)	Inlet flow (m³/m² h)	Permeate Flow (L/m²h)	PFR (L/m² h bar)	$\alpha_{Cl/SO4}$	% Rejection				
						Ca (II)	Mg (II)	S (VI)	Na (I)	Cl (-I)
1	9	21.4	7.3	0.8	7.7	15.3	60.1	87.3	3.6	2.6
2	10	34.3	8.5	0.8	8.4	15.5	60.5	88.5	2.6	3.5
3	20	21.4	20.0	1.0	13.2	28.9	70.2	92.8	6.2	5.1
4	20	34.3	20.4	1.0	13.4	27.6	70.1	92.8	3.9	3.3
5	30	21.4	32.6	1.1	15.0	35.5	73.3	93.9	8.6	9.3
6	30	34.3	33.6	1.1	14.8	34.5	74.5	93.9	5.8	9.7

Table 6.2. Results obtained with the XUS membrane using different operation conditions.

XUS	Transmembrane Pressure (bar)	Inlet flow (m³/m²h)	Permeate Flow (L/m²h)	PFR (L/m² h bar)	$\alpha_{Cl/SO4}$	% Rejection				
						Ca (II)	Mg (II)	S (VI)	Na (I)	Cl (-I)
1	9	21.4	3.0	0.3	9.1	25.7	71.2	89.2	-0.4	1.7
2	10	34.3	4.0	0.4	9.4	26.7	71.4	89.9	-0.7	5.1
3	20	21.4	9.5	0.5	16.0	44.6	84.2	93.9	-0.5	2.3
4	20	34.3	12.0	0.6	16.7	46.7	84.8	94.1	1.1	1.3
5	30	21.4	22.2	0.7	20.0	56.8	88.0	95.4	2.4	7.8
6	30	34.3	22.4	0.7	23.6	53.5	87.6	96.1	-5.6	8.3

The negative sodium rejections using XUS membrane can be explained due to the Donnan effect of electromigration. It can be observed that XUS membrane had high rejection of calcium and magnesium and, in consequence, sodium was concentrated in permeate in order to maintain the chemical equilibrium of the solution. This effect is beneficial for the reuse of this brine in the chlor-alkali industry, where almost purely saturated NaCl brine is needed.

It can be observed from Table 6.1 and Table 6.2 that XUS membrane had higher rejections in all cases studied but much lower permeate fluxes. Selectivity of XUS towards chloride was also higher than the one showed by NF270 and XUS rejected much more calcium than NF270.

In Figure 6.2, comparison of PFR and selectivity of NF270 and XUS membranes according to transmembrane pressure and inlet flow used can be found. It can be observed that in general terms, at higher inlet flows, more permeate flow and higher rejections of undesired ions could be obtained. The same occurred with the pressure, but an optimum should be searched for energy consumption in higher scales.
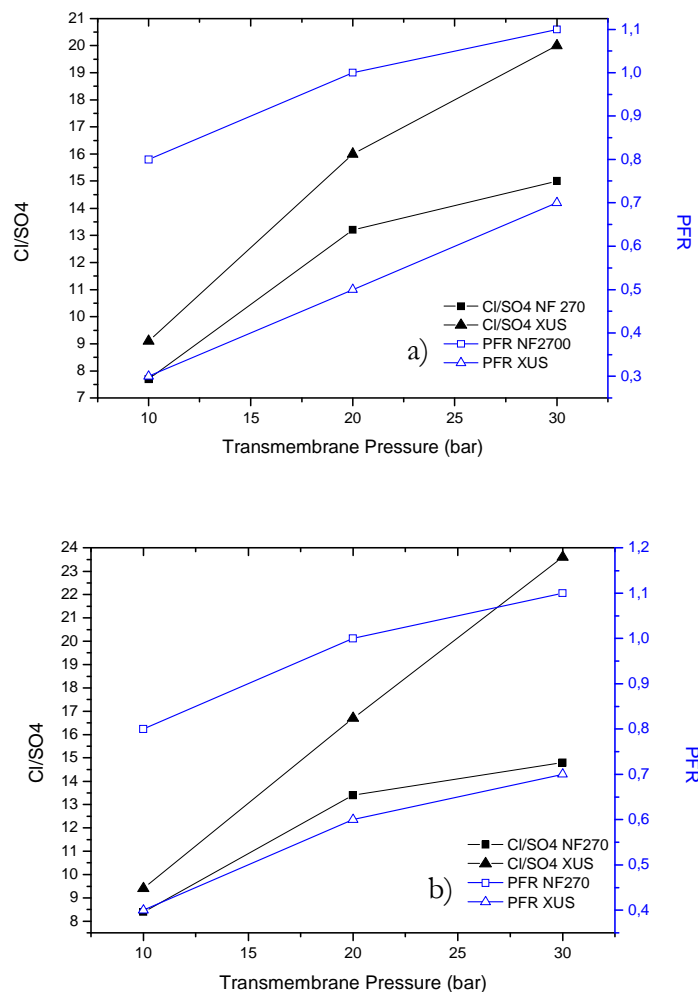

Fig. 6.2. Selectivity and PFR (L/m^2 h bar) of the NF270 and XUS membranes as a function of transmembrane pressure when a) inlet flow is 21.4 m^3/m^2h or b) 34.3 m^3/m^2h of collecting pipe brine.

Although high rejections were obtained with nanofiltration, the composition requirements for the reuse of the brine in the chlor-alkali industry were not achieved in any case tested in the lab. Since high permeate flow was desired in the NF pilot plant in order to feed the ED pilot plant, it was decided to study the purification of SWD-RO brines with NF270 membranes, that provided more flux. It can be observed in Figure 6.2 that NF270 selectivity towards chloride ion quickly increased from 10 to 20 bars, but this increase slightly diminished from 20 to 30 bars. The same occurred with permeability. This fact makes us suppose that the optimal operation pressure would be somewhere between 20 and 30 bar for the mine brine tested. This fact should be confirmed with more experiments. However, as it was difficult to transport and get samples from the mine brine as well as the brine had a variable composition, it was decided to focus the next experiments on the SWD-RO brine.

6.2. SWD-RO brine nanofiltration using spiral wound modules.

6.2.1. SWD-RO brine composition and nanofiltration membranes used.

The NF pilot plant was fed with the SWD-RO brine obtained from desalination of Mediterranean seawater in the Desalination Plant of Barcelona. Composition of this brine is further detailed in Chapter 4.

The design of the pilot plant was done in collaboration with DOW using the software ROSA. Although ROSA was not validated for high salinity brines, it was used as a first step for NF design in the worst-case scenario. The objective of the design was to achieve enough brine to feed the ED plant. In consequence, from the membranes previously tested in the lab equipment and the previous work reviewed (*Hilal et al., 2005*), NF270 membranes were chosen according to their higher production flux and medium hardness removal capacity.

NF270 membrane is composed of a semiaromatic piperazine-based polyamide layer on top of a polysulfone microporous support reinforced with nonwoven polyester (*Pereira, 2006*). The main characteristics of these membranes and operation conditions described by the manufacturer can be found in Table 6.3; these membranes were kindly supplied by DOW to develop this thesis.

Table.6.3. NF270 4040 characteristics and operation parameters of the pilot plant

Membrane Type	Polyamide Thin-Film Composite
Maximum Operating Temperature	45°C
Maximum Operating Pressure	41 bar
Maximum Feed Flow rate	3.6 m³/h
Maximum Pressure Drop	1.0 bar
pH Range, Continuous Operation	2 – 11
pH Range, Short-Term Cleaning	1- 12
Maximum Feed Silt Density Index	SDI 5
Free Chlorine Tolerance	< 0.1 mg/L

6.2.2. NF pilot plant description and operation.

The inlet brine flow rate was approximately 1250 L/h (33 L/m^{2}h) of SWD-RO brine which was previously filtered with 5 microns filter. In order to treat this feed stream, five NF270 4" 40" were used in serial, as detailed in Figure 6.3. The total effective area for the pilot plant was 38 m^2 of active membrane. Conductivity and flow rate of the feed stream was continuously monitored and registered. Parameters monitored from the different streams are detailed in Figure 6.3.

Recovery rate was determined with a valve in the reject flow. The pilot plant was designed to test different inlet pressures up to a maximum of 40 bars, limited by the maximum operating tolerance of the membranes. Nevertheless, 20 bars was the maximum value operated as higher pressure could not be obtained due to the fixed inlet flow.

All the materials used in the construction of the pilot plant were especially chosen to resist corrosion of highly concentrated brine and to resist high pressures in order to prevent membrane deterioration.
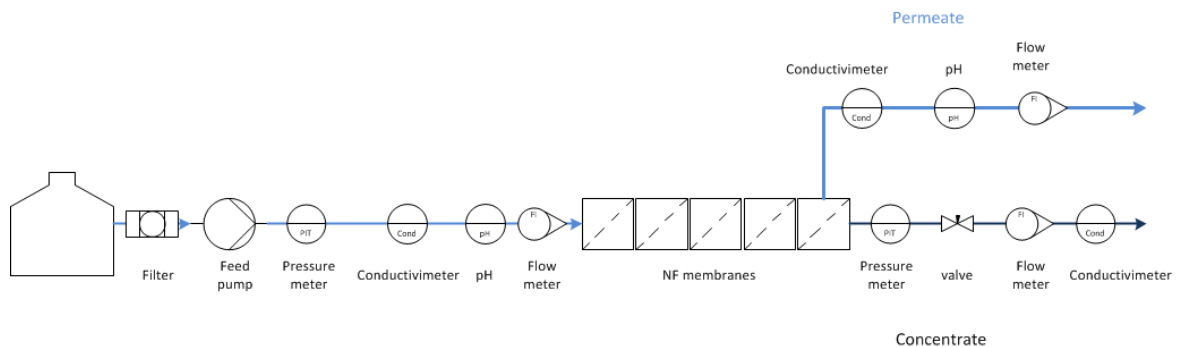

Fig. 6.3. Scheme of the NF pilot plant of Barcelona

Fig.6.4 Picture of the NF pilot plant

The NF pilot plant was operated for 24 hours a day with an automatic control of the main parameters. Different inlet pressures were evaluated in the range of 8 to 20 bar. The parameters monitored during the operation of the pilot plant are detailed in Table 6.4. pH and temperature were measured in all the flows to control the performance of the plant. Permeate flow was maintained at pH between 6 and 7.5. 1 mg/L of antiscalants were added to the feed brine in order to avoid calcium and sulphate precipitation. The antiscalant addition was small because the brine already contained the antiscalants of the reverse osmosis process.

Samples of feed brine, permeate and reject brine were collected twice a day when the system was stabilized after 48h of continuous operation. Flushing with permeate of the NF process or tab water was done every time the plant was shut down. Cleaning with acids or bases to remove precipitation or fouling was done when the salt removal efficiency was reduced by 10%, the nominal permeate flux diminished by 15% or when the difference between inlet and outlet pressure was higher than 15%. Temperature of the cleaning solutions could be controlled with a resistance in the feed tank to increase their cleaning efficiency.

Table 6.4. Parameters monitored during NF pilot plant operation

Feed flow	Concentrate flow	Permeate flow
Pressure	Pressure	Flow rate
Flow rate	Flow rate	Conductivity
Conductivity	Conductivity	Pressure
Temperature	Temperature	Temperature
pH		pH

6.2.3. Analytical methodologies and chemical analysis.

The sodium chloride, sulphate, calcium and magnesium levels in the samples were analyzed using different analytical methods Chloride was determined through precipitation with $AgNO_3$ and a silver chloride electrode in a METHROM 721 instrument. Calcium and magnesium were analyzed through atomic absortion using *AAnalyst 300* Perkin Elmer. Sulphate was determined by ionic chromatography using 761 Compact IC Methrom with the column Anion Dual 2-6.1006.100. Sodium chloride was determined by chemical balance of the major ions of the solution. Trace metals like aluminium, copper, iron, nickel and strontium were determined using ICP-OES Variant 725. Potassium was determined also with ICP-OES. Detection limits were determined at 0.0225 mg/L of aluminium, 0.007 mg/L of copper, 0.0375 mg/L of iron, 0.0011 mg/L of potassium, 0.0150 mg/L of nickel and 0.0075 mg/L of strontium.

6.2.4. Data analysis. Determination of permeate flow rate, rejection and selectivity .

Permeate flow rate (PFR) was calculated according to equation 6.4, rejection (R) and selectivity were calculated according to equations 6.2 and 6.3 described in section 6.2.2.

$$PFR = \frac{Q_{permeate\ at\ 25^{\underline{a}}C}}{A_{membrane} \cdot P} \qquad (6.4)$$

Where $Q_{permeate}$ is the permeate flow rate obtained at 25ºC, $A_{membrane}$ is the total area of membranes (38 m^2) and P is the pressure of the system (bar). The normalized permeate flow rate at 25ºC was calculated through the program FTNORM supplied by Dow Chemical (*Dow, 2011*) that provides for automatic standardization of operating data.

6.2.5. Experimental results of brine purification using spiral wound NF membranes.

6.2.5.1. Purification performance

The NF pilot plant was operated using different inlet pressures from 8 to 21 bar. Pressures higher than 21 bars were not used because of the fixed inlet flow rate that limited operating at higher pressures in the pilot plant. General results obtained when the system was stabilized after some days of continuous operation are detailed in Table 6.5. pH of the inlet brine was kept constant at around 7, where permeability and retention properties have been reported optimum for NF270 membranes (*Mänttäri et al. 2004*). In Figure 6.5 and Figure 6.6, rejection of major and minor elements of the SWD-RO as a function of the transmembrane pressure is represented.

Table 6.5. General purification results obtained with Barcelona NF pilot plant using SWD-RO brine.

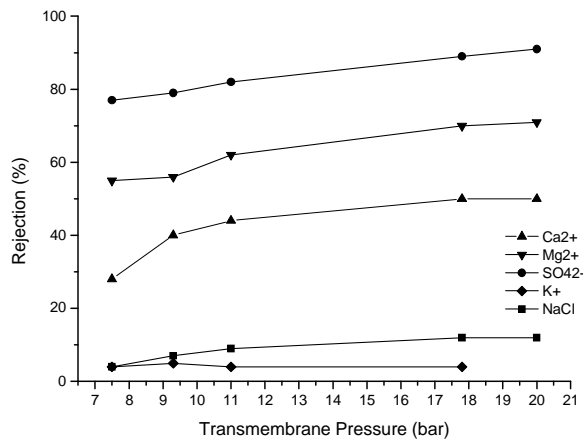| Transmembrane Pressure (bar)	Permeate Flow at 25ªC (L/m²h)	PFR (L/m²h bar)	Water Recovery %	α$_{Cl/SO4}$	% Rejection at 22-26ºC								
					Ca (II)	Mg (II)	S (VI)	K (I)	Al (III)	Sr (II)	Cu (II)	Ni (II)	NaCl
7.5	8.7	1.2	25%	4.2	28	55	77	4	>33	33	17	0	4
9.3	13.9	1.5	42%	4.4	40	56	79	5	>33	41	23	0	7
11	15.7	1.4	46%		44	62	-	4	>33	47	33	10	9
14.5	19.7	1.4	62%	4.8	50	65	80	-	-	-	-	-	10
17.8	23.7	1.3	74%	8.0	50	70	89	4	>33	70	66	23	12
20	25.0	1.3	76%	9.8	50	71	91	5	>33	70	66	35	12

Fig. 6.5. Rejection of major elements from SWD-RO brine as a function of transmembrane pressure applied.
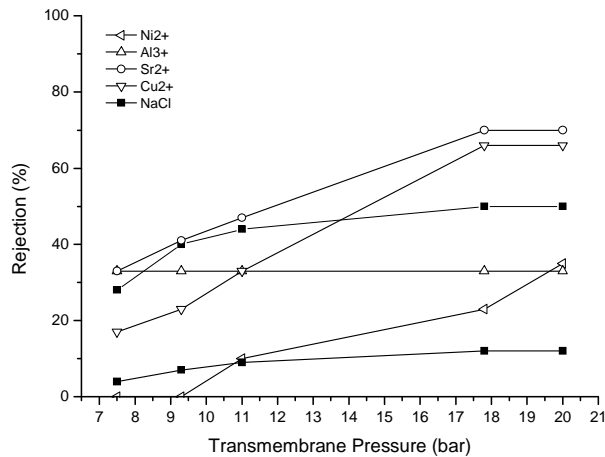
Fig. 6.6. Rejection of minor elements from SWD-RO brine as a function of transmembrane pressure applied.

It can be observed from Table 6.5 that permeate flow increased with pressure, but PFR reached a maximum between 10 and 15 bar. Pure Water Permeability (PWP) of NF270 membrane was determined by Hilal *et al.* (2005) at 27.45 L/m^2 h bar, so due to the high salinity of the SWD-RO brine, it was reduced by 18 times when SWD-RO reject was used, reaching a maximum of 1.5 L/m^2 h bar.

Rejection of univalent ions was lower than polyvalent ions, as can be observed from Figures 6.5 and 6.6. . Selectivity towards chloride ions increased in the pressure range studied. Rejection of polyvalent ions generally increased with pressure in the range studied, but undesired NaCl rejection was increased reaching a maximum of 12% at 20 bar. Major ion rejection got more or less steady at 18bar, but minor elements rejection increased from 18 to 20 bar. Rejection order with SWD-RO brine at 20 bar was S (VI) > Mg (II) > Sr (II) > Cu (II) > Ca (II) > Ni (II) > Na (I) > K (I). NF270 is a negatively charged membrane, so higher rejections are obtained with anions. Ionic size, shape and initial concentration play a significant role in rejections

obtained. When high concentrated brines are used, screen phenomenon strongly happens on membrane surface and Donnan effect of electric repulsion is minimized. Counter ions screen membrane surface charge and in consequence, sieving becomes the significant mechanism for ion rejection (*Madeni et al., 2009*), ions with lower hydrated radius like Na^+ and K^+ would be less rejected that the other ions from the brine (*Hussain et al., 2007*). It has to be pointed out that at high concentration, formation of ion pairs is significant and their radii are different from the radii of the free ions. Speciation of ions represented in Table 6.6 shows that most of the ions studied are not present in charged form, but high rejections can be obtained anyway confirming the sieving effect.

In conclusion, despite the complex mechanism of rejection that occurs on nanofiltration, ion size can be used as a first step to predict the performance of NF. In Table 6.6, hydrated radius, especiation of ions and rejection obtained at 20 bar can be found. It can be observed that ions with higher hydrated radius tend to have higher rejection than all other ions.

Table 6.6. Hydrated radius of ions studied, especiation and rejection obtained with SWD-RO brine at 20bar.

Element	Especiation of ions in the inlet brine	Considered Form	Hydrated radius (nm) *	Rejection at 20 bar
K(I)	K^+ (0.82) KCl_{aq} (0.18)	K^+	0.275	5%
Na(I)	Na^+ (0.98) $NaSO_4^-$ (0.02)	Na^+	0.365	12%
Ni(II)	$NiCl_2$ (0.73) $NiCl^+$ (0.18) Ni^{2+} (0.07) $Ni(OH)_{2\ aq}$ (0.02)	Ni^{2+}	0.6	35%
Ca(II)	Ca^{2+} (0.45) $CaCl^+$ (0.35) $CaSO_{4(aq)}$ (0.20)	Ca^{2+}	0.349	50%
Cu(II)	$CuCl^+$ (0.48) $CuCl_2$ (0.28) Cu^{2+} (0.17) $CuSO_{4aq}$ (0.07)	Cu^{2+}	0.6	66%
Sr(II)	Sr^{2+} (0.65) $SrSO_{4aq}$ (0.30) $SrSO_{4(s)}$ (0.05)	Sr^{2+}	0.410	70%
Mg(II)	Mg^{2+} (0.65) $MgSO_{4\ aq}$(0.35)	Mg^{2+}	0.429	71%
Al(III)	$AlSO_4^+$(0.60) $Al(OH)^{2+}$ (0.12) $AlOH^{+2}$ (0.11) Al^{3+} (0.11) $Al(SO_4)^{2-}$ (0.6)	Al^{3+}	0.9	>33%
Cl(-I)	Cl^-(1)	Cl^-	0.347	12%
S(VI)	$MgSO_{4aq}$ (0.70) $NaSO_4^-$ (0.18) SO_4^{2-} (0.4) $CaSO_{4aq}$ (0.8)	SO_4^{2-}	0.380	91%

Source: Madeni et al. 2007, Tansel et al. 2006 and Kielland 1937

Rejections are also slightly dependent on inlet temperature, especially when it is higher than 30ºC , due to concentration polarization reduction (*Madaeni et al, 2007*). All tests in the pilot plant were carried out between 22-26ºC and flow rates were normalized so, the results obtained can be considered comparable. It can be observed that the highest rejections were obtained at 20bar. Moreover, higher production fluxes were obtained at this pressure, so this point was considered the optimal operation parameter.

At 20 bar, brine with approximately 415 **mg/L** of calcium, 760 **mg/L** of magnesium, 500 **mg/L** of sulphate and 52 g/L of NaCl was obtained, as can be seen in Table 6.7, where composition of the SWD-RO obtained as a function of transmembrane pressure is compared to the membrane electrolysis cell requirements. The concentrations obtained were far from the requirements of the membrane electrolysis cell but were useful for a primary purification step, especially before the ED concentration where precipitation problems related to calcium carbonate and sulphate were observed when pH was not controlled. Further treatments like primary precipitation and ion exchange resins would be advisable to reuse this brine. Calcium, magnesium, niquel and copper needed further treatments to be removed.

Table 6.7. Comparison of brine composition obtained in the NF pilot plant and electrolysis cell requirements.

Brine composition obtained	SWD-RO brine	8 bar	10bar	12bar	18bar	20 bar	Membrane cell requiremens
NaCl (g/L)	59	57	55	54	52	52	300
K (I) (g/L)	0.7	0.7	0.7	0.7	0.7	0.7	-
Ca (II) (mg/L)	830	*598*	*498*	*465*	*415*	*415*	0.02
Mg (II) (mg/L)	2,600	*1,200*	*1,160*	*1,000*	*920*	*760*	
S (VI) (g/L)	5.4	1.2	1.1	1.1	0.6	0.5	8
Al (III) (mg/L)	0.3	*DL*	*DL*	*DL*	*DL*	*DL*	0.1
Ni (II) (mg/L)	0.07	*0.03*	*0.03*	*0.027*	*0.023*	*0.015*	0.01
Sr (II) (mg/L)	16	*9.2*	*8.1*	*7.3*	*6.6*	*6.5*	0.4
Cu (II) (mg/L)	0.03	*0.02*	*0.02*	*0.02*	*0.01*	*0.01*	0.01

DL: 0.0225 mg/L of aluminium

Results obtained with NF270 membranes at the pilot plant were compared with the results obtained negative charged membranes similar to NF270. Madaeni *et al.* (2007) treated saturated chlor-alkali brine for calcium, magnesium, sulphate and iron removal, Hilal *et al.* (2005) studied NF for seawater desalination with synthetic solutions of 25 g/L NaCl, Eriksson *et al.* (2005) studied NF for SWD-RO pre-treatment, Telzhensky *et al.* (2011) studied NF for magnesium recovery of seawater and Bader (2007, 2008) treated seawater and Paradox Valley Brine for sulphate

removal. Composition of the inlet brines used in these works is summarized in Table 6.8. Results obtained at the optimal operation point in the NF pilot plant are compared to the purification results of these works in Table 6.9. Results at 7.5 and 21 bar from the pilot plant are detailed in Table 6.9, so comparison with the work reviewed at the same operation conditions can be done.

Hilal *et al.* (2005) determined that at higher inlet concentrations, lower rejections could be observed due to concentration polarization. It can be observed that, in general terms, SWD-RO brine nanofiltration present slighlty lower polyvalent ion rejections than seawater nanofiltration but higher rejections that the other concentrated brines studied. Concentration polarization occurs when the convective flux that forces the ion pass through the membrane and the diffusion flux of ions from the membrane to the bulk solution are unbalanced, creating an accumulation of ions on the membrane surface. In consequence, lower rejections can be observed due to ion repulsions. In order to reduce this phenomenon, higher inlet flow to create turbulence on the membrane surface can be used. In consequence, solution on membrane surface is renewed and less accumulation is produced.

It can be observed from Table 6.9, that rejections obtained in the pilot plant are in the range of the values reviewed when highly concentrated brines are used. NF270 presented a reduction of permeate flow when SWD-RO brine was used because of the high salinity flow used. Permeates flow obtained with seawater were up to 5 times higher than the one obtained in the pilot plant, but rejection of NaCl were also higher.

Madeni *et al.* (2007) used different membranes to treat saturated chlor-alkali brine and optimized the purification results. The optimal point for Madaeni *et al.* (2007) to treat the brine was determined at 8 bar when PVD Hydranautics membranes were used. It can be observed that NF270 had lower permeate flow at the same pressure but rejections were similar in all ions analyzed. NF270 rejected more NaCl than most of the membranes reviewed; this was not considered significant, as the next treatment step for the SWD-RO brine should be a selective concentration to saturate it at 300g/L NaCl.

If ED concentration step was done before NF treatment, lower rejections could be expected, as concentration polarization phenomena would increase. It can be observed that higher inlet concentrations lead to slightly lower rejections and fouling/scaling phenomena increased. Moreover, ED also concentrated some minor elements like nickel and copper and higher rejections would be required during the post-treatment step.

Table 6.8. Composition of the brines used in the works reviewed.

Brine composition	Eriksson *et al.* (2005), Abdullatef *et al.* (2007), Telzhensky *et al.* (2011) *	Hilal *et al.* (2005)	Bader (2007)	Bader (2008)	Madeni *et al.* (2007)	This work
NaCl (g/L)	35	25	35	220	290	59
K (I) (g/L)	0.7	-	0.7	4.2	-	0.7
Ca (II) (mg/L)	530	-	530	1.380	8.4	830
Mg (II) (mg/L)	1642	-	1642	1.500	9.2	2,600
S (VI) (g/L)	3.6	-	3.6	5.9	8	5.4
Fe (II, III) (mg/L)	-	--	-	0.25	0.8	< 0.2
Sr (II)(mg/L)	15	-	15	26.4	-	16

* SW approximate composition

*Table 6.9. Comparison of chlor-alkali brine nanofiltration with two different membranes*

Reference	Membrane	L:Lab plant P:Pilot plant	Pressure (bar)	Recovery (%)	Permeate Flow at 25ªC (L/m²h)	% Rejection					
						Ca (II)	Mg (II)	S (VI)	K (I)	Sr (II)	NaCl
This work	NF270	P	7.5	25%	9	28	55	77	4	33	4
			21	76%	25	50	71	91	5	70	12
Hilal et al. (2005)	NF270	L	9	n.s	50	-	-	-	-	-	10
Eriksson et al. (2005)	DK8040F	P	25	65%	43	91	98	99	-	-	-
Abdullatef el al. (2007)	n.s.	P	-	50%	n.s	82	95	99	-	-	11
Telzhensky et al. (2011)	DS-5L	P	14	50%	n.s	35	56	92	8	-	7
	NE2540-70		14	50%	n.s	56	82	98	-1	-	8
Bader (2007)	n.s	P	-	30-40%	n.s	50	69	98	17	58	16
Bader (2008)	n.s	L	30	n.s	n.s	42	71	99	15	63	8
Madeni et al. (2007)	PVD	L	8	n.s	16	32	40	-	-	-	1

*n.s. not specified.

SWD-RO brine NF pilot plant was operated in a continuous mode during two months and no decrease on permeate flow or increasure on pressure indicating fouling on membrane surface was observed. Pilot plant is still on operation to evaluate the fouling and scaling phenomena, after some months of operation, analysis of membrane surface will be carried out to determine scaling and fouling potential of the treatment system.

6.2.5.2. Energy consumption

Energy consumption depending on the pressure applied can be found on Figure 6.7. It can be observed that power consumption decreased when increasing pressure, as the amount of permeate produced increased too. Moreover, energy consumption was maintained steady at 3 kWh/h during all tests, which corresponded to the minimum energy consumption of the high-pressure pumps. At higher pressures this consumption should increase, but it could not be tested in the pilot plant during the realization of this thesis. In consequence the optimum of power consumption in the pilot plant was obtained around 20 bar at 3.2 kWh/m^3, from this point on the reduction of power consumption was not considered significant. Adding some energy recovery systems in the concentrate stream produced could reduce this energy consumption and make the process economically feasible.
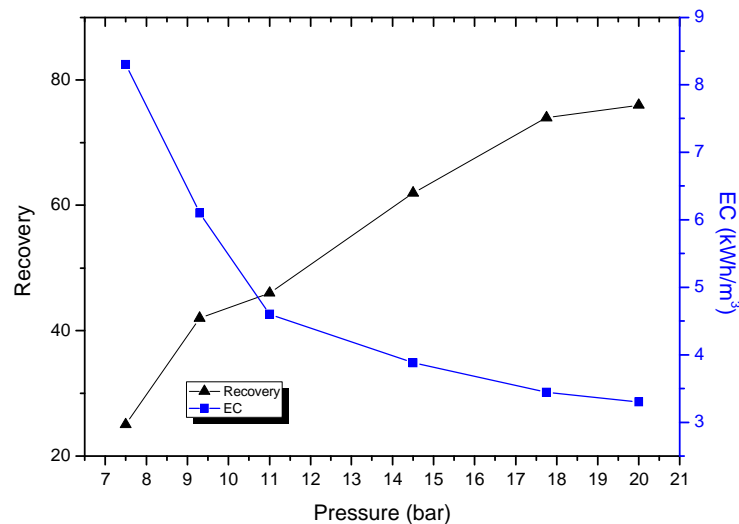
Fig.6.7. Energy consumption and recovery obtained in function of the transmembrane pressure applied on the NF pilot plant.

Taking that into account, it was concluded that the optimum operation point, both in terms of economics and element purification performance, would be at 20 bar in the pilot plant. Higher pressures should be tested in future experiments with a modified pilot plant to determine if the optimal operation point would be somewhere higher.

6.3. Conclusions

Nanofiltration has been tested with the two types of brines: potash mine brine and SWD-RO brine rejects. NF of collector brine was carried out in the lab using two membranes, NF270 and XUS, in a flat sheet membrane equipment. SWD-RO brine nanofiltration was carried out in the NF pilot plant designed with NF270 spiral wound membranes.

Nanofiltration of collector brine was evaluated in the range of 10 to 30 bar, reaching an optimum operation point between 20 and 30 bar, where selectivity towards sodium chloride reached a maximum. Slightly higher rejections of undesired ions were obtained with XUS membranes, that were special for highly concentrated solutions treatment; nevertheless, higher permeate flow was obtained with NF270 membranes. Concentration of univalent ions was observed when using XUS membranes due to Donnan effect. No scaling or fouling was observed on membrane surface after all the experiments carried out.

NF270 was considered more suitable for the design of brine treatment as more steps would be needed to purify the brine and higher fluxes would be required. Rejections in the range of 35% of calcium, 74% magnesium, 94% sulphate, 7% of sodium and 9.5% chloride were obtained with NF270 at 20-30bar. Calcium and magnesium should be further purified to reach the requirements..

NF pilot plant was designed for SWD-RO brine treatment; it was operated in the range of 8 to 21 bar with 1.25 m^3/h inlet flow. Temperature was maintained in the range of 22-26ºC in all the experiments carried out. Higher pressures could not be evaluated during this thesis as fixed inlet flow limited the maximum operating pressure to 21 bar. Pilot plant is currently under revision to evaluate higher inlet pressures.

The optimal operation point in the pilot plant, both in terms of economics and purification performance was determined at 20 bar. Rejection of undesired ions increased with pressure, undesired NaCl rejection also increased but only maximums of 12% were reached. Permeate flow rate (PFR) was constant in all the experiments. At 20 bar, 25L/m^{2}h permeate flow was obtained, which was enough to feed the ED pilot plant. The cation rejection order observed was Mg (II) > Sr (II) > Cu (II) > Ca (II) > Ni (II)> Na (I) > K (I), mainly dependant on the hydrating ionic radii and speciation.

At 20 bar, brine with approximately 415 **mg/L** of calcium, 760 **mg/L** of magnesium, 500 **mg/L** of sulphate and 52 g/L of NaCl was obtained with an energy consumption of 3.2 kWh/m^3. In the pressure range studied, energy consumption was steady at 3kWh/h. Energy consumption could be optimized when higher inlet pressures were tested, as higher productions flows could be obtained. Calcium, magnesium and sulphate contents were reduced by 50%, 71% and 91% respectively. Nickel, strontium, copper and aluminium contents were reduced by 35%, 70%, 66% and

33% respectively. Nevertheless, further purification steps would be needed to meet the electrolysis requirements.

Results obtained with NF pilot plant were compared with the results previously presented in the literature. It was observed that the results obtained were in the range of the reviewed works with different membranes and inlet solutions. Nevertheless, lower permeate fluxes were obtained due to the high salinity of the brines and membranes used.

NaCl concentration slightly decreased after NF treatment. NF effectively removed calcium, magnesium and sulphate, which could precipitate in the concentration process; it was concluded that nanofiltration could be a suitable pre-treatment before ED concentration or even before RO process. Eriksson *et al.* (2005) studied the use of nanofiltration for seawater pretreatment in the Umm Lujj RO plant of Kuwait. Results obtained demonstrated that higher quality of brine could be obtained when NF was used as a pretreatment: purities of 98% of NaCl could be obtained by this method, which would benefit its further reuse.

Chapter 7

Precipitation process for brines purification and reuse

Primary treatment through precipitation with sodium carbonate and sodium hydroxide was evaluated with three kinds of brines: a) mine brine from the collector pipe, b) reject brines from the SWD-RO process and c) concentrated SWD-RO brines using ED technology. The composition and origin of these brines is detailed in Chapter 4 and 5.

This precipitation treatment was carried out using the operating conditions used by the chlor-alkali industry as has been described in Chapter 2. This treatment consists of a primary precipitation with sodium carbonate and sodium hydroxide to remove calcium, magnesium and some metals thay may precipitate. Finally, if it is required, the brine is polished using ion exchange resins to meet the chlor-alkali cell's requirements.

Excess of reagent and high temperatures are needed to optimize the purification process by precipitation. The excess of reagents needed is usually comprised between 0.1 to 0.5 g/L NaOH and 0.3 to 1.5 g/L Na_2CO_3. Literature reflects some disagreement regarding the order of chemical additions, some recommend additions of reagents together while others suggest sequential additions (*ICCP, 2001*). Temperatures over 60ºC are recommended to speed up the purification process, which otherwise can take several hours to complete. Nevertheless, high brine temperatures can increase the precipitate settling rate as it reduces the crystal size (*Elliot, 1999*).

It has been reported that brines with relations of Ca/Mg lower than 2 or even 4, which is the case for the brines studied in this thesis, tend to present complex settling processes. Flocculating addition can help to some extend to improve precipitates settling from these brines. Prepurification to reduce the amount of magnesium in the brine has also been studied for high magnesium content brines (*Turek et al, 1995*), and so, settling times and purification results were improved in the cases studied. Other methods, such as increasing the Ca/Mg ratio by adding $CaCl_2$ has also been studied (*Elliot, 1999*) but can generate an extra cost on the treatment system. Agitation should also be controlled in order to avoid breaking the floc into small particles and increase the settling time.

Design of an effective purification treatment by precipitation requires the optimization of the process where the amount of reactant added, addition order and temperature of the brine are the main variables. Moreover, studies on the purity and composition of the precipitates obtained should be carried out in order to assess its reuse and reduce the economic cost of the global purification treatment.

Finally, in this thesis precipitation is studied for SWD-RO brine, ED-SWD-RO brine and collector brine in order to remove mainly calcium and magnesium. This precipitation was carried out in the lab using the operation conditions used by the chlor-alkali industry and different inlet temperatures, reagent amount dose and addition order were evaluated to optimize the purification process.

7.1 Experimental technique and procedures. Materials and Methods.

7.1.1 Brines composition

For the purification assays three different types of brines were used in the lab:

a) Sea water reverse osmosis (SWD-RO) desalination brines. Brines were produced by Sea Water Reverse Osmosis pilot plants operating in the Sostaqua Desalination Research Platform in Barcelona (Spain).

b) Concentrated SWD-RO brine by Electrodialysis (ED). Brines produced by the ED pilot plant of Barcelona, as detailed in Chapter 5.

c) Potash salt mine brines. Brines were extracted from the brine collector from the Suria and Cardona mines. Sampling point was located in Sant Joan Despí, near the Solvay's factory in Martorell, as explained in Chapter 4.

General composition of the brines used and saturation indexes (SI) calculated by using PhreeqC with Pitzer database are detailed in Table 7.1.

Table 7.1. Composition of the brines used and composition requirements of the membrane electrolysis cell

		K (I)	Na (I)	Ca (II)	Mg (II)	Cl (-I)	S (VI)	SI CaCO$_3$	SI MgCO$_3$	SI CaSO$_4$
Mine Collector Brine	g/L	14.97	60.00	0.67	5.49	120.05	4.28	1.00	1.58	-0.23
SWD-RO Brine	g/L	0.76	20.72	0.83	2.62	38.82	5.41	0.59	0.80	-0.27
Concentrated ED-SWD-RO	g/L	4.31	88.66	0.56	1.30	140.65	1.41	0.93	1.31	-0.88
Membrane Electrolysis cell requirements	g/L	-	118.00	Ca (II) + Mg (II) <20 ppb		182.00	8.00			

Some of the brines were oversaturated with calcium or magnesium carbonate, as can be seen in Table 7.1. Although brines were oversaturated, the RO brines contained the antiescalants used in the desalination process that avoided carbonate and sulphate precipitation.

It can also be seen from Table 7.1 that the three brines need major purification for calcium and magnesium for being used in the membrane electrolysis cells. The collector brine has high potassium content compared to other brines. That can be a disadvantage for the reuse in the chlor-alkali industry, as a mixture of NaOH/KOH will be produced in the membrane based electrolysis cell. The levels of KOH could not be suitable for pharmaceutical uses where the content of potassium is a limitation.

7.1.2. Methods for precipitation assays.

Batch experiments were carried out to investigate the purification of the three types of brines by precipitation with sodium hydroxide, sodium carbonate and mixtures of both reagents. Two temperatures were used: 25 and 65ºC. 65ºC were chosen because is the brine loop temperature in the chlor-alkali industry and moreover, temperatures higher than 60ºC are recommended to speed up the purification process (*ICCP, 2001*).

In order to avoid dilutions of the samples during the purification tests, the reactants were prepared with NaCl to reach the same composition of the brine used. Additionally, the volume of reagents added was negligible compared to the brine sample volume.

The concentrations of the reactants were 37 g/L Na$_2$CO$_3$ and 250 g/L NaOH, which are the same concentration used for the purification of salt brines by the chlor-alkali industry of Solvay in Martorell (Barcelona). The individual solutions of NaOH and Na$_2$CO$_3$ were prepared by dissolving respective salts in micro-filtered (with 0.22 μm Millipore filter) distilled water and were further filtered with 0.22 μm Millipore filter

after preparation to ensure no impurities or undissolved salts were present. All the chemicals and reagents used were of analytical grade.

Batch experiments were conducted using low-density polyethylene batch reactors, maintained at constant temperature using a thermostatized water bath (at 65±1ºC). For each run, variables amounts of reagents and 20 ml of an initial solution were placed in the reactor.

Batch experiments: using one reagent

Experiments with one reactant, Na_2CO_3 or NaOH, were carried out to determine the optimum reagent excess to purify the brines. These experiments were done adding different volumes of just one reactant each time and analyzing the content of calcium, magnesium and pH in the brine after every addition, as detailed in Figure 7.1a.

Batch experiments: using two reagents

Experiments with to reagents were done to determine the optimum excess and addition order, as detailed in Figure 7.1b. Also, these experiments were done at 65ºC and room temperature and the methodology used was the same as the one used in first experiments with just one reactant.
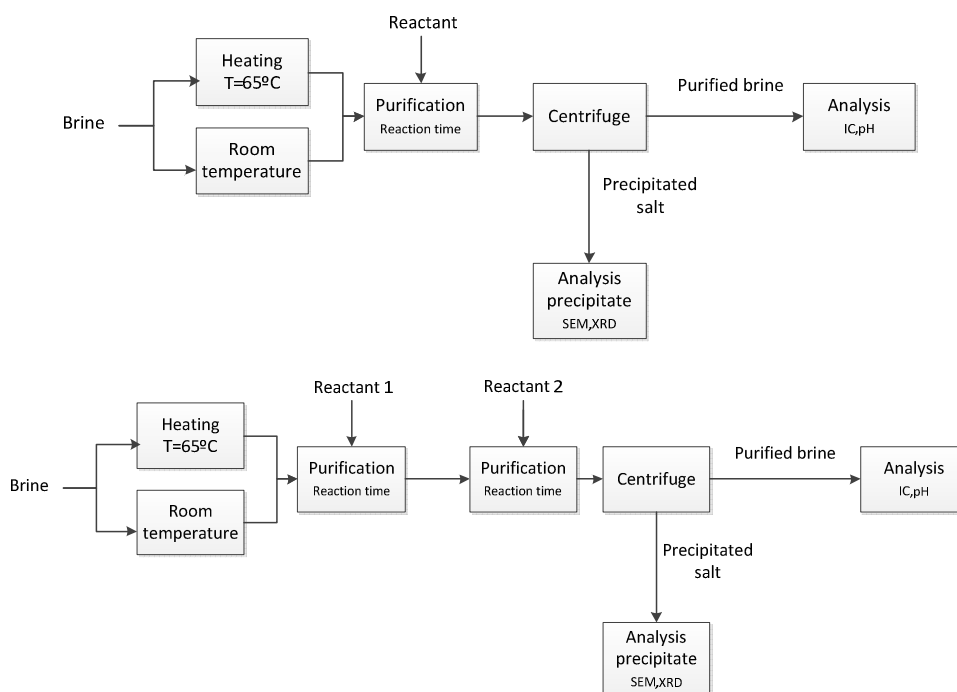

Figure 7.1a) Scheme of the methodology used in purification tests done with one reactant. b) Scheme of the methodology used in purification tests done with one reactant.

7.1.3. Analytical methods.

Treated brines were filtered with 0.20 μm filter and were analysed to determine calcium and magnesium content. First, pH was determined in every sample. Calcium and magnesium from all samples were analyzed using ionic chromatograph Dionex ICS1000 CS-16. Because of the high salinity of the brines used, it was needed to dilute the samples (1:100 and 1:250 dilutions were used). This affected the quantification limit (QL) of ionic chromatography that was established at 20mg/L of calcium and 20mg/L of magnesium for the SWD-RO brine, 25 mg/L of magnesium and 25 mg/L of calcium for the collector brine and for the concentrated ED-SWD-RO brine. The detection limit of the ionic chromatograph was determined at 10 mg/L of calcium and magnesium for SWD-RO brines and 15 mg/L of calcium and magnesium for the collector brine and the concentrated ED-SWD-RO brine.

7.1.4. Precipitates analysis

The precipitates samples collected from the reactors were observed after experiments under a JEOL 3400® Scanning Electron Microscopy with Energy Dispersive System (SEM-EDS). Precipitates were extracted from the samples by centrifugation and were washed with deionised water to remove soluble components present on the brine, mainly NaCl, and avoid interferences in the analysis. The EDS allows detection of light elements, such as C and O, which are very useful to identify solids. Mineral phases were identified with a BRUKER D5005® X-Ray Diffractometer (XRD), with Cu Lα radiation.

From the batch assays on the optimal conditions, the precipitates were extracted and finally milled and digested in 5% HNO_3. After filtration of the insoluble fraction (basically quartz determined by XRD), the concentration of Ca, Mg was determined by diluting 1:50 the sample. The different minor elements were directly determined by ICP-AES. Analytical errors were estimated to be approx 2% in accordance with the reproducibility of the standard. Analytical detection limits were in (mg/L): 5 for Na; 1 for P; 0.5 for K, Al and S; 0.1 for Mg , Ca, Ni and B; 0.02 for Zn; 0.01 for Cu and Fe; 0.005 for Ba, Mn and Al.

7.1.5. Chemical precipitation modelling.

Precipitation processes were modelled using PHREEQ-C code (*Parkhurst, 1995)*. Measured Ca and Mg concentrations were compared when necessary with those predicted using PHREEQ-C code. The database from Pitzer thermodynamics was used to calculate the chemical equilibrium because of the high ionic strength of the used brines moving from 60 g/l NaCl in SWD-RO desalination brines to 230 g/l NaCl of ED concentrated brine. The effect of salinity on single salt solubility and formation of pure precipitates is usually taken into account through assessment of

the ionic strength of the solution. Recently, Sheikholeslami and Ong (2003) when studying the scaling potential of brines in sea water reverse osmosis refered two issues previously not addressed: the effect of salinity on kinetics of scale formation and the effect of salinity on co-precipitation. The kinetics of the precipitation processes was not considered and reaction times were fixed according to the reaction times used on the primary purification units of the chlor-alkali industry.

7.2 . Primary brine precipitation results and discussion.

7.2.1 One reactant addition.

7.2.1.1. Na$_2$CO$_3$ addition for calcium removal

Calcium composition of the treated brines versus the pH achieved after dosing of Na$_2$CO$_3$ at both temperatures (25 and 65 ºC) is represented in Figures 7.2 and 7.3. The induction time for CaCO$_3$ precipitation was very short, lower than 1 minute in all the temperatures tested. As a general trend, Ca is efficiently removed from solution with the increase of pH, carbonate content and temperature. Table 7.2 shows a summary of the removal efficiency ratios for the three types of brines. In general recovery ratios higher than 97-99% are achieved for pH higher than 10. The calcium content requirement for the application on membrane based electrolysis processes was never achieved in all the cases studied, as can be seen in Table 7.3.
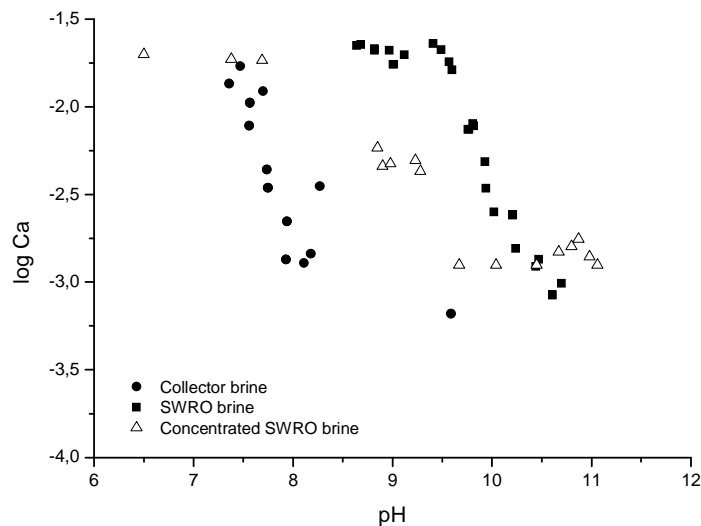

Figure 7.2. Evaluation of Ca concentrations: log Ca versus pH of the treated brines for experiments using Na$_2$CO$_3$ as reagent. Experiments at room temperature (25ºC).

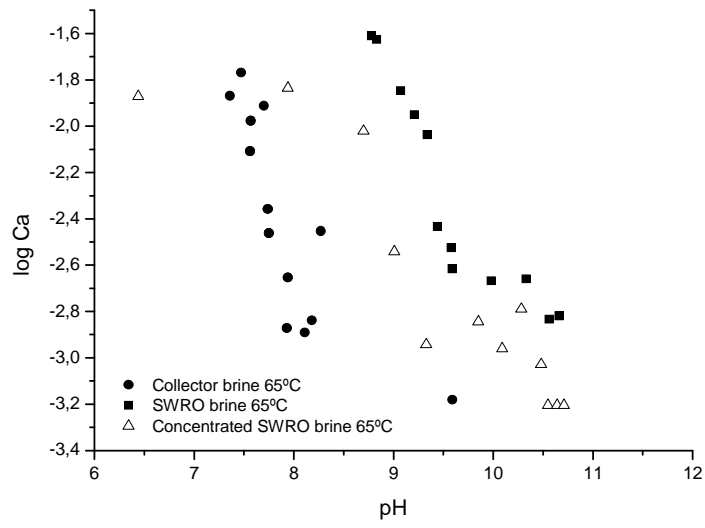*Figure 7.3. Evaluation of Ca concentrations: log Ca versus pH of the treated brines for experiments using Na_2CO_3 as reagent. Experiments at 65ºC .*

Table 7.2. Calcium removal efficiencies (%) for the brines studied at different temperatures when Na_2CO_3 was used as reagent.

Collector brine						SWD-RO Brine						Concentrated ED-SWD-RO Brine					
Room temperature 25ºC			T 65ºC			Room temperature 25ºC			T 65ºC			Room temperature 25ºC			T 65ºC		
pH	Ca (II) [M]	% removal	pH	Ca (II) [M]	% removal	pH	Ca (II) [M]	% removal	pH	Ca (II) [M]	% removal	pH	Ca (II) [M]	% removal	pH	Ca (II) [M]	% removal
7.2	0.02	0%	7.2	0.02	0%	8.6	0.02	0%	8.8	0.02	0%	2.7	0.02	0%	2.6	0.02	0%
7.9	0.01	43.6%	7.75	0.003	67.2%	9.8	0.01	66.8%	9.3	0.01	61.2%	8.9	0.01	67.8%	6.4	0.01	33.2%
8.8	0.002	85.4%	7.93	0.001	87.2%	10.2	0.002	93.0%	9.6	0.003	87.4%	9.3	0.004	76.4%	9.0	0.003	85.8%
10.5	0.001	94.7%	9.59	0.0007	93.4%	10.6	0.001	96.2%	10.7	0.002	93.6%	9.7	0.001	93.1%	10.5	0.001	95.4%

Table 7.3.Residual concentrations of Calcium and Magnesium in the brines studied as a function of temperature and excess of Na_2CO_3 used.

	Room temperature 25ºC				Temperature 65ºC			
	Excess CO_3^{2-}	pH	Ca (II) (mg/L)	Mg (II) (mg/L)	Excess CO_3^{2-}	pH	Ca (II) (mg/L)	Mg (II) (mg/L)
Collector brine	0.35g/L	7.9	105	4245	0.35 g/L	7.7	176	3689
SWD-RO Brine	14.0g/L	10.4	49	771	8.5 g/L	9.9	42	463
Concentrated ED-SWD-RO Brine	9.6 g/L	10.0	50	202	8 g/L	9.8	57	74

SEM-EDS examination of the precipitate obtained when Na_2CO_3 reagent was used, detected the presence of layers with crystalline form of precipitates of Ca-C-O (Fig. 7.4 a). However Mg also was detected, indicating that also some precipitates of Mg, as $MgCO_3$ or $Mg(OH)_2$ could also be found in the precipitates as a consequence of the increase of the carbonate content or the increase of pH. XRD patterns of newly precipitated materials from the three types of brines revealed the presence of detectable crystalline phases containing Ca and identified as calcite ($CaCO_{3(s)}$) (Figure 7.4b). Some SiO_2, $FeCO_3$ and $MgCa(CO_3)$ could be observed in SWD-RO brine.

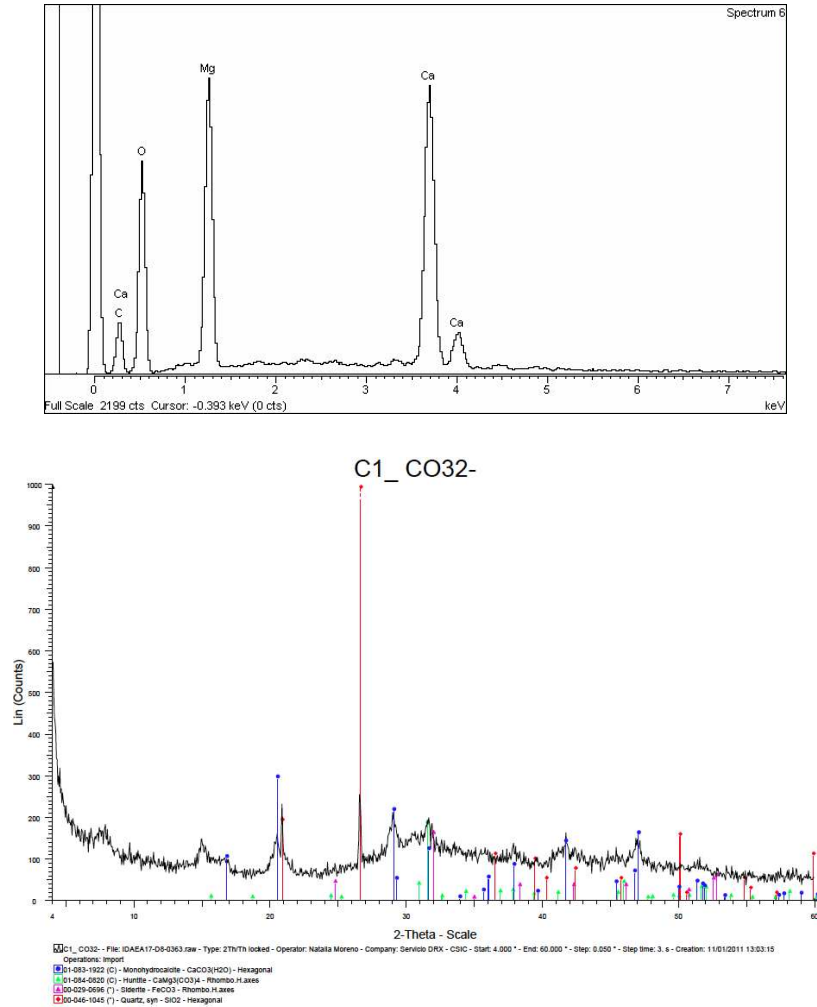*Fig. 7.4 a) SEM of the solid precipitated when Na_2CO_3 was added. b) DRX of the solid precipitated*

Calcium carbonate is one of the most common and widely dispersed minerals, occurring as limestone, chalk, and also biominerals. It has three polymorphs forms: calcite (hexagonal), aragonite (orthorhombic) and vaterite (hexagonal), in order of increasing solubility and decreasing thermodynamic stability. Water chemistry parameters such as pH and ionic strength have significant effects upon the form of calcium carbonate, which will precipitate from a supersaturated solution. Actually,

with [Mg (II)]/[Ca (II)] ratios higher than 3, which is the case for SWD-RO brine and collector brine, vaterite is the first phase to precipitate. Vaterite successively recrystallizates into a more stable phase such as aragonite and calcite (*Drioli et al. 2004*). Calcite and aragonite polymorphs during carbonate precipitations from seawater have been previously reported in the literature *(Morse et al. 1997, Drioli et al. 2004, Pokrovsky 1998, Kitamura 2001)*

When comparing the data at room temperature and 65°C represented in Figures 7.5-7.8, it can be observed that the increase of temperature affects the precipitation, favouring the formation of $CaCO_{3(s)}$ at lower pH values. This is in agreement with the effect of the temperature on the solubility constant as far as the enthalpy of the precipitation process is -1207.6 kJ/kmol. At pH values of 10, measured calcium concentrations are stabilized around $10^{-3.8}$ mol for the collector brine, $10^{-2.8}$ mol for the SWD-RO brine and $10^{-3.0}$ mol for the ED-SWD-RO brine.

The solubility data of the Ca(II)- CO_3^{2-} mineral phases from the PHREEQC database, using the PITZER data base, were used to evaluate the variation of Ca concentration with pH during the precipitation experiments (Fig. 7.5-7.7). Concentration of aqueous Ca in the equilibrated solution brines was compared with the expected for equilibrium with calcium carbonate $CaCO_{3(s)}$. The general trend show higher values of measured Ca concentration in solution than the predicted for three types of brines and for both temperatures. The higher differences between measured and predicted concentrations were obtained for the SWD-RO brines, both characterized by presence of phosphate based antiscalants (between 1- 2.5 mg/l). The presence of the antiscalants used in the pre-treatment steps of the RO desalination plants as super-threshold agents to reduce the carbonate precipitation could explain the higher differences between the predicted and measured concentrations.
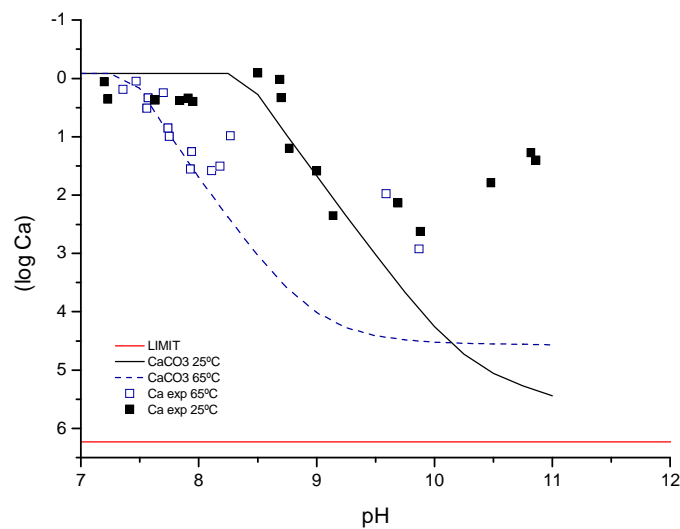

Figure 7.5. Modelled $CaCO_3$ precipitation at different temperatures and experimental results obtained with the brine from the collector. The limit for the electrolysis process was considered to be 20ppb of Calcium.
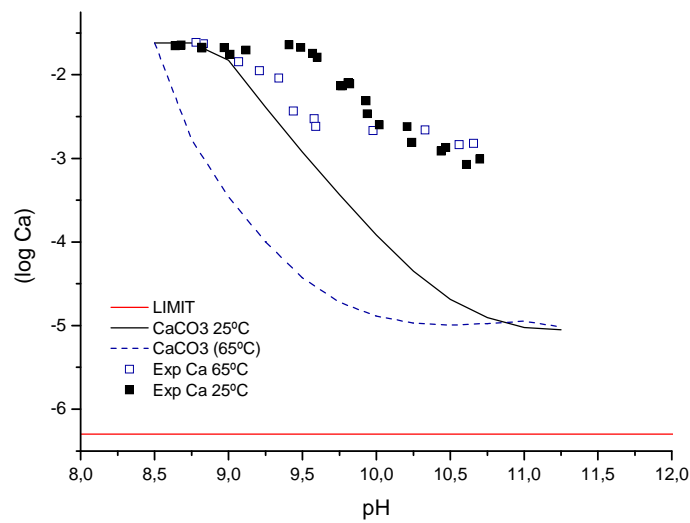
Figure 7.6. Modelled CaCO₃ precipitation at different temperatures and experimental results obtained with the SWD-RO brine. The limit for the electrolysis process was considered to be 20ppb of Calcium.
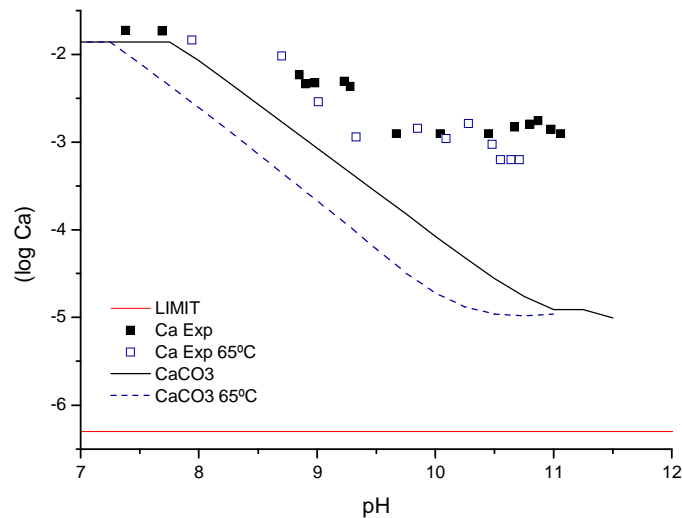

Figure 7.7. Modelled CaCO₃ precipitation at different temperatures and experimental results obtained with the concentrated ED-SWD-RO brine. The limit for the electrolysis process was considered to be 20ppb of Calcium.

Precipitation of calcium carbonate from different type of brines containing antiscalants has been was used to increase the RO process recovery using a secondary RO stage *(Greenlee et al. 2010a, 2010b, 2011, Rahardianto et al. 2010)*. When antiscalants are present in the brine, reduction of CaCO₃ precipitation was observed, as is also corroborated with the data obtained in this study. Also antiscalant adsorption onto nucleating crystals and smaller particle size distribution was noticed *(Greenlee et al. 2010a, 2010b)*. Studies on antiscalants degradation by oxidation *(Greenlee*

et al. 2011) acceleration of precipitation by seeded precipitation *(Rahardianto et al. 2010)* demonstrated that higher precipitation rates could be obtained with these brines when they were previously treated. Treatment to remove antiscalants would increase the total reuse cost but it would benefit the calcium purification process.

In the precipitation assays at room temperature the maximum hardness reduction took place for 3 g/L Na_2CO_3 dose for the collector brine, 27 g/L Na_2CO_3 for the SWD-RO brine and 20 g/L Na_2CO_3 for the concentrated ED-SWD-RO brine, as can be seen in Fig. 7.8 and Fig.7.9. That corresponds to 0.6, 25 and 19 Na_2CO_3 g/L excess respectively. At 65ºC, the maximum hardness reduction took place for 3 g/L, 18 and 16 g Na_2CO_3 /L dose for the collector brine, the SWD-RO brine and concentrated ED-SWD-RO brine respectively, as can be seen in Figures 7.8 and 7.9. That corresponds to an excess of 0.6, 15 and 14 g Na_2CO_3/L respectively.

In the case of SWD-RO brine and concentrated ED-SWD-RO brine, the excess of CO_3^{2-} needed to achieve the maximum reduction was much higher than the values reported in the literature due to the presence of antiscalans. However, due to the selective concentration process using ED, the antiscalants content in concentrated brine is reduced (below 0.05 mg/L) and then this effect was probably minimized. The amount of Na_2CO_3 needed in these two brines significantly diminished with the increase of temperature due to the effect on the antiscalant performance. The effect of temperature on the antiscalant efficiency diminished at higher temperatures (e.g. 65ºC), and then the purification process improves as has been previously reported in the literature *(Ketrane et al. 2009)*.

The calcium membrane electrolysis limit was never achieved in all the cases studied, as can be seen in Table 7.3. The model predicted that at room temperature the limit could be achieved using the collector brine, but the experimental results showed higher residual calcium concentrations than the predicted.
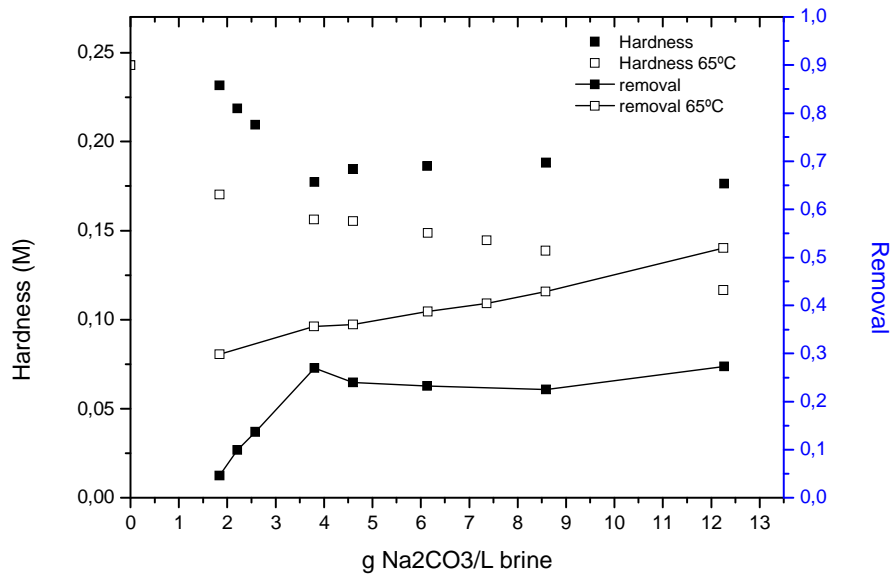
Figure 7.8. Hardness of the collector brine according to the Na_2CO_3 added at different temperatures and removal achieved.
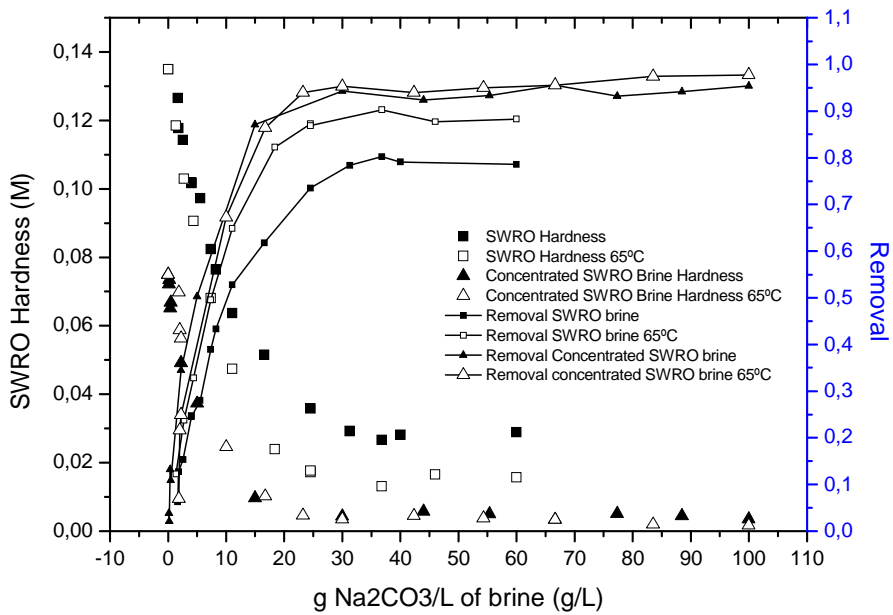
Figure 7.9. Hardness of the SWD-RO brine and concentrated ED-SWD-RO brine according to the Na_2CO_3 added at different temperatures and removal achieved.

7.2.1.2. NaOH addition for magnesium removal

Magnesium composition on the treated brines versus the pH achieved after dosing of NaOH at both temperatures (25 and 65 °C) is presented in Figures 7.10 and 7.11. The induction time for $Mg(OH)_{2(s)}$ precipitation was lower than 1 minute at both

temperatures. As a general trend Mg is efficiently removed from solution with the increase of pH and temperature. Table 7.4 shows a summary of a set the removal efficiency ratios for the three types of brines. In general recovery rations higher than 97-99% are achieved for pH higher than 11. The magnesium content requirement to be achieved for application on membrane based electrolysis process for chloride production was never achieved in all the cases studied, as can be seen in Table 7.5
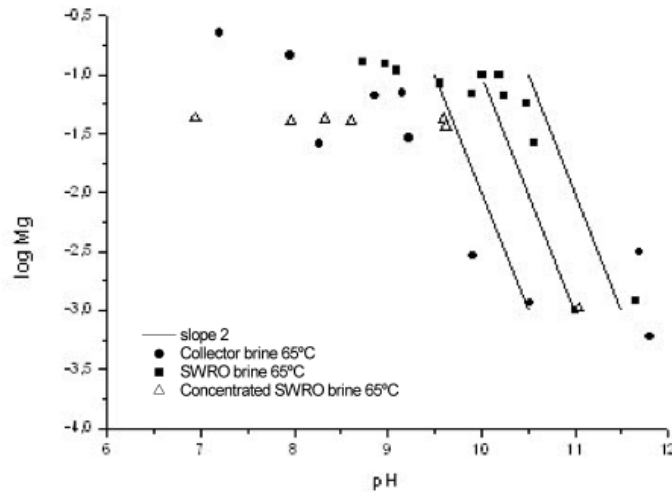

Figure 7.10. Evaluation of Mg (II) concentrations: log Mg versus pH of the treated brines for experiments using NaOH as reagent. Experiments at room temperature (25ºC).
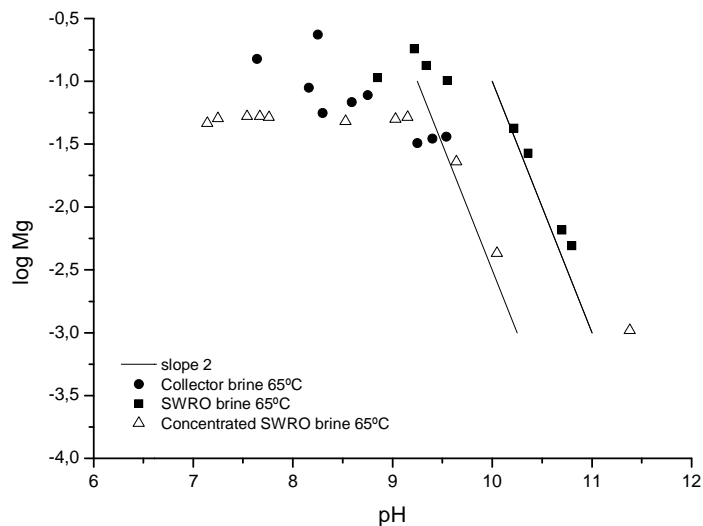

Figure 7.11. Evaluation of Mg (II) concentrations: log Mg versus pH of the treated brines for experiments using NaOH as reagent. Experiments at 65ºC.

Table 7.4. Magnesium removal efficiencies (%) for the brines studied at different temperatures when NaOH was used as reagent.

Collector brine						*SWD-RO Brine*						*Concentrated ED-SWD-RO Brine*					
Room temperature 25ºC			*T 65ºC*			*Room temperature 25ºC*			*T 65ºC*			*Room temperature 25ºC*			*T 65ºC*		
pH	Mg (II) [M]	% removal	pH	Mg (II) [M]	% removal	pH	Mg (II) [M]	% removal	pH	Mg (II) [M]	% removal	pH	Mg (II) [M]	% removal	pH	Mg (II) [M]	% removal
7.2	0.15	0%	7.6	0.15	0%	9.1	0.11	0%	8.9	0.11	0%	2.8	0.05	0%	2.7	0.05	0%
8.8	0.07	54.2%	8.6	0.07	54.7%	10.3	0.07	41.1%	9.6	0.10	4.7%	3.5	0.04	15.7%	9.6	0.02	50.9%
9.2	0.03	80.0%	9.4	0.03	76.8%	10.6	0.03	75.9%	10.8	0.005	95.4%	9.6	0.03	22.9%	10.1	0.004	90.8%
10.5	0.001	99.2%	12.7	0.001	99.2%	12.9	0.001	99.1%	12.7	0.0004	99.6%	11.0	0.001	97.8%	11.4	0.001	97.77%

Table 7.5. Residual concentrations of Calcium and Magnesium in the brines studied as a function of temperature and excess of NaOH used.

	Room temperature 25ºC				Temperature 65ºC			
	Excess OH⁻	pH	Ca (II) (mg/L)	Mg (II) (mg/L)	Excess OH⁻	pH	Ca (II) (mg/L)	Mg (II) (mg/L)
Collector brine	0.85	11.7	448	75	0.85	11.1	25*	184
SWD-RO Brine	0.85	11.0	596	155	0.85	10.8	538	118
Concentrated ED-SWD-RO Brine	0.85	12.9	276	25*	0.85	12.9	280	25*

*QL quantification limit

The SEM-EDS examination of the precipitates obtained from the brines studied when NaOH was used as reagent detected the presence of layers with amorphous precipitates of Mg-O as major component (Fig. 7.12 a). Ca also was detected (in a minor percentage), indicating that also some precipitates of Ca, as $Ca(OH)_2$ or $CaCO_3$ could also found as a consequence of the presence of carbonate on the samples or in sodium hydroxide solutions used as, in some cases, high pH values were achieved. XRD patterns of newly precipitated materials from the three types of brines revealed the presence of detectable crystalline phases in the Mg identified as brucite $(Mg(OH)_{2(s)})$ and small amounts of calcite was also detected (Figure 7.12 b).
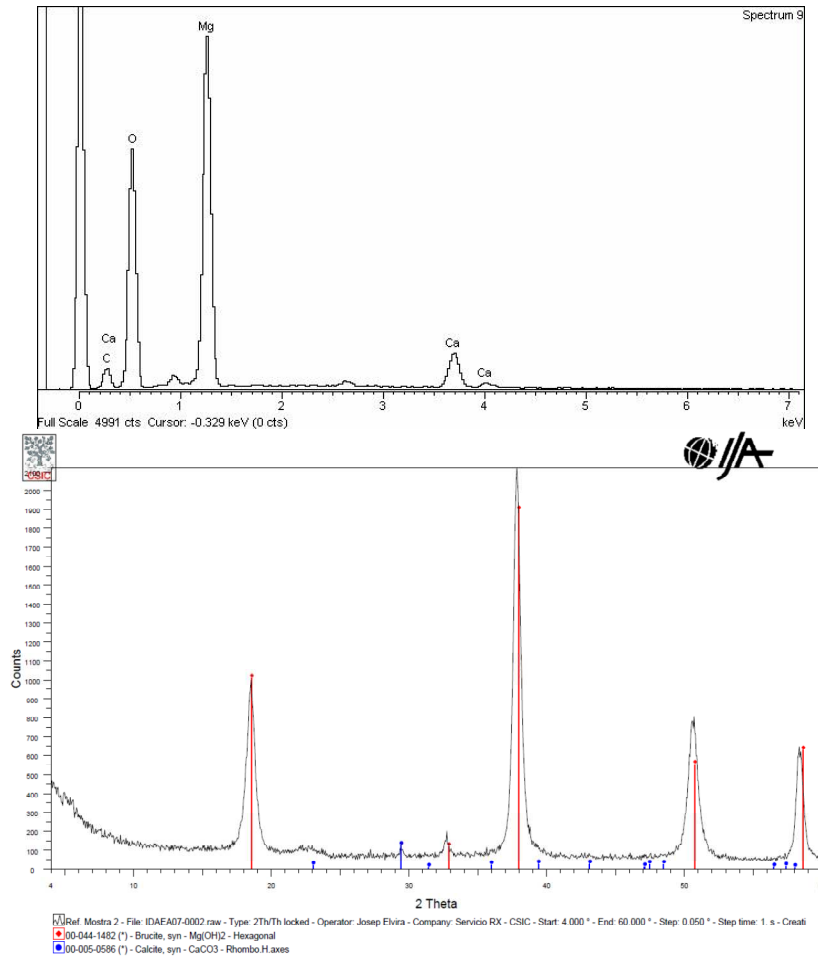
Figure 7.12. a) SEM of the solid salt precipitated when adding sodium hydroxide b) XRD analysis of the salt precipitated

In Figures 7.13-7.15, the evolution of log Mg versus the pH reached at different temperatures can be found. The increase of pH favoured the precipitation of $Mg(OH)_2$ and the decrease of Mg (II) concentration in solution. The type of brines affects the start-up of the precipitation; in the case of the collector brine this takes place when pH is around 9-9.5, for the ED-SWD-RO brine it occurs between 10 and 10.5 while for SWD-RO this takes place at 9.5-10. Contrary to the case of CaCO3, the increase of temperature did not affect the precipitation process.

The solubility data of the Mg(II)-OH$^-$ mineral phases from the PHREEQC code, using the PITZER data base, were used to evaluate the variation of Mg concentration with pH during the precipitation experiments (Fig. 7.13-7.15). Concentration of aqueous Mg in the equilibrated solution brines was not in accordance with that expected for equilibrium with $Mg(OH)_{2(s)}$ however, the predicted and measured variation as a function of pH shows the same shape. The general trend shows higher values of measured Mg total concentration in solution than the predicted for three types of brines and for both temperatures. The induction time for $Mg(OH)_2$ precipitation was lower than 1 minute for both temperatures tested following published results of salts precipitation under saturation conditions where small induction times, lower than 1 second, were reported (*Turek, 1995b*). Higher precipitation rates of magnesium were reported in literature when antiscalants were present, so antiscalants could be an advantage for magnesium purification in RO brines (*Greenlee et al. 2010b*). Nevertheless, this effect was not observed on the brines studied.
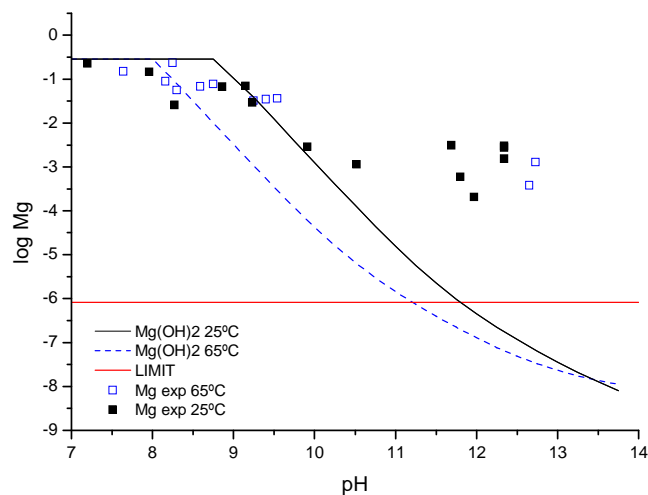
Figure 7.13. Modelled Mg(OH)₂ precipitation at different temperatures and experimental results obtained with the collector brine. The limit for the electrolysis was considered to be 20ppb of Magnesium.
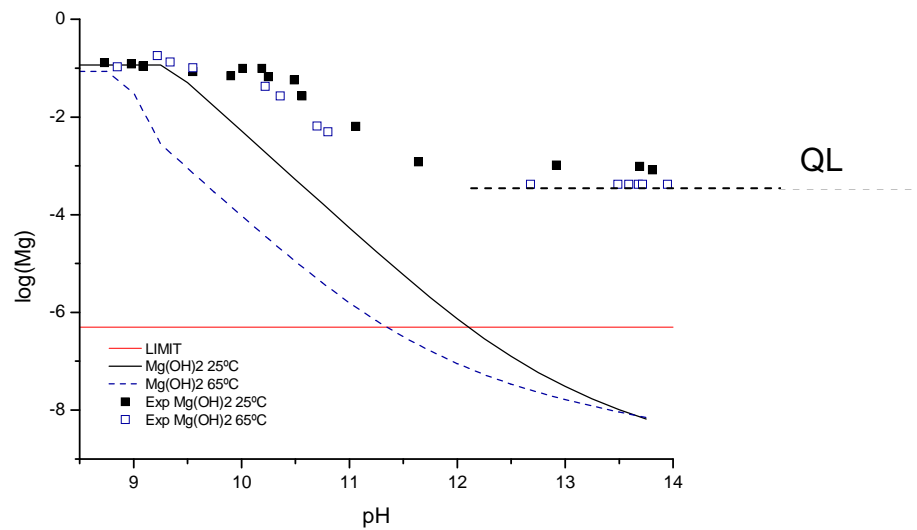
Figure 7.14. Modelled Mg(OH)$_2$ precipitation at different temperatures and experimental results obtained with the SWD-RO brine. The limit for the electrolysis was considered to be 20ppb of Magnesium.
QL: quantification limit
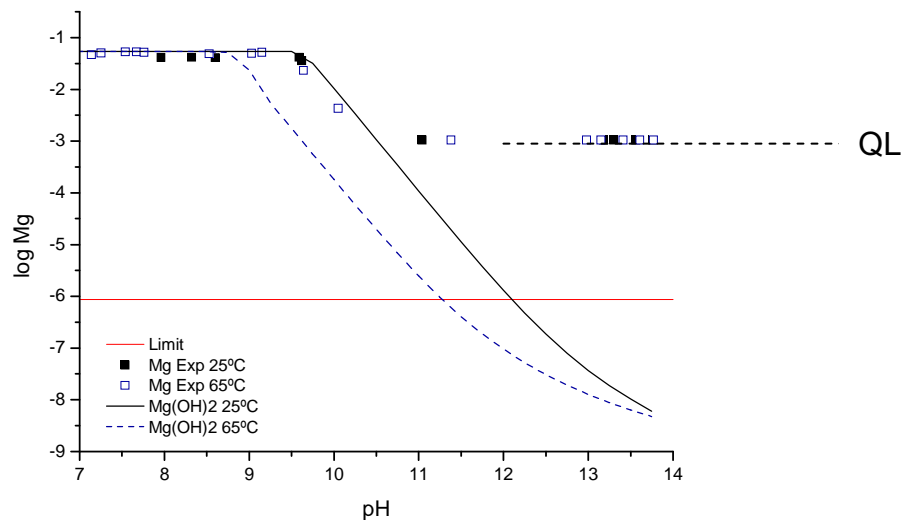
Figure 7.15. Modelled Mg(OH)$_2$ precipitation at different temperatures and experimental results obtained with the concentrated ED-SWD-RO brine. The limit for the electrolysis was considered to be 20ppb of Magnesium.
QL: quantification limit

In the precipitation assays at room temperature the maximum hardness reduction took place for 20 g/L NaOH dose for the collector brines, 11 g/L Na2CO3 for the SWD-RO brine and 7.5 g/L NaOH for the concentrated ED-SWD-RO brine, as it can be seen in Fig. 7.16 and Fig. 7.17. That corresponds to 2 g/L NaOH (0.85 g OH$^-$/L) excess for the three brines. The excess needed was out of the range determined by the literature; this fact can be due to precipitation of other metallic ions. That

excess can also be explained because the brines commonly used in the chlor-alkali industry had lower amount of magnesium compared to the calcium concentration, but in this case it happens just the opposite. Moreover, with such higher amount of calcium and magnesium, simultaneous precipitation of calcium increases the amount of hydroxide needed to purify the brine.

At 65ºC, the maximum hardness reduction took place for 20 g/L, 9 and 7.5 g NaOH /L dose for the collector brines, the RO brine and concentrated RO brine respectively, as it can be seen in Figures 7.16 and 7.17. That corresponds to an excess of 2g NaOH/L (0.85 g OH⁻/L) for the three brines. It can be seen from Table 7.5 that the levels of magnesium reached in the two experiments at different temperatures are quite similar in all brines. However, at higher temperatures purification of calcium was usually higher with lower pHs.
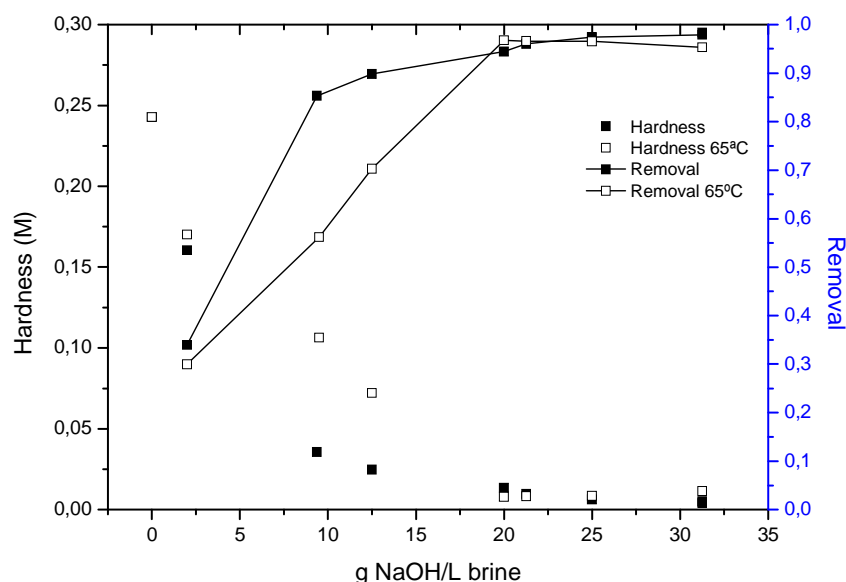

Figure 7.16. Hardness of the collector brine according to the NaOH added at different temperatures and removal achieved.
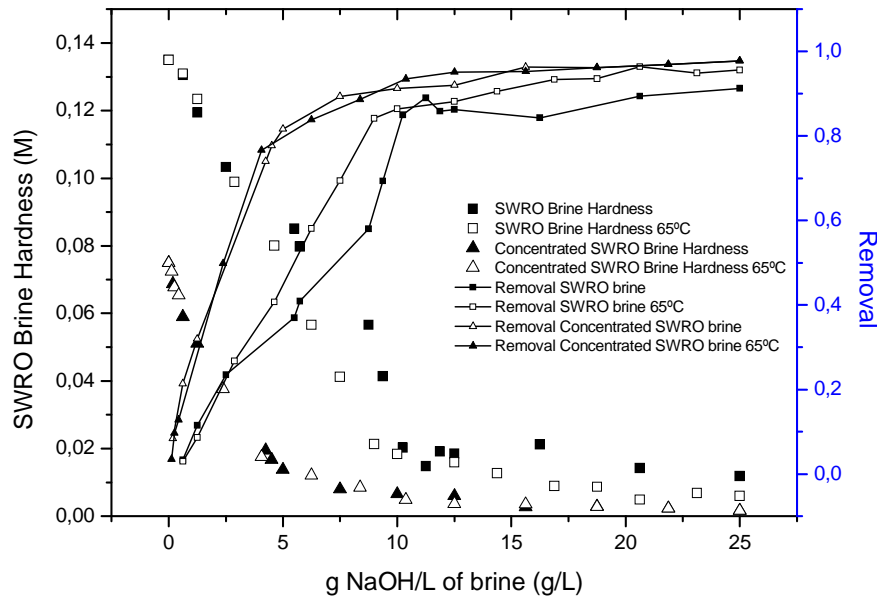
Figure 7.17. Hardness of the RO brine according to the NaOH added at different temperatures and removal achieved.

7.2.1.3. Two reactants addition

Results obtained when different amounts of the two reactants were added are represented in Tables 7.6, 7.7 and 7.8. Since the previous experiments showed that the removal efficiency of calcium increases with temperature purification trials were performed at 65°C. Different order additions were studied with the SWD-RO brines. As can be seen in Tables 7.7 and 7.8, no significant difference on hardness removal efficiency results were observed when changing the reactants addition order. The small differences found, in the purification efficiency, for the dose of 6g/L Na_2CO_3 and 0.13 g/L NaOH could be due to the fact that the measured value was close to the hardness quantification limit (0.001 mol/L).

The hardness removal efficiency was higher than 95% in the optimal additions for the conditions tested. Then, and following the reported experience of chlor-alkali industries, as the Solvay Plant in (Martorell, Spain) it was decided to use the order of first sodium carbonate addition followed by a second addition of sodium hydroxide as described in Chapter 2. As can be seen in Tables 7.6-7.8 at the optimum Ca and Mg purification ratios the measured values of Ca and Mg where below the quantification limit (QL) with the analytical technique used in this work. Analysis of samples with ICP-AES shown however that the requirements of the membrane base electrolysis chlor-alkali plants were never reached. Results in Tables 7.6 and 7.7 also shown that purification was more effective in the ED-SWD-RO brine, as was

previously purified by the selective ED concentration process and the concentration of antiscalants was dramatically diminished.

Table 7.6. Hardness results and removal reached when adding different amounts of two reactants on the SWD-RO brine at 65ºC
QL: quantification limit: 10 mg/L of Calcium and 10 mg/L of Magnesium

		Temperature 65ºC NaOH		
		0.6 g/L	**9.0 g/L**	**25g/L**
Na₂CO₃	**39 g/L**	CO_3^{2-} + OH^- : 0.01M	CO_3^{2-} + OH^- : QL	CO_3^{2-} + OH^- : QL
		OH^- + CO_3^{2-}: 0.01M	OH^- + CO_3^{2-}: QL	OH^- + CO_3^{2-}: QL
	18 g/L	CO_3^{2-} + OH^- : 0.03M	CO_3^{2-} + OH^- : QL	CO_3^{2-} + OH^- : QL
		OH^- + CO_3^{2-}: 0.03M	OH^- + CO_3^{2-}: QL	OH^- + CO_3^{2-}: QL
	0.10 g/L	CO_3^{2-} + OH^- : 0.12M	CO_3^{2-} + OH^- : 0.007M	CO_3^{2-} + OH^- : 0.006 M
		OH^- + CO_3^{2-}: 0.12M	OH^- + CO_3^{2-}: 0.007M	OH^- + CO_3^{2-}: 0.007M

Table 7.7. Hardness results reached when adding different amounts of two reactants on the concentrated ED-SWD-RO brine at 65ºC
QL: quantification limit: 25 mg/L of Calcium and 25 mg/L of Magnesium

		Temperature 65ºC NaOH		
		0.13 g/L	**7.5 g/L**	**25.0g/L**
Na₂CO₃	**39 g/L**	CO_3^{2-} + OH^- : QL	CO_3^{2-} + OH^- : QL	CO_3^{2-} + OH^- : QL
		OH^- + CO_3^{2-} QL	OH^- + CO_3^{2-}: QL	OH^- + CO_3^{2-}: QL
	16 g/L	CO_3^{2-} + OH^- : QL	CO_3^{2-} + OH^- : QL	CO_3^{2-} + OH^- : QL
		OH^- + CO_3^{2-}: 0.003M	OH^- + CO_3^{2-}: QL	OH^- + CO_3^{2-}: QL
	0.10 g/L	CO_3^{2-} + OH^- : 0.05 M	CO_3^{2-} + OH^- : 0.002M	CO_3^{2-} + OH^- : QL
		OH^- + CO_3^{2-}: 0.05 M	OH^- + CO_3^{2-}: 0.002M	OH^- + CO_3^{2-}: QL

Table 7.8. Hardness results reached when adding different amounts of two reactants on the collector brine at 65ºC
QL: quantification limit: 20 mg/L of Calcium and 20 mg/L of Magnesium

		Temperature 65ºC NaOH		
		0.13 g/L	**7.5 g/L**	**25.0 g/L**
Na₂CO₃	**8.5 g/L**	CO_3^{2-} + OH^- :0.07M	CO_3^{2-} + OH^- : QL	CO_3^{2-} + OH^- : QL
	3.0 g/L	CO_3^{2-} + OH^- : 0.09M	CO_3^{2-} + OH^- : QL	CO_3^{2-} + OH^- : QL
	0.7 g/L	CO_3^{2-} + OH^- : 0.11M	CO_3^{2-} + OH^- : 0.003M	CO_3^{2-} + OH^- : 0.002M

Precipitated salt was analyzed by DRX and SEM, the analysis showed that was formed mainly by calcium carbonate and magnesium hydroxide, as can be seen in Figure 7.18. The SEM-EDS examination detected the presence of layers with crystalline form of precipitates of Ca-C-O (Fig. 7.18) and amorphous layers of Mg-O. XRD patterns of newly precipitated materials from the three types of brines revealed the presence of detectable crystalline phases of Ca identified as calcite ($CaCO_{3(s)}$) and Mg identified as $Mg(OH)_{2(s)}$ (Figure 7.18). In consequence, if that purification was done in two different vessels and the precipitated salt was extracted and washed, it could be reused as a by-product of the purification process.
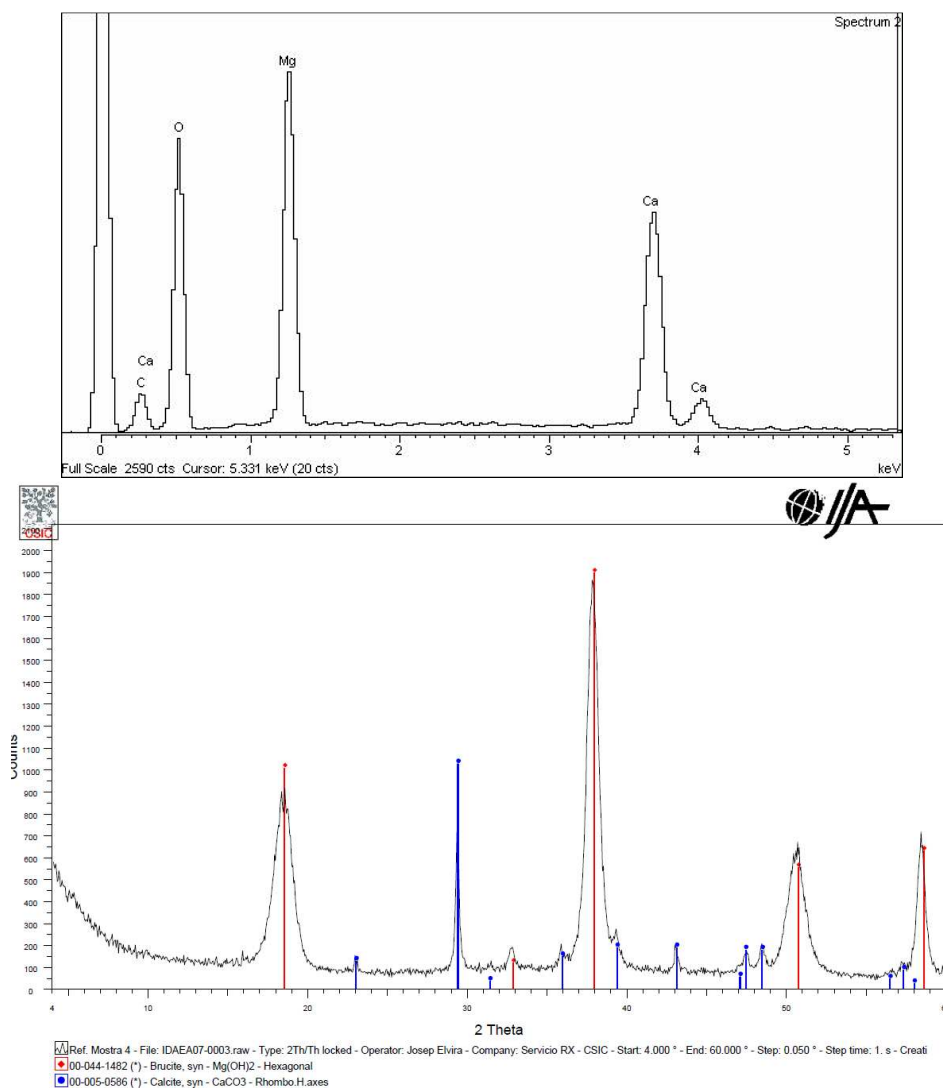
Figure 7.18. a) SEM analysis of precipitated salt when two reagents were used. b)XRD analysis of the precipitated salt when adding two reactants.

7.2.1.4. Prepurification of magnesium

According to the experiments carried out by Turek *et al.* (1995a), it was beneficial to prepurify magnesium in order to improve the clarification of the solution and obtain higher cristallinity degree in the precipitates. With these prepurification step, better purification performance could be achieved.

In order to test if pre-purification would be helpful for the removal of calcium and magnesium, different test were carried out adding NaOH in two stages in the collector brine. In consequence, the addition order was NaOH followed by Na_2CO_3 and finally NaOH, using the optimal previously determined with just one reactant addition. The tests were carried out at room temperature to simplify the experimental.

Results were compared with the ones obtained with previous additions at room temperature and no significant difference was observed in the purification rate obtained. Final hardness content was approximately similar to the previous values reported at room temperature, as can be seen in Table 7.9. In conclusion, prepurification of magnesium was discarded.

Table 7.9. Results obtained with the pre-purification of collector brine at room temperature. Total additions: 3g Na_2CO_3/L and 20 g NaOH/L.

	% addition			Final Hardness (M)	Final Hardness obtained without prepurification at 25C (M)
	NaOH (1)	Na₂CO₃ (2)	NaOH (3)		
1	88%	100%	12%	0.02	
2	50%	100%	50%	0.01	
3	12%	100%	88%	0.02	0.01
4	100%	100%	0%	0.01	
5	0%	100%	100%	0.01	

7.3. Chemical characterization of precipitation by products: potential material valorization.

Samples of precipitates from the single reagent primary purification with both Na_2CO_3 and NaOH were analyzed for both minor and major components, results are summarized in Table 7.10. Analysis of the dissolved precipitates from the Na_2CO_3 precipitation showed a Ca:Mg relation of 1.4 in all cases, except for the SWD-RO brine where the relation was 0.5. Collector brine precipitates had the higher content of calcium carbonate compared to the SWD-RO brine precipitates with higher total Ca (II) content. Major elements in dissolved precipitates analyzed were Ca, Mg, Sr, S, K and P. Minor components detected were Ba, Na, Cu, Mn, Fe, Ni, B and Zn. The high content of K could be associated to the precipitation of K_2CO_3. The presence of priority pollutants as As, Hg, Pb and Cd were not detected in the samples. In Table 7.11 , results of % $CaCO_3$ and $Mg(OH)_2$ in the solid are represented considering that all Ca analyzed was in form of $CaCO_3$ and magnesium in form of $Mg(OH)_2$.

Table 7.10. Analysis of the different precipitates obtained during purification of brines

	g/Kg				mg/kg																							
	Ca	Mg	Na	K	Sr	P	S	Si	Mn	Pb	Zn	Cu	Al	Be	Fe	Li	Mo	Ni	Sb	Ti	V	As	B	Cr	Ba	Cd	Co	Hg
Precipitate when Na₂CO₃ was added																												
Collector brine	139	98	13	4	1612.6	306.7	1064.0	48.2	144.6	DL	153.8	12.5	DL	DL	23.3	DL	DL	12.5	DL	DL	DL	DL	22.4	0.8	34.1	DL	1.7	DL
SWD-RO brine	69	127	5	0.1	1001.5	111.3	98.9	DL	0.4	DL	3.6	0.8	DL	DL	5.1	DL	DL	DL	DL	DL	DL	DL	8.7	0.2	3.4	DL	DL	DL
Concentrated ED-SWD-RO brine	54	41	17	0.8	609.8	49.2	65.1	DL	0.5	DL	5.6	1.8	DL	DL	14.2	DL	DL	1.1	DL	DL	DL	DL	3.0	1.6	3.7	DL	DL	0.2
Precipitate when NaOH was added																												
Mine brine	11	213	1	0.05	15.0	77.1	176.6	193.9	14.0	DL	13.3	1.7	21.2	DL	4.8	DL	DL	2.7	DL	DL	DL	DL	DL	DL	0.6	DL	DL	DL
SWD-RO brine	66	245	22	0.4	82.4	671.3	765.5	DL	5.9	DL	41.2	DL	DL	DL	70.7	DL	DL	DL	DL	DL	DL	DL	DL	11.8	5.9	DL	DL	DL
Concentrated ED-SWD-RO brine	103	238	11	0.2	45.0	361.4	269.1	101.6	2.3	DL	28.9	4.6	69.3	DL	73.9	DL	DL	21.9	DL	DL	DL	DL	DL	DL	6.9	2.3	DL	DL
Detection Limit (mg/L)	0.1	0.1	5	0.005	0.005	1	0.5	0.25	0.005	0.2	0.02	0.01	0.5	0.1	0.01	0.1	0.1	0.1	0.1	0.02	0.1	0.5	0.2	0.01	0.005	0.01	0.02	4.00E-03

Table 7.11. Percentage of CaCO₃ and Mg(OH)₂ in the precipitates analyzed by ICP when Na₂CO₃ is added to the brines.

	% weight in the precipitate	
	CaCO₃	Mg(OH)₂
Collector brine	35%	24%
SWD-RO Brine	17%	31%
Concentrated ED-SWD-RO Brine	13%	10%

Analysis of the dissolved precipitates in 5% HNO_3 from the NaOH purification assays showed a Ca:Mg relation of 0.3 for the two RO brines and 0.05 for the collector brine. Around 55% content was $Mg(OH)_2$ although some traces of Ba, Sr, Na, K, Ni, Fe, Al, Zn, Mn, Cu, P and S could be found. In Table 7.12, results on % of $CaCO_3$ and $Mg(OH)_2$ are represented considering that all the Ca and Mg of the samples analyzed were in these forms.

Table 7.12. Percentage of $CaCO_3$ and $Mg(OH)_2$ in the precipitates analyzed by ICP when NaOH was added to the brines.

	% weight in the precipitate	
	$CaCO_3$	**$Mg(OH)_2$**
Collector brine*	3%	52%
SWD-RO Brine	17%	59%
Concentrated ED-SWD-RO Brine	26%	57%

*some insoluble salts were present in the precipitate

Recently, Steinhauser (2008) reviewed the management of the waste management options at the production of soda ash using the Solvay process. The solid and liquid effluents from the soda ash production have been a target of investigation since decades or centuries, often attempting to make use of the wastes. In the case of the brines generated, rich in Ca, Mg and Sulphate ion purification is performed by precipitation of these ions. In the first step, milk of lime (CaO) is added to remove Mg (II) ions. Since the brine is saturated with gypsum in many cases the addition of Ca^{2+} ions leads to the precipitation of $CaSO_4 \cdot 2H_2O$. The precipitates are separated from the purified brine by decantation and/or filtration and form the brine purification mud (containing $Mg(OH)_2$, $CaSO_4 \cdot 2H_2O$, $CaCO_3$). This mud is sometimes used as a fertilizer after a proper separation of mud from the brine or has been proposed as amendment option for acidic soils. Rechently, Shi and Huo (2009) developed a novel method to prepare soil nutrient amendment by calcining a mixture of white mud from the soda ash process and potassium feldspar (blending mass ratio of 70:30 for white mud to potassium feldspar). In conclusion, reuse of the precipitates generated during the primary treatment of these brines should be further studied, nevertheless it could be used as fertilizants due to its high content in carbonate and hydroxide or as additive or fillers in the cement industry or in the plastic industry. The use in these two sectors requires a reduction of the chloride content on the solids, that is the major problem to be solved. Samples analyzed in this study were washed several times to reduce the soluble chloride salts, however, this process could not be feasible at industrial scale.

7.4. Conclusions

The results showed better purification results at 65ºC than at 25ºC for calcium removal for the three types of brines. Contrary, no significant effect was measured for magnesium removal. The excess of reagents to reach the optimum of purification was higher than the reported in the literature. This need of reagent excess was due to the presence of antiscalants in the RO brines. When the ratio of Ca:Mg is lower than 6, it has been suggested to add $CaCl_2$ to provide enough calcium to sweep down the magnesium or to prepurificate the brine with NaOH to reduce the settling time and improve the performance of the system (*Elliot, 1999*). Nevertheless, $CaCl_2$ addition was not studied because of the increase in operation costs to treat these brines. Prepurification of magnesium did not present significant improvements in the general purification performance, so it was finally discarded.

Despite using the Pitzer database for high ionic strength, the model developed using PHREEQC was not able to predict the amount of calcium and magnesium remaining in the brines because of the high salinities of brines and antiscalants content. Nevertheless, the model was considered valid to predict the main precipitating reactions in each case and was corroborated with XRD and SEM analysis. Removal of antiscalants through degration by oxidation *(Greenlee et al. 2011)* or acceleration of precipitation by seeded precipitation (*Rahardianto et al. 2010*) could be studied in future works to improve the purification results.

It was observed from the results that reactants order addition did not produce a significant difference in the purification values obtained. A second purification step should be studied in order to determine the viability to reach the limits of the membrane and diaphragm electrolysis process with these brines.

The collector brine and concentrated ED-SWD-RO brine were purified up to 15 mg/L of calcium and magnesium, and the SWD-RO brine was purified up to 10 mg/L of calcium and magnesium. The purification efficiency was higher than 95% in all cases studied.

When two reactants were added, precipitation should be carried out in two separate vessels in order to recover valuable salts. The precipitates obtained did not had high purities, so its reuse would be conditioned and studies to obtain better by-product qualities should be carried out in the next future. Nevertheless, reuse in the cement industry and in the plastic industry like additives or fillers, or like fertilizants could be studied. Possible reuses should be further studied in future works.

Precipitation alone is not enough to reduce the levels of calcium and magnesium for the membrane electrolysis cell, so an additional polishing step is required. The secondary brine treatment usually consists of a filtration step and an ion exchange unit to decrease alkaline earth metals to ppb levels.

Chapter 8

Conclusions and future work

8.1. Summary of results

Reuse of SWD-RO brine and collector brine in chlor-alkali industry to produce NaOH and chlorine was evaluated in this thesis. Membrane electrolysis cells will be the predominant electrolysis technology in the next future due to environmental considerations. In consequence reuse of these brines in this membrane electrolysis cell was studied.

Membrane electrolysis cells have strict composition requirements that demand high purity brines. Usually, a primary purification by selective precipitation with NaOH and Na_2CO_3 and a secondary purification step with ion-exchange resins is enough to treat the brines currently used in the membrane chlor-alkali industry. These brines are obtained by directly dissolving purified mine salt, and low content of impurities can be observed on the brine produced. This treatment must be modified in order to reuse alternative brines proposed in this thesis that contain several impurities to be treated.

Characterization of the brines was carried out in this thesis as a first step to determine the treatments needed. Samples of both brines studied were analyzed frequently during one year. The brine circulating in the Llobregat pipe collects the potash mine drainages and the runoffs coming from rainfalls on mine tailings; in consequence, collector brine presented composition and flow rate variations due to

the weather conditions that generated runoffs and diluted the brine. In contrast, SWD-RO brine composition was steady, as RO process was considered stable. The composition variability of collector brine could be a disadvantage when designing a treatment system, as steady production and quality could not be assured.

Collector brine had higher salinity content (from 80 to 180 g/L NaCl) than SWD-RO (60g /L NaCl), which was an advantage as concentration step could be simplified by just adding small amounts of solid salt. Concentration by salt addition was not studied in this thesis because it has been widely applied. In general terms, both brines studied needed concentration of NaCl up to saturation levels (300g/L NaCl) and major purification of calcium, magnesium and strontium to meet the membrane electrolysis requirements. Moreover, iron and manganese should be removed from collector brine and nickel, copper and aluminium from SWD-RO brines. In addition, collector brine had high potassium content (17 g/L) that will contaminate the final NaOH produced with KOH; this fact will limit its application in the pharmaceutical industry.

Electrodialysis and nanofiltration pilot plants were specially designed for SWD-RO brine treatment. Precicipitation was evaluated in the lab simulating the operational conditions at sodium chloride purification plants. Nanofiltration of collector brine was also carried in the lab due to difficulties in brine availability and transport. Final concentrations and removal obtained with these treatments are detailed in Table 8.1. Moreover, the composition obtained in all the cases is compared with the membrane electrolysis cell's requirements It can be observed that each of these treatments alone was not enough to meet the electrolysis requirements. Nevertheless, a combined system could efficiently reach these requirements and is further discussed in section 8.2.

Electrodialysis was a feasible technology for SWD-RO brine concentration. It concentrated the brine and at the same time produced some useful by-products that could be further valorized (chlorine and hydrogen gas). Performance obtained was highly dependent on inlet temperature and current densities used. At higher inlet temperatures lower concentrations could be obtained, but higher production flows and lower energy consumptions could be reached. At higher current densities applied, higher production flows and concentrations could be obtained but higher energy consumptions were recorded. ED pilot plant was designed in one single pass for diluate, which allowed working with higher current densities and to get higher concentrations. Decarbonation of SWD-RO by pH control was needed in order to avoid precipitations on the membrane surface and so, to avoid the increase of resistance inside the stack, which increased energy consumption and reduced the current efficiency.

The optimal ED operation point was determined when working in a continuous mode at 0.5kA/m^2 were 18L/h of 244 g/L NaCl with 0.16 kWh/kg NaCl energy consumption were obtained. This energy consumption values were in the range of

the industrial cells used in Japan to produce solid salt from seawater, however, higher concentrations can be obtained with SWD-RO brine. More optimization will be needed to reach the technical target to get brines with NaCl contents higher than 200g/L with less than 0.12 kWh/kg. ED intrinsically purified polyvalent ions, which were diluted due to osmosis and electro-osmosis phenomena. Nickel and copper were an exception and were concentrated on the brine produced. In the pH operated, these ions were in form of univalent compounds and so, could pass through the membranes.

Nanofiltration efficiently removed polyvalent ions from both brines. The optimal operation point for collector brine was determined at 20-30 bar in a flat-sheet membrane equipment. Two membranes, XUS and NF270, were tested. NF270 presented higher production flows whereas XUS presented higher rejections. No membrane fouling or scaling was observed after the experiments with collector brine.

NF pilot plant could operate in the range of 8- 20 bar with SWD-RO brines. Higher pressures could not be evaluated, as inlet flow was fixed and limited the maximum operational pressure. The optimal operation point for SWD-RO brine nanofiltration was 20 bar, where 25 L/m^{2}h of purified brine with and energy consumption of 3.2 kWh/m^3 was obtained. This energy consumption could be optimized when higher pressures could be evaluated. Energy consumption of the pilot plant was steady in the pressure range studied at 3 kWh/h and was only reduced by increasing the produced permeate flow.

Rejection results obtained with NF were in the range of the ones reported in the literature. Sulphates were reduced by 90%, magnesium rejection was 71% and calcium rejection was 50% at 20 bar, whereas NaCl was reduced by 12%. The cation rejection order observed was Mg (II) > Sr (II) > Cu (II) > Ca (II) > Ni (II)> Na (I) > K (I), mainly dependant on the hydrating ionic radii and speciation. Lower permeate flows were obtained in the pilot plant compared to literature reported due to higher salinity brines used that increased concentration polarization and membranes chosen. No membrane fouling or scaling was observed after the experiments with SWD-RO brines.

Precipitation using NaOH and Na$_2$CO$_3$ reagents was tested in SWD-RO brine, concentrated ED-SWD-RO brine and collector brine. The effect of reagents order addition in the purification performance was determined not significant. Prepurification of magnesium by adding a primary addition of NaOH followed by the usual treatment system (Na$_2$CO$_3$ addition followed by NaOH) did not have a significant effect on the purification results obtained. Temperatures over 65ºC increased calcium purification performance, especially on SWD-RO and ED-SWD-RO brines which contained all the antiscalants of the RO process that avoided calcium carbonate and sulphate precipitation. Higher temperatures speeded up the precipitation reactions as well as diminished the antiscalant effect. In conclusion, it was recommended to purificate the brines at temperatures higher than 60ºC.

The amount of reactants needed to reach the optimal purification point was higher than the values reported in the literature due to the complexity of the brines evaluated and the antiscalants present on SWD-RO and ED-SWD-RO brines. ED-SWD-RO brines required less reactant than SWD-RO brines because ED process slightly diluted the antiscalant present in the brine. Different studies have been reported to remove antiscalants from the brine in order to optimize the precipitation processes. Removal of antiscalants through degration by oxidation *(Greenlee et al. 2011)* or acceleration of precipitation by seeded precipitation (*Rahardianto et al. 2010*) could be studied in future works to improve the purification results.

Brine compositions obtained after precipitation treatment were not enough to meet the membrane electrolysis requirements. Nevertheless, purifications efficiencies higher than 95% could be obtained. A secondary treatment will be required to polish the brines to reach the ppb levels required.

The precipitates obtained during the purification process could be further valorized. Precipitates analyzed in this thesis did not had high purities, but its reuse in precipitation applications, such as struvite production, could be studied. Studies to obtain better by-product qualities should be carried out in the next future.

Finally, modelization of SWD-RO brine concentration by ED and purification of brines by precipitation was carried out in this thesis. Nerst-Planck equations describing mass transport phenomena were used to model ED process. Parameters needed were extracted from literature reviewed and ideal assumptions were made in order to simplify the solving process. Modelization of precipitation treatment was carried out using PHREEQC code with Pitzer database to simulate the chemical equilibrium of high ionic strength solutions.

ED modelization accurately fitted the results obtained in the pilot plant despite the ideal assumptions made. The model was able to predict the NaCl concentration, time required to reach the maximum concentration and production flow rate obtained when current densities and feed inlet characteristics were introduced. The model was useful to predict the results obtained and optimize the pilot plant. Relative errors of 2% were obtained at temperatures lower than 25ºC. At higher inlet temperatures, the model presented some deviations on the maxium concentration reached due to deviation on the parameters used. Experimental parameters should be determined in order to optimize the model at different temperatures.

Precipitation model was useful to predict the major salt precipitated. Nevertheless, due to antiscalants present in the brine and high complexity of the brines studied, it could not predict the amount of calcium and magnesium remaining in the solution. Results predicted by the model were corroborated by precipitate analysis with DRX and SEM

Table 8.1. Final compositions obtained and % removal using different treatment technologies on the brines studied

	SWD-RO brine				ED-SWD-RO brine	Collector brine			Membrane cell's requirements
	ED		NF		Precipitation	Precipitation	NF		Precipitation	
	0.50 kA/m² (28ºC)		NF270 20 bar (25ºC)		18g/L Na$_2$CO$_3$ and 9g/L NaOH (65ºC)	16g/L Na$_2$CO$_3$ and 7.5g/L NaOH (65ºC)	NF270 30 bar (25ºC)		3g/L Na$_2$CO$_3$ and 7.5 g/L NaOH (65ºC)	
g/L	C_f	%	C_f	%	C_f %	C_f %	C_f	%	C_f %	
NaCl	244		52	12%	59		152	8%	165	300
K (I)	3.2	-220%	0.7	5%						-
Mg (II)	1.3	40%	0.4	71%	0.01 99%	0.015 99%	1.2	75%	0.015 99%	< 20 ppb
Ca (II)	0.3	60%	0.8	50%			0.6	34%		
S (VI)			0.5	91%			0.3	94%		8
mg/L										
Al (III)	0.10	0%	DL	33%						0.1
Ni (II)	0.20	-230%	0.02	35%						0.01
Sr (II)	14.0	0%	6.5	70%						0.4
Cu (II)	0.2	-560%	0.01	66%						0.01
Energy consumption	0.16 kWh/kg		3.2 kWh/kg							

8.2. Treatment system for alternative brines reuse in the chlor-alkali industry.

It can be observed from Table 8.1 that none of the treatments studied alone could reach the membrane cell requirements. In conclusion, a combination of these treatments should be used to polish the brines and make them suitable to be reused in the chlor-alkali industry using membrane cells.

Collector brine presented composition variability so, a steady treatment will not be able to produce a brine with constant quality. Moreover, the high content of potassium in the brine could contaminate the final NaOH produced with KOH that limited its application in the pharmaceutical industry. Due to all of these drawbacks, this brine was finally discarded for chlor-alkali reuse and was not considered suitable for this application. However, this brine could be studied for other purposes, such as a magnesium salt source when precipitation was used.

In the case of SWD-RO brines, it was observed that the highest rejections of undesired ions were obtained with precipitation treatment. However, this treatment required higher amounts of reactants due to antiscalants presents and high amounts of solid sludge were produced, so a pretreatment to reduce the antiscalant present would benefit its application. Moreover, this treatment was not enough to remove metals like nickel and strontium to membrane electrolysis cell requirements, so complementary treatment such as nanofiltration and ion-exchange resins should be used to minimize these drawbacks and reduce the amount of reactants needed. Precipitation was proved more effective after ED concentration because antiscalants were diluted during this process, in consequence, it is recommended to use precipitation after the concentration stage.

ED was an useful technology for brine concentration at high inlet temperatures. It is suggested to use ED with preheated brine in order to reduce the energy consumption. This technology produced some by-products, such as chlorine and hydrogen that could be further valorized. Intrinsical purification of polyvalent ions was obtained for SWD-RO brines, but some metals like nickel and copper were further concentrated during the process. Moreover, exhaustive pH control was needed in order to avoid calcium and magnesium precipitation inside the stack. As a consequence, it is suggested to use NF before ED process in order to remove sulphate, calcium and magnesium as well as some minor elements that could be troublesome for the concentration process and reduce the reactant needs. Finally, an addition of NaCl (approx. 60g/L NaCl) would be required in order to saturate the brine.

Nanofiltration for SWD-RO brine was proved effective and could be an useful pretreatment. Removal efficiencies of NF were lower than the ones obtained by precipitation, however NF could be useful as some metals and sulphate could be

removed without producing sludge. Eriksson *et al.* (2005) reported that 98% purity NaCl brine could be obtained when NF was used before RO process in seawater desalination. In consequence, it is recommended to use NF before RO process whereas it is possible.

In consequence, in order to reuse SWD-RO brines in the chlor-alkali industry, the treatment system proposed in Figure 8.1 is recommended. Further studies could be used to improve performances of the system by removing antiscalants. Ion exchange resins could be used at the end of the treatment system in order to polish some elements that could not be highly removed in all the processes, like strontium and nickel, and to reach the levels required by the chlor-alkali membrane cells. In current on-going projects in the Chemical Engineering Dept. of BarcelonaTech, alternative brine heating through solar ponds is being studied to store energy in Solvay-Martorell (*Valderrama et al. 2008*). Solar ponds are brine reservoirs that collect solar thermal energy, as a result, density gradients are created inside the pond and different layers of brine with different temperatures and salt concentrations can be found. This system could be used to preheat the SWD-RO brine up to 65ºC in the brine treatment system designed and optimize the reuse process of alternative brines in the chlor-alkali industry without increasing the energy consumption requirements.
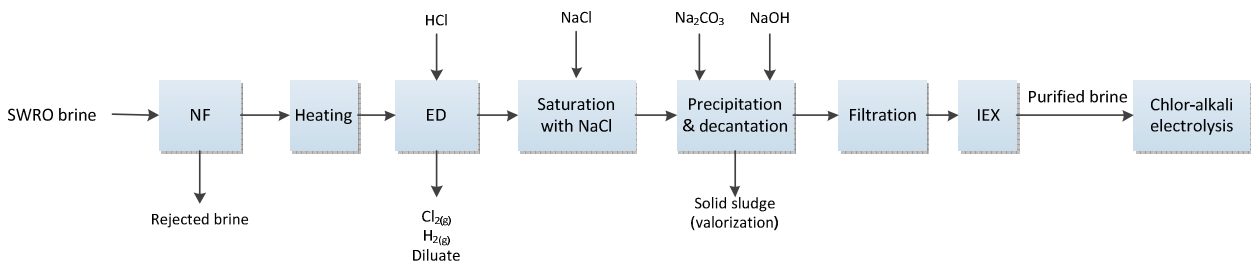

Fig. 8.1. Scheme of the SWD-RO brine treatment process proposed for its reuse in the chlor-alkali industry.

8.3. Future work

There are different questions arising from the results of this thesis and that can be treated as future work. Here we point out the most interesting ones.

- To study the option to preheat the inlet brine for ED process in order to reduce the energy consumption.
- To improve the hydrogen degas design of the ED stack in order to test higher current densities up to 0.7 kA/m^2
- To study the reuse of the by-products currently produced during ED process (hydrogen, chlorine, diluate produced).
- To redesign the ED unit in order to obtain diluate with low salinities that could be further valorized (diluate stream in recirculation mode).
- To experimentally determine the parameters needed to correct the model and to extend it to other major ions such as calcium and magnesium.
- To determine the concentration mechanism of transition metals when high salinity brines are used.
- To redesign the NF unit to evaluate inlet pressures higher than 20 bar and reduce energy consumption.
- To study the temperature effect on NF results obtained with SWD-RO brine.
- To evaluate the use of SWD-RO brine NF without antiscalant addition.
- To evaluate the operation of NF unit in a continuous mode and to determine cleaning needs.
- To test different membranes for NF of SWD-RO brines in order to reduce energy consumption and increase rejections obtained.
- To study the viability of magnesium recovery by precipitation and further valorization from collector brine.
- To study antiscalant removal from SWD-RO brines in order to improve purification efficiency and reduce the amount of reactant needed.
- To obtain higher purities in the precipitation process in order to valorize the salts produced.
- To evaluate complete treatment systems proposed and determine the needs of further purification.

References

- Abdullatef A.Z., Farooque A.M., Al-Otaibi G.F., Kither N.M.,Al Khames S.I (2007) "Optimum Nanofiltration Membrane Arrangements in Seawater Pretreatment: Part-1" IDA World Congress-Maspalomas (Spain)

- Ahmad A.L., Ooi B.S., Mohammad A.W., Choudhury J.P., (2004) "Development of a highly hydrophilic nanofiltration membrane for desalination and water treatment" Desalination 168, pp.215-221.

- Ahmed M, Shayya W, Hoey D, Mahendran A, Morris R, Al-Handaly J (2000) "Use of evaporation ponds for brine disposal in desalination plants" Desalination 130, pp. 155-168

- AGUA, (2007). "Dossier Bibliográfico de publicaciones sobre política y gestión del agua"

- Ameridia (2011) http://www.ameridia.com/html/elep.html

- Aquatec (2010) "Method for treatment and purification of seawater to recover high purity sodium chloride for industrial usage" Patent WO2010/135561A2.

- Bader M.S.H. (2007) "Sulfate removal technologies for oil fields seawater injection operations" Journal of Science and Engineering 55, pp. 93-110.

- Bader M.S.H. (2008) "Analysis of the Paradox Valley brine desulfation by Nanofiltration" Desalination 229, pp. 33–51

- Badruzzaman M., Oppenheimer J., Adham S, Kumar M. (2009) "Innovative beneficial reuse of reverse osmosis concentrate using bipolar membrane electrodialysis and electrochlorination processes" Journal of Membrane Science 326, pp. 392–399

- Baker R.W. (2004) "Membrane Technology and Applications" Second Edition. John Wiley & Sons Ltd.

- Barr A. (2001). "Sulphate Removal by Nanofiltration" Filtration+Separation. Volume 38, Issue 6, pp. 18-20.

- Bessarabov, D, Twardowski Z (2002) "Industrial Applications of Nanofiltration" Membrane Technology 9, pp. 6-9

- Blancke W. (2006) UNITA DI RICERCA ELETTROLISI ROSIGNANO. "Production of NaCl concentrated brine from seawater for chlor-alkali membrane electrolysis: 4 months exploitation of an Asahi Glass micro pilot cell" SOLVAY

- Blancke W. (2007) UNITA DI RICERCA ELETTROLISI ROSIGNANO. "Production of NaCl concentrated brine from seawater for chlor-alkali membrane electrolysis: exploitation of saturated super purified seawater in a chlor-alakli micro pilot cell " SOLVAY

- Brown C.J., Russer A. , Sheedy M. (2000) "New ion exchange processes for brine purification" 8th World Salt Symposium Volume 1.

- Canaragua (2010) "Brine reuse" Sostaqua Project. Results obtained in line 1D of the project.
  http://www.sostaqua.com/publications/publications.php?act=1&task=11.

- Casado-Martínez M.C., Fernández N., Lloret J., Marín L., Martínez-Gómez C., Beiras R., Riba I., Saco-Alvarez L., del-Valls T.A. (2006) "Interlaboratory assessment of marine bioassays to evaluate the environmental quality of coastal sediments in Spain. III Bioassay using embryos of teh sea urchin Paracentrotus lividus" Ciencias Marinas Magazine, volume 32 Number 12.

- Chen T. Neville A. Yuan M. (2006)" Influence of Mg^{2+} on $CaCO_3$ formation—bulk precipitation and surface deposition". Chemical Engineering Science. Volume 61, Issue 16, pp. 5318 – 5327.

- Danoun R. (2007) "Desalination Plants: Potential impacts of brine discharge on marine life". The Ocean Technology Group. University of Sidney.

- Drioli E, Criscuoli A, Curcio E. (2002) "Integrated membrane operations for seawater desalination." Desalination 147, pp.78-81.

- Drioli E., Curcio E., Criscuoli A., Di Profio G. (2004), "Integrated system for recovery of CaCO3, NaCl and MgSO4·7H2O from nanofiltration retentate" Journal of Membrane Science 239, pp.27-38.

- Dow (2011)

  http://www.dowwaterandprocess.com/support_training/design_tools/ftnorm.htm

- Elliott D. (1999). "Primary Brine Treatment Operations" Eltech Chlorine/Chlorate Seminar. Cleveland, Ohio.

- El-Naas M., Al-Marzouqi, A.H, Chaalal O. (2010) "A combined approach for the management of desalination reject brine and capture of CO_2" Desalination 251, pp.70-74

- Ericsson B, Hallmans B. (1996) "Treatment of saline wastewater for zero discharge at the Debiensko coal mines in Poland" Desalination 105 p.115-123

- Eriksson P., Kyburz M., Pergande W. (2005) "NF membrane characteristics and evaluation for seawater processing applications" Desalination 184, pp.281 – 294.

- Eurochlor (2010). "Chlorine Industry Review 2009-2010"

- Fidaleo M., Moresi M . (2005) "Optimal strategy to model the electrodialytic recovery of a strong electrolyte". Journal of Membrane Science 260, pp. 90-111.

- Fidaleo M., Moresi M. (2011) "Electrodialytic desalting of model concentrated NaCl brines as such or enriched with a non-electrolyte osmotic component" Journal of Membrane Science 367, pp. 220–232

- Firdaous L., Saheb T., Schlumpff J.P., Malériat J.P., Bourseau P. Jaouen P. (2005). "A mathematical model of multicomponent mass transfer in electrodialysis" SIMS2005 - Scandinavian Conference on Simulation and Modeling.

- Fritzmann C., Löwenberg Wintgens T., Mellin T. (2007) "State-of-the-art of reverse osmosis desalination" Desalination 216, pp. 1-76

- Fernández Torquemada Y., Sánchez Lisazo J.L.   "Effects of salinity on growth and survival of Vymodocea nodosa (Ucria) Aschernon and Zostera noltii Hornemann". Biology Marine Mediterranean 13 (4) (2006) pp. 46-47

- Fujita, T. (2009), "Current challenges of salt production technology", Bull. Soc. Sea Water Sci., Jpn., 63, pp. 15-20.

- Gacia E, Invers O, Manzanera M, Ballesteros E, Romero J. (2007) "Impact of the brine from a desalination plant on a shallow seagrass (Posidonia Oceanica) meadow" Estuarine, Coastal and Shelf Science 72, pp. 579- 590.

- Gibert O., Valderrama C., Peterkóva M., Cortina J.L. (2010) "Evaluation of Selective Sorbents for the Extraction of Valuable Metal Ions (Cs, Rb, Li, U) from Reverse Osmosis Rejected Brine" Solvent Extraction and Ion Exchange, 28, pp. 543–562

- Greenlee L.F., Testa F., Lawler D.F., Freeman B.D., Moulin P. (2010a) "The effect of antiscalant addition on calcium carbonate precipitation for a simplified synthetic brackish water reverse osmosis concentrate" Water research 44, pp. 2957-2969.

- Greenlee L.F., Testa F., Lawler D.F., Freeman B.D., Moulin P. (2010b) "Effect of antiscalant on precipitation of an RO concentrate: Metals precipitated and particle characteristics for several water compositions". Water research 44, pp. 2672-2684.

- Greenlee L.F., Testa F., Lawler D.F., Freeman B.D., Moulin P. (2011) "Effect of antiscalant degradation on salt precipitation and solid/liquid separation of RO concentrate" Journal of Membrane Science 366 pp. 48-61.

- Hassan A.M, Farooque A.M., Jamaluddin A.T.M., Al-Amoudi A.S., Al-Sofi M.AK., Al-Rubaian A.F., Kither N.M., Al-Tisan I.A.R., Rowaili A. (2000) "A demonstration plant based on the new NF-SWD-RO process" Desalination 131, Issues 1-3, pp. 157-171.

- Hayashi Y, Fukui S., Nakamura Y. (2000) "Method of and apparatus for producing potable water and salt" US Patent 6.030.530

- Hilal N, Al-Zoubi H, Darwish N.A., Mohammad A.W., Abu Arabi M. (2004) "A comprehensive review of nanofiltration membranes: treatment, pretreatment, modelling and atomic force microscopy". Desalination 170, pp. 281-308.

- Hilal N, Al-Zoubi H, Mohammad A.W., Darwish N.A (2005) "Nanofiltration of highly concentrated salt solutions up to seawater salinity" Desalination 184, pp. 315–326.

- Hong S.U., Malaisamy R., Bruening M.L. (2006) " Optimization of flux and selectivity in Cl-/SO42- separations with multilayer polyelectrolyte membranes" Journal of Membrane Science 283, pp.266-372.

- Hussain A.A., Abashar M.E.E. ,Al-Mutaz. I.S. (2007) "Influence of ion size on the prediction of nanofiltration membrane systems". Desalination 214, pp. 150-166.

- IPPC Integrated Pollution Prevention and Control (2001),"Reference Document on Best Available Techniques in the Chlor-Alkali Manufacturing industry".

- Jeppesen T, Shu, L, Keir G., Jegatheesan V. (2009) "Metal recovery from reverse osmosis concentrate". Journal of Cleaner Production 17, pp. 703–707

- Ji X., Curcio E., Al Obaidani S., Di Profio G., Fontananova E. , Drioli E. (2010) "Membrane distillation-crystallization of seawater reverse osmosis brines" Separation and Purification Technology 71, pp. 76-82

- Kielland J. (1937) "Individual activity coefficients of ions in aqueous solutions" J. Am. Chem. Soc. 59,pp.1675-1678.

- Kim D.H. (2011) "A review of desalting process techniques and economic analysis of the recovery of salts from retentates" Desalination doi:10.1016/j.desal.2010.12.041.

- Kitamura M. (2001) "Crystallization and Transformation Mechanism of Calcium Carbonate Polymorphs and the Effect of Magnesium Ion" Journal of Colloid and Interface Science. Volume 236, Issue 2, pp. 318-327

- Ketrane R. Saidani B. Gil O. Leleyter L. Baraud F. (2009) "Efficiency of five scale inhibitors on calcium carbonate precipitation from hard water:Effect of temperature and concentration" Desalination 249, pp. 1397-1404.

- Korngold E., Aronov L. , Daltrophe N. (2009) "Electrodialysis of brine solutions discharged from an RO plant" Desalination 242, pp. 215-227

- Krieg H.M., Modise S.J., Keizer K. , Neomagus H.W.J.P. (2004) "Salt rejection in nanofiltration for single and binary salt mixtures in view of sulphate removal" Desalination 171, pp. 205-215

- Latorre M. (2004). "Costes económicos y medio ambientales de la desalación de agua de mar". Congreso Ibérico de Gestión y Planificación del Agua.

- Leblanc J, Andrews J. (2007) "Solar-Powered Desalination: A modelling and an experimental study" Renovable Energy for Sustainable Development Conference.

- Le Dirach J, Nisan S, Poletiko C. (2005) "Extraction of strategic materials from the concentrated brine rejected by integrated nuclear desalination systems" Desalination 182, pp. 449–460.

- Lee H-J., Strathmann H, Moon S-H. (2006) "Determination of the limiting current density in electrodialysis desalination as an empirical function of linear velocity" Desalination 190, pp.43–50.

- Li N, Yin F, Sun W, Zhang C, Shi Y. (2010) "Turbidity study of solar ponds utilizing seawater as salt source" Solar Energy 84 , pp. 289–295.

- Llansana A., Ferrero E., Ayala V., Malfeito J.J. (2007) "Characterization of Nanofiltration Membranes and their evaluation for RO desalination pre-treatment" IDA World Congress-Maspalomas (Spain)

- M'nif A, Bouguecha S, Hamrouni B, Dhahbi M. (2007) "Coupling of membrane processes for brackish water desalination" Desalination 2003, pp. 331-336.

- Macedonio F, Di Profio G, Curcio E , Drioli E (2006) "Integrated membrane Systems for seawater desalination" Desalination 200, pp. 612-614.

- Macedonio F, Di Profio G, Drioli E (2007) "Integrated membrane systems for seawater desalination: energetic and exergetic analysis, economic evaluation, experimental study" Desalination 203, pp. 260-276

- Madeni S S, Kazemi V. (2007) "Treatment of saturated brine in chlor-alkali process using membranes" Separation and Purification Technology 61, pp. 72-78.

- Madeni S.S., Salehi E. (2009) "A new adsorption-transport and porosity combined model for passage of cations through nanofiltration membrane" Journal of Membrane Science 333, pp. 100-109.

- Mänttäri M., Pekuri T., Nyström M. (2004) "NF270, a new membrane having promising characteristics and being suitable for treatment of dilute effluents from paper industry" Journal of Membrane Science 242, pp. 107-116.

- Marcus, Y. (1997) "Ion properties"; Marcel Dekker: New York.

- Martín-Alonso, J. (2006) "Managing Resources in an European Semi-Arid Environment: Combined use of Surface and Groundwater for Drinking Water Production in the Barcelona Metropolitan Area" Riverbank Filtration Hydrology Nato Science Series: IV: Earth and Environmental SciencesVolume 60, pp.281-298.

- Martinez S. (2003) "Documents de referència sobre les millors tècniques disponibles aplicables a la indústria. La indústria del clor-àlcali" Departament de Medi Ambient. Catalan Goverment.

- Meneses M., Pasqualino J.C., Céspedes-Sánchez R., Castells F. (2010) "Alternatives for Reducing the Environmental Impact of the Main Residue from a Desalination Plant" Journal of Industrial Ecology, Volume 14, Number 3. Pp. 512-527.

- Mericq J-P., Laborie S., Cabassud C. (2010) "Vacuum membrane distillation of seawater reverse osmosis brines" Water Research 44, pp. 5260 -5273

- Mickley, M. (2006). "Membrane Concentrate Disposal: Practices and Regulation", Second Edition. U.S. Department of the Interior, Bureau of Reclamation, Technical Service Center, Water Treatment Engineering and Research Group.

- Moch I. (2002) "A 21st Century Study of Global Seawater Reverse Osmosis Operating and Capital Costs", Proceedings of the IDA World Congress on Desalination and Water Reuse.

- Moon P, Sandí G, Stevens D, Kizilel R. (2004) "Computational Modeling of Ionic Transport in Continuous and Batch Electrodialysis" SEPARATION SCIENCE AND TECHNOLOGY. Vol. 39, No. 11, pp. 2531–2555.

- Morse J.W., Wang Q., Tsio M.Y. (1997) "Influences of temperature and Mg:Ca ratio on $CaCO_3$ precipitates from seawater" Geology v.25 no. 1. pp. 85-87.

- Muttoo T., Dean D. (2001) "Development of Chlorine Dioxide Gas Transport Contactor (ERCO R101TM Generator) for Use in Drinking Water Disinfection" North American Membrane Society Meeting, Lexington, Kentucky.

- Ochoa J - R., (1996) "Electrosíntesis y Electrodiálisis, Fundamentos, aplicaciones tecnológicas y tendencias", Madrid. pp 136 -144.

- Ohya H, Suzuki T, Nakao S. (2001) "Integrated system for complete usage of components in seawater" Desalination 134, pp. 29-36.

- Oren Y., Korngold E., Daltrophe N., Messalem R., Volkman Y., Aronov L., Weismann M., Bouriakov N., Glueckstern P., Gilron J. (2010), "Pilot studies on high recovery BWRO-EDR for near zero liquid discharge approach" Desalination 261, pp. 321-330.

- Ortiz J.M., Sotoca J.A., Exposito E., Gallud F., García-García V., Montiel V. Aldaz A. (2005) "Brackish water desalination by electrodialysis: batch recirculation operation modeling." Journal of Membrane Science 252, pp. 65–75.

- Palomar P., Losada I.J. (2010) "Desalination in Spain: Recent developments and recommendations" Desalination 225, pp. 97-106.

- Parkhurst, D.L. (1995) "PHREEQC: a computer program for speciation, reaction-path, advective transport, and inverse geochemical calculations." U.S. Geol. Surv., Water Resour. Invest. Rep. pp. 95 – 4227

- Pastacaldi, A. (2001) " Le sel, la saumure leurs impuretés et les traitements" Réunion Inter-Usines « jeunes électrolyseurs » NOH. Unité de Recherche Electrolyse ROSIGNANO

- Pereira S., Peinemann K-V. (2006) "Membrane Technology in the Chemical Industry" 2nd Edition. WILEY-VCH Verlag GmbH & Co. KGaA,Weinheim, Germany pp. 274-280.

- Pokrovsky O.S. (1998) "Precipitation of calcium and magnesium carbonates from homogeneous supersaturated solutions" Journal of Crystal Growth 186 pp. 233-239

- Qdais, H. (2008). "Environmental Impacts of the mega desalination project: the Red-Dead Sea conveyor" Desalination 220, pp. 16-23.

- Rahardianto A., McCool B.C., Cohen Y. (2010) "Accelerated desupersaturation of reverse osmosis concentrate by chemically-enhanced seeded precipitation" Desalination 264 pp. 256-267

- Randall D.G., Nathoo J., Lewis A.E. (2011) "A case study for treating a reverse osmosis brine using Eutectic Freeze Crystallization—Approaching a zero waste process" Desalination 266, pp. 256-262.

- Ravizki A, Nadav N (2007) "Salt production by the evaporation of SWD-RO brine in Elliat. A success story" Desalination 205, pp. 374-379

- Reddy S.T., Lewisa A.E.,. Witkamp G.J, Kramera H.J.M., van Spronsenb J. (2010) "Recovery of Na2SO4· 10H2O from a reverse osmosis retentate by eutectic freeze crystallisation technology" Chemical Engineering Research and Design 88, pp.1153–1157

- ROSA (2011) http://www.dowwaterandprocess.com/support_training/design_tools/rosa.htm

- Rovira M., Casas J.M, Saler A (2006)." Saline balance in the basin of the Llobregat river" Afinidad: Revista de química teórica y aplicada, ISSN 0001-9704, Vol. 63, Nº. 526 , pp. 438-443.

- Rovira M. (2008) "La conca salina del Bages i la qualitat de l'aigua del Llobregat" PhD Thesis. Barcelona_Tech.

- Sadrzadeh M. , Razmi A., Mohammadi T. (2007a) "Separation of different ions from wastewater at various operating conditions using electrodialysis" Separation and Purification Technology 54, pp.147-156.

- Sadrzadeh M., Kaviani A., Mohammadi T. (2007b) "Mathematical modeling of desalination by electrodialysis" Desalination 206, pp. 538–546.

- Sánchez-Lizaso J.L., Romero J., Ruiz J., Gacia E., Buceta J.L., Invers O., Fernández Torquemada Y. Mas A., Ruiz-Mateo A., Manzanera M. (2008) "Salinity tolerance of the Mediterranean seagrass Posidonia oceánica: recommendations to minimize the impact of brine discharges from desalination plants" Desalination 221, pp.602-607.

- Sheikholeslami R., Ong H.W.K., (2003) Kinetics and thermodynamics of calcium carbonate and calcium sulfate at salinities up to 1.5 M, Desalination 157 pp.217-234.

- Shi L., and Luos H.(2009) "Preparation of soil nutrient amendment using white mud produced in ammonia-soda process and its environmental assessment, Transactions of on ferrous". Metals Society of China, 19, 5, pp. 1383-1388.

- Sostaqua (2011) www.sostaqua.com

- Steinhauser G. (2008) "Cleaner production in the Solvay Process: general strategies and recent developments" Journal of Cleaner Production 16, pp. 883-841.

- Strathmann H. (2010) "Electrodialysis, a mature technology with a multitude of new applications". Desalination 264, pp. 268–288.

- Tanaka Y., Ehara R., Itoi S., Goto T. (2003) "Ion-exchange membrane electrodialytic salt production using brine discharged from a reverse osmosis seawater desalination plant" Journal of Membrane Science 222, pp. 71-86.

- Tanaka Y. (2007) "Ion exchange membranes: fundamentals and applications" Elsevier B.V. ISBN: 978-0-444-51982-5

- Tanaka Y. (2009) "A computer simulation of continuous ion exchange membrane electrodialysis for desalination of saline water". Desalination 249, pp. 809-821.

- Tanaka Y.(2010a) "A computer simulation of ion exchange membrane electrodialysis for concentration of seawater". Membrane Water Treatment Vol. 1, No. 1. pp. 13-37.

- Tanaka Y. (2010b) "A computer simulation of feed and bleed ion exchange membrane electrodialysis for desalination of saline water" Desalination 254, pp. 99–107

- Tansel B., Sager J., Rector T., Garland J., Strayer R., Levine L., Roberts M., Hummerick M., Bauer H. (2006) "Significance of hydrated radius and hydration shells on ionic permeability during nanofiltration in dead end and cross flow modes" Separation and Purification Technology, 51, pp. 40-47.

- Telzhensky M., Birnhack L., Lehmann O., Windler E., Lahav O. (2011) "Selective separation of seawater Mg2+ ions for use in downstream water treatment processes" Chemical Engineering Journal. doi:10.1016/j.cej.2011.09.082

- Turek M, Mrowiec-Bialon J, Gnot W. (1995 a). "Utilitzation of coal mine brines in the chlorine production process" Desalination 101, pp. 57-67.

- Turek M, Gnot W. (1995 b), "Precipitation of Magnesium Hydroxide from Brine" Industrial& Engineering Chemistry Research 34, pp. 244-250

- Turek M., Gonet M. (1996) "Nanofiltration in the utilization of coal-mine brines". Desalination 108, pp.171-177

- Turek M (2002a) "Seawater desalination and salt production in a hybrid membrane-thermal process" Desalination 153 pp.173-177

- Turek M (2002b) "Dual-purpose desalination-salt production electrodialysis" Desalination 153 pp. 377-381.

- Turek M. (2004) "Electrodialytic desalination and concentration of coal-mine brine" Desalination 162, pp. 355-359.

- Turek M. , Dydo P. , Klimel R. (2005 a) "Salt Production from coal-mine brine in ED-evaporation-crystallization system" Desalination 184, pp.439-446.

- Turek M. , Dydo P., Surma A. (2005 b) "Zero discharge utilization of saline waters from "Wesola" coal-mine" Desalination 185, pp. 275- 280

- Turek M, Dydo P, Klimek R (2008a) "Salt production from coal-mine brine in NF — evaporation — crystallization system" Desalination 221, pp.238-243.

- Turek M, Bandura B, Dydo P. (2008b) "Power production from coal-mine brine utilizing reversed electrodialysis" Desalination 221 pp.462-466.

- Turek M., Was J., Dydo P. (2009) " Brackish water desalination in RO–single pass EDR system" Desalination and water treatment 7,pp. 263–266.

- Twardowski Z. (1996) "Nanofiltration of concentrated aqueous salt solutions" US Patent 5,587,083

- Twardowski Z, Ulan J.G. (1999) "Nanofiltration of concentrated aqueous salt solutions" US Patent 5,858,240

- University of South Carolina Research Foundation (2006) " Zero Discharge Seawater Desalination: Integrating the Production of Freshwater, Salt, Magnesium and Bromine" Desalination and Water Purification Research and Development Program Report No. 111

- Valderrama C., Gibert O., Cortina J.L., Larrotcha E., Flores J. (2008) "Estanques solares de salmuera". Semana Agbar de la Innovación 2008.

- Valero F., Barceló A., Arbos R. (2011) "Electrodialysis Technology - Theory and Applications" Desalination, Trends and Technologies.

- Van der Bruggen B., Lejon L., Vandecasteele C. (2003). "Reuse, Treatment, and Discharge of the Concentrate of Pressure-Driven Membrane Processes" Environmental Science and Technology 37, no.17. pp. 3733–3738.

- Van der Bruggen B. , Koninckx A., Vandecasteele C. (2004) '' Separation of monovalent and divalent ions from aqueous solution by electrodialysis and nanofiltration'' Water Research 38, pp. 1347–1353.

- Van der Bruggen B., Mänttäri M., Nyström M. (2008) "Drawbacks of applying nanofiltration and how to avoid them: A review" Separation and Purification Technology 63, pp. 251−263

- Velmurugan V, Sritha K. (2008) "Prospects and scopes of solar pond: A detailed review" Renewable and Sustainable Energy Reviews 12, pp. 2253–2263.

- Wang K., Chung T., Rajagopalan R., (2007) "Novel Polybenzimidazole (PBI) Nanofiltration Membranes for the separation of sulfate and chromate from high alkalinity brine to facilitate the chlor-alkali process" Ind. Eng. Chem. Res. 46, pp. 1572-1577.

- WHO. Public Health and the Environment World Health Organization (2007) "Desalination for Safe Water Supply Guidance for the Health and Environmental Aspects Applicable to Desalination"

- WWC. World Water Council (2000). "World water vision: Making water everybody's business".

- Yacubowicz, J. (2005) "Nanofiltration properties and uses" Filtration+Separation 42, pp. 16-21

- Yamane R., Ichikawa M., Mituzani Y., Onoue Y. (1969) " Concentrated Brine production from seawater by electrodialysis using ion exchange membranes" I&EC Process Design and Development. Vol 8. pp. 159-164

- Zhang Y., Ghyselbrecht K., Meesschaert B., Pinoy L., Van der Bruggen B. (2010) "Electrodialysis on RO concentrate to improve water recovery in wastewater reclamation" Journal of Membrane Science 378, pp. 101– 110.